

CHAPTER 5

Trends in Stratospheric Temperatures

Lead Authors:

M.-L. Chanin
V. Ramaswamy

Coauthors:

D.J. Gaffen
W.J. Randel
R.B. Rood
M. Shiotani

Contributors:

J.K. Angell
J. Barnett
P. Forster
M. Gelman
J. Hansen
P. Keckhut
Y. Koshelkov
K. Labitzke
J.-J.R. Lin
E.V. Lysenko
J. Nash
A. O'Neill
M.D. Schwarzkopf
K.P. Shine
R. Swinbank
O. Uchino

CHAPTER 5

TRENDS IN STRATOSPHERIC TEMPERATURES

Contents

SCIENTIFIC SUMMARY	5.1
5.1 INTRODUCTION	5.5
5.2 OBSERVATIONS	5.6
5.2.1 Data	5.6
5.2.1.1 Radiosonde Datasets	5.8
5.2.1.2 Rocketsonde and Lidar Datasets	5.9
5.2.1.3 MSU and SSU Satellite Datasets	5.9
5.2.1.4 Analyzed Datasets	5.10
5.2.2 Summary of Various Radiosonde-Based Investigations of Trends	5.11
5.2.3 Zonal, Annual-Mean Trends	5.15
5.2.3.1 Trends Determination	5.15
5.2.3.2 Trends at 50 and 100 hPa	5.15
5.2.3.3 Vertical Profiles	5.18
5.2.3.4 Rocket Data and Trends Comparisons	5.19
5.2.4 Latitude-Season Trends	5.22
5.2.5 Uncertainties in Trends Estimated from Observations	5.25
5.2.5.1 Uncertainties Associated with Radiosonde Data	5.26
5.2.5.2 Uncertainties Associated with Analyses of SSU Satellite Data	5.28
5.2.5.3 Uncertainties in Satellite-Radiosonde Trend Intercomparisons	5.28
5.2.5.4 Uncertainties Associated with Rocket Data	5.28
5.2.5.5 Uncertainties Associated with the Lidar Record	5.29
5.2.6 Issues Concerning Variability	5.29
5.2.6.1 Volcanic Aerosol Influences	5.29
5.2.6.2 Solar Cycle	5.30
5.2.6.3 QBO Temperature Variations	5.32
5.2.6.4 Planetary Wave Effects	5.33
5.2.6.5 El Niño-Southern Oscillation (ENSO)	5.33
5.2.7 Changes in Tropopause Height	5.33
5.3 MODEL SIMULATIONS	5.34
5.3.1 Background	5.34
5.3.2 Well-Mixed Greenhouse Gases	5.35
5.3.3 Stratospheric Ozone	5.38
5.3.3.1 Lower Stratosphere	5.38
5.3.3.2 Sensitivities Related to Ozone Change	5.44
5.3.4 Aerosols	5.46
5.3.5 Water Vapor	5.47
5.3.6 Other (Solar Cycle, QBO)	5.47
5.4 CHANGES IN TRACE SPECIES AND OBSERVED TEMPERATURE TRENDS	5.48
5.4.1 Lower Stratosphere	5.48
5.4.2 Middle and Upper Stratosphere	5.50
5.4.3 Upper Troposphere	5.51
REFERENCES	5.51

SCIENTIFIC SUMMARY

Observations

- Datasets available for analyzing stratospheric temperature trends comprise measurements by radiosonde (1940s-present), satellite (1979-present), lidar (1979-present), and rocketsonde (periods varying with location, but most terminating by ~mid-1990s); meteorological analyses based on radiosonde and/or satellite data; and products based on assimilating observations using a general circulation model (GCM).
- The temporary global, annual-mean lower stratospheric (~50-100 hPa) warming (peak value ~1 K) associated with the aerosols from the Mt. Pinatubo volcanic eruption (see WMO, 1992, 1995), which lasted up to about 1993, has now given way to a relatively colder stratosphere.
- Radiosonde and satellite data indicate a cooling trend of the global, annual-mean lower stratosphere since ~1980. Over the period 1979-1994, the trend is ~0.6 K/decade. For the period prior to 1980, the radiosonde data exhibit a substantially weaker long-term cooling trend.
- Over the period 1979-1994 there is an annual-mean cooling of the Northern Hemisphere midlatitude lower stratosphere (~0.75 K/decade at 30-60°N). This trend is coherent amongst the various datasets with regard to the magnitude and statistical significance. Over the longer period 1966-1994, the available datasets indicate an annual-mean cooling at 30-60°N of ~0.3 K/decade.
- In the ~15-45° latitude belt of the Southern Hemisphere, the radiosonde record indicates an annual-mean cooling of the lower stratosphere of up to ~0.5-1 K/decade over the period 1979-1994. The satellite record also indicates a cooling of the lower stratosphere in this latitude belt; the cooling is statistically significant between about November and April.
- Substantial cooling (~3-4 K/decade) is observed in the polar lower stratosphere during late winter/springtime in both hemispheres. An approximate decadal-scale cooling trend is evident in the Antarctic since about the early 1980s, and in the Arctic since about the early 1990s. However, the dynamical variability is large in these regions, particularly in the Arctic, and this introduces difficulties in establishing a high statistical significance of the trends.
- A cooling of the upper stratosphere (pressure < 3 hPa; altitude > 40 km) is apparent over the 60°N-60°S region from the annual-mean Stratospheric Sounding Unit (SSU) satellite data over the 1979-1994 period (up to ~3 K/decade near 50 km). There is a slight minimum in cooling in the middle stratosphere (~30-40 km) between the maxima in the lower and upper stratosphere.
- Lidar and rocket data available from specific sites generally show a cooling over most of the middle and upper stratosphere (~30-50 km) of 1 to 2 K/decade since ~1970, with the magnitude increasing with altitude. The influence of the 11-year solar cycle is relatively large (>1 K) at these altitudes (>30 km).
- The vertical profile of the annual-mean stratospheric temperature change observed in the Northern Hemisphere midlatitude (45°N) over the 1979-1994 period is robust among the different datasets. The overall trend (Figure 5A) consists of a ~0.8 K/decade cooling of the ~20-35 km region, with the cooling trend increasing with height above (~2.5 K/decade at 50 km).

STRATOSPHERIC TEMPERATURE TRENDS

Model Results and Model-Observation Comparisons

- Model simulations based on the known changes in the stratospheric concentrations of various radiatively active species indicate that the depletion of lower stratospheric ozone is the dominant factor in the explanation of the observed global-mean lower stratospheric cooling trend ($\sim 0.5\text{-}0.6$ K/decade) for the period 1979-1990. The contribution to this trend from increases in well-mixed greenhouse gases is estimated to be less than one-fourth that due to ozone loss.
- Model simulations indicate that ozone depletion is an important causal factor in the latitude-month pattern of the decadal (1979-1990) lower stratospheric cooling. The simulated lower stratosphere in Northern and Southern Hemisphere midlatitudes, and in the Antarctic springtime, generally exhibits a statistically significant cooling trend over this period, consistent with observations.
- The Fixed Dynamical Heating (FDH; equivalently, the pure radiative response) calculations yield a mid- to high-latitude annual-mean cooling that is approximately consistent with a GCM's radiative-dynamical response (Figure 5B); however, changes in circulation simulated by the GCM cause an additional cooling in the tropics, besides affecting the meridional pattern of the temperature decrease.
- FDH model results indicate that both well-mixed greenhouse gases and ozone changes are important contributors to the cooling in the middle and upper stratosphere; however, the computed upper stratospheric cooling is smaller than the observed decadal trend. Increased water vapor in the lower to upper stratosphere domain could also be an important contributor to the cooling; however, decadal-scale global stratospheric water vapor trends have not yet been determined.
- Model simulations of the response to the observed global lower stratospheric ozone loss in mid to high latitudes suggest a radiative-dynamical feedback leading to a warming of the middle and upper stratospheric regions, especially during springtime; however, while the modeled warming is large and can be statistically significant during the Antarctic spring, it is not statistically significant during the Arctic spring. Antarctic radiosonde observations indicate a statistically significant warming trend in spring at ~ 30 hPa (24 km) and extending possibly to even higher altitudes; this region lies above a domain of strong cooling that is approximately collocated with the altitude of the observed ozone depletion.
- There is little evidence to suggest that tropospheric climate changes (e.g., induced by greenhouse gas increases in the troposphere) and sea surface temperature variations have been dominant factors in the global-mean stratospheric temperature trend over the 1979-1994 period. The effect of potential shifts in atmospheric circulation patterns upon the decadal trends in global stratospheric temperatures remains to be determined.

STRATOSPHERIC TEMPERATURE TRENDS

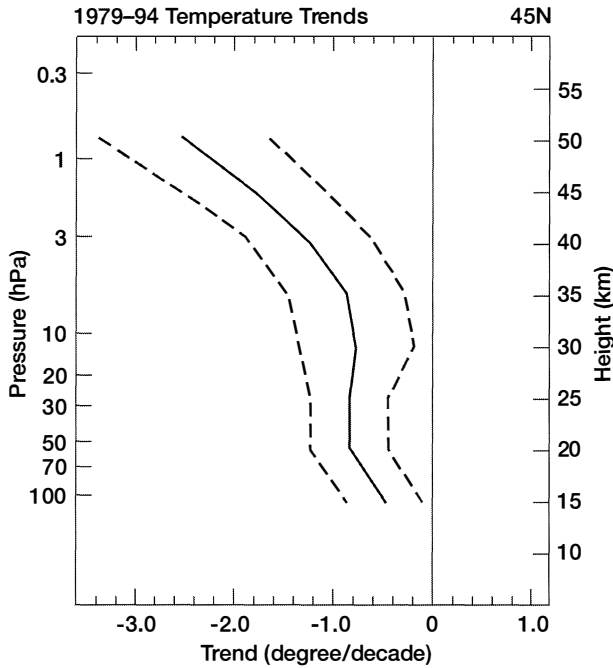


Figure 5A. Summary figure illustrating the overall mean vertical profile of temperature trend (K/decade) over the 1979-1994 period in the stratosphere at 45°N, as compiled using radiosonde, satellite, and analyzed datasets (Section 5.2.3.3). The vertical profile of the averaged trend estimate was computed as a weighted mean of the individual system trends shown in Figure 5-9, with the weighting being inversely proportional to the individual uncertainty. The solid line indicates the weighted trend estimate while the dashed lines denote the uncertainty at the 2-sigma level (note: Table 5-6 lists the numerical values of the trends and the uncertainty at the one-sigma level). (Figure assembled for this chapter in cooperation with the SPARC-Stratospheric Temperature Trends Assessment project.)

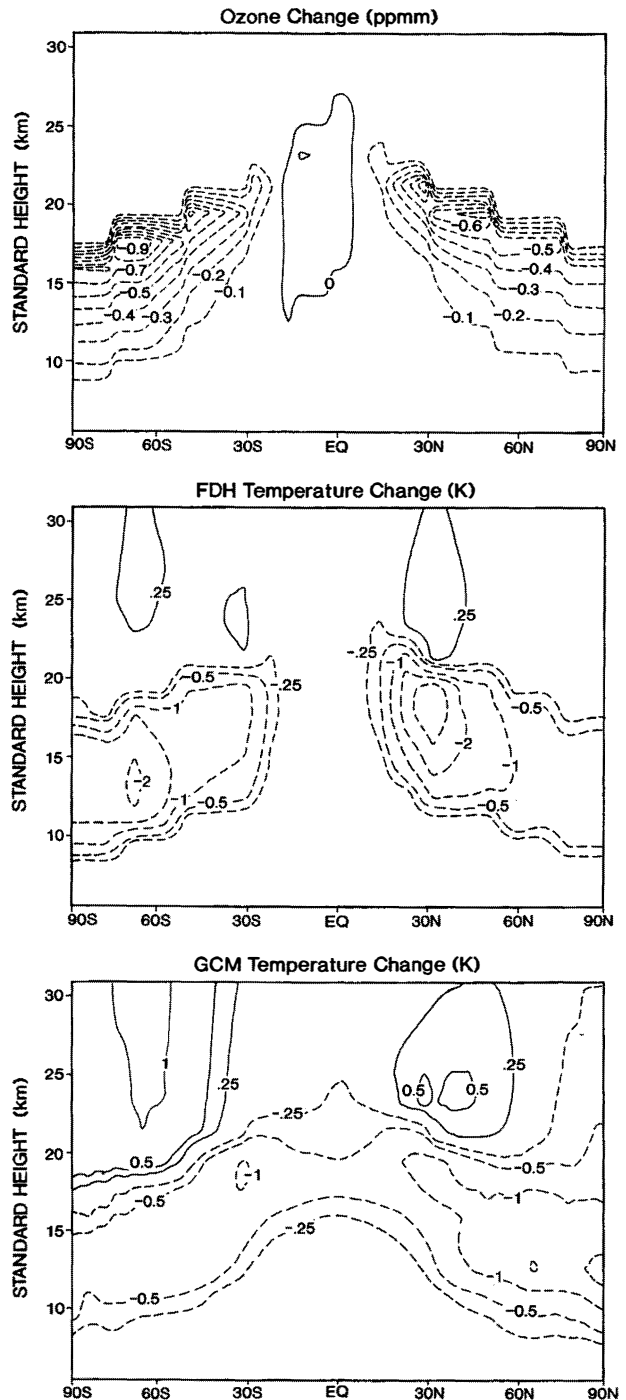


Figure 5B. Top panel: Idealized, annual-mean stratospheric ozone loss profile, based on Total Ozone Mapping Spectrometer (TOMS) and Stratospheric Aerosol and Gas Experiment (SAGE) satellite-observed ozone trends. Middle panel: Corresponding temperature change, as obtained using a Fixed Dynamical Heating (FDH) model, which illustrates the pure radiative response, and (bottom panel) a general circulation model (GCM), which illustrates the radiative-dynamical response (Section 5.3.3.1). (Adapted from Ramaswamy *et al.*, 1992, 1996).

5.1 INTRODUCTION

For at least a decade now, the investigation of trends in stratospheric temperatures has been recognized by the World Meteorological Organization (WMO) to be an integral part of the ozone trends report. A comprehensive international scientific assessment of stratospheric temperature changes was undertaken in WMO (1990a). Analyses of the then-available datasets (rocketsonde, radiosonde, and satellite records) over the period 1979/80 to 1985/86 indicated that the observed temperature trend was inconsistent with the then-apparent ozone losses inferred from Solar Backscatter Ultraviolet (SBUV) spectrometer data, but consistent with Stratospheric Aerosol and Gas Experiment (SAGE) ozone changes. The largest cooling in the observed datasets was in the upper stratosphere, while the lower stratosphere had experienced no significant cooling except in the tropics and Antarctica. It is interesting to note that the period analyzed by WMO (1990a) was one when severe ozone losses were just beginning to be recognized in the Antarctic springtime lower stratosphere. It was also a period from sunspot maximum to sunspot minimum. Standard interactive photochemical-radiation models then available that incorporated trace-gas changes (including ozone) were found to yield a cooling in the upper/middle stratosphere that was broadly consistent with the available observations but under-predicted the observed cooling in the lower stratosphere. A warming due to the El Chichón volcanic eruption (1982-1983) was also reported, with simple models using imposed aerosol inputs reproducing the observed transient warming.

Since the time of the 1988 WMO Assessment (WMO, 1990a), there has been an ever-growing impetus for observational and model investigations of stratospheric temperature trends (WMO, 1990b, 1992, 1995). This has occurred owing to the secular increases in greenhouse gases and the now well-documented global and seasonal losses of stratospheric ozone, both of which have a substantial impact on the stratospheric radiative-dynamical equilibrium. The availability of various temperature observations and the ever-increasing length of the data record have also been encouraging factors. In addition, models have progressively acquired the capability to perform more realistic simulations of the stratosphere. This has provided a motivation for comparing model results with observations, and thereby

the search for causal explanation(s) of the observed trends. The developments seen in modeling underscore the significance of the interactions between radiation, dynamics, and chemistry in the interpretation of linkages between changes in trace species and temperature trends. Temperature changes are also instrumental in the microphysical-chemical processes of importance in the stratosphere (see Chapter 7).

The assessment of stratospheric temperature trends is now regarded as a high priority in climate change research inasmuch as it has been shown to be a key entity in the detection and attribution of the observed vertical profile of temperature changes in the Earth's atmosphere (Hansen *et al.*, 1995; Santer *et al.*, 1996; Tett *et al.*, 1996). Indeed, the subject of trends in stratospheric temperatures is of crucial importance to the Intergovernmental Panel on Climate Change assessment (IPCC, 1996) and constitutes a significant scientific input into policy decisions.

We summarize here the principal results concerning stratospheric temperature trends from the previous WMO ozone assessments. In general, the successive assessments since the WMO (1986) and WMO (1990a) reports have traced the evolution of the state of the science on both the observation and model simulation fronts. On the observational side, WMO has reported on available temperature trends from various kinds of instruments: radiosonde, rocketsonde, satellite, and lidar. On the modeling side, since the 1986 report, WMO has reported on model investigations that illustrate the role of greenhouse gases and aerosols in the thermal structure of the stratosphere, and the effects due to changes in their concentrations upon stratospheric temperature trends. The 1989 Assessment (WMO, 1990b) began to recognize, from observational and modeling standpoints, the substantial lower stratospheric cooling occurring during springtime in the Antarctic as a consequence of the large ozone depletion. The low- and middle-latitude lower stratosphere were inferred to have a cooling of less than 0.4 K/decade over the prior 20 years. The upper stratosphere was estimated to have cooled by 1.5 ± 1 K between 1979/80 and 1985/86.

The 1991 Assessment (WMO, 1992) reported that, based on radiosonde analyses, a global-mean lower stratospheric cooling of ~ 0.3 K had occurred over the previous 2-3 decades. Model calculations indicated that the observed ozone losses had the potential to yield substantial cooling of the global lower stratosphere. At

STRATOSPHERIC TEMPERATURE TRENDS

44°N during summer, an observed cooling of the upper stratosphere (~1 K/decade at ~35 km) and mesosphere (~4 K/decade) was also reported. However, in general, for assessment purposes, the global stratospheric temperature record and understanding of temperature changes were found to be not as sound as those related to ozone changes.

The 1994 Assessment (WMO, 1995) discussed the observational and modeling efforts through 1994, focusing entirely on trends in lower stratospheric temperatures. That Assessment concluded, based on radiosonde and satellite microwave observations, that there were short-term variations superposed on the long-term trends. A contributing factor to the former was stratospheric aerosol increases following the El Chichón and Mt. Pinatubo volcanic eruptions, which resulted in an increase of the global stratospheric temperature. These transient warmings posed a complication when analyzing the long-term trends and inferring their causes. The long-term trends from the radiosonde and satellite data indicated a cooling of 0.25 to 0.4 K/decade since the late 1970s, with suggestions of an acceleration of the cooling during the 1980s. The global cooling of the lower stratosphere suggested by the observations was reproduced reasonably well by models considering the observed decreases of ozone in the lower stratosphere. For altitudes above the lower stratosphere, a clear conclusion concerning trends could not be made. The 1991 and 1994 Assessments (WMO, 1992, 1995) laid the basis for the conclusion that the observed trends in the lower stratosphere during the 1980s were largely attributable to halocarbon-induced ozone losses.

This 1998 Assessment extends the evaluations of the earlier ones by focusing on the decadal-scale lower to upper stratospheric temperature trends arising out of observational (Section 5.2) and model simulation (Section 5.3) analyses. The temperature observations considered span at least 10 years; the period considered for evaluation is typically at least 15 years. The trend estimates discussed here include (i) a long-term period that spans two decades or more, (ii) the period since 1979 and extending to either 1994 or the present (i.e., up to 1998), and (iii) the period extending from 1979 to about the early 1990s. The last-mentioned period is that for which several model simulations have been compared with observations. In Section 5.4, we use the results from Sections 5.2 and 5.3 to investigate the extent to which the observed temperature trends can be attributed to changes in the concentrations of radiatively active species.

5.2 OBSERVATIONS

5.2.1 Data

The types of observational data available for investigation into stratospheric temperature trends are diverse. They differ in type of measurement, length of time period, and space-time sampling. There have been several investigations of trends that have considered varying time spans with the different available datasets, as will be discussed shortly. In recent years, the World Climate Research Programme's SPARC-STTA (Stratospheric Processes and their Role in Climate-Stratospheric Temperature Trends Assessment) group has initiated a project to bring together various datasets covering the period 1966-1994 and to intercompare the resulting global stratospheric temperature trends. The authors and contributors of this current WMO/UNEP 1998 Assessment chapter largely constitute the working group of the SPARC-STTA. The data and trends obtained by this group are used in some of the intercomparisons reported here. The chapter prepared for the current WMO/UNEP Assessment will serve as an input to the ongoing SPARC investigation of stratospheric temperature trends.

SPARC-STTA chose two different time periods to examine the trends, based on the availability of the data, viz., 1979-1994 and 1966-1994. The former period coincides with the period when severe global ozone losses have been detected and also coincides with the period of global satellite observations. The second period is a longer one for which radiosonde (and a few rocketsonde) datasets are available.

The updated datasets made available to and employed by the SPARC-STTA for the analyses are shown (with the exception of rocketsonde datasets) in Table 5-1 along with their respective latitudes, altitudes, and periods of coverage. Additionally, independent of the STTA activity, some investigations (Dunkerton *et al.*, 1998; Keckhut *et al.*, 1998; Komuro, 1989; Golitsyn *et al.*, 1996; Kokin and Lysenko, 1994; Lysenko *et al.*, 1997) have analyzed trends from rocketsonde observations made at a few geographical locations and over specific time periods (see Table 5-2). We utilize these datasets in some of the presentations to follow. It is convenient to group the currently known datasets in the following manner:

- *Ground-based instruments:* radiosonde, rocketsonde, and lidar

STRATOSPHERIC TEMPERATURE TRENDS

Table 5-1. Zonal temperature time series made available to and considered by SPARC-STTA. For the MSU and Nash satellite data, the approximate peak levels “sensed” are listed. References to earlier versions of the datasets are also listed. See Section 5.2.1 for details.

Dataset	Period	Latitude Coverage	Averaging	Levels (hPa)
<u>Radiosonde Datasets</u>				
Angell (Angell, 1988)	1958-1994	8 bands 4 bands	3-monthly 3-monthly	100-50 50, 30, 20, 10
Oort (Oort and Liu, 1993)	1958-1989	85°S-85°N	monthly	100, 50
Russia (Koshelkov and Zakharov, 1998)	1959-1994 1961-1994	70°N, 80°N 70°N, 80°N	monthly monthly	100 50
UK RAOB (or RAOB) (Parker and Cox, 1995)	1961-1994	87.5°S-87.5°N	monthly	100, 50, 30, 20
Berlin (Labitzke and van Loon, 1994)	1965-1994	10-90°N	monthly	100, 50, 30
<u>Lidar Dataset</u>				
Lidar (Hauchecorne <i>et al.</i> , 1991)	1979-1994	44°N, 6°E (Haute Provence)	monthly	10, 5, 2, 1, 0.4
<u>Satellite Datasets</u>				
MSU (Spencer and Christy, 1993)	1979-1994	85°S-85°N	monthly	90
Nash (Nash and Forrester, 1986)	1979-1994	75°S-75°N	monthly	50, 20, 15, 6, 5, 2, 1.5, 0.5
<u>Analyzed Datasets</u>				
CPC (Gelman <i>et al.</i> , 1994)	1979-1994 1964-1978	85°S-85°N 20°N-85°N	monthly monthly	70, 50, 30, 10, 5, 2, 1 50, 30, 10
Reanal (Kalnay <i>et al.</i> , 1996)	1979-1994	85°S-85°N	monthly	100, 70, 50, 30, 10
GSFC (Schubert <i>et al.</i> , 1993)	1979-1994	90°S-90°N	monthly	100, 70, 50, 30, 20
UKMO/SSUANAL (Bailey <i>et al.</i> , 1993)	1979-1994	90°S-90°N	monthly	50, 20, 10, 5, 2, 1

STRATOSPHERIC TEMPERATURE TRENDS

- *Satellite instruments:* microwave and infrared sounders
- *Analyses:* employing data from one or both of the above instrument types, without/with a numerical model

The datasets indicated in Table 5-1 are a collection of monthly-mean, zonal-mean temperature time series. All but one of these datasets cover the years 1979-1994, and some extend farther back in time. The pressure-altitude levels of the datasets vary, but overall they cover the range 100 to 0.4 hPa (approximately 16-55 km). Most datasets provide temperatures at specific pressure levels, but some provide data as mean temperatures representative of various pressure layers. The instrumental records from radiosondes, rocketsondes, lidar, and satellite (Microwave Sounding Unit (MSU) and Stratospheric Sounding Unit (SSU)) are virtually independent of each other. General characteristics of the different datasets are discussed below (see also WMO, 1990a,b).

5.2.1.1 RADIOSONDE DATASETS

Radiosonde data are available dating back to approximately the early 1940s. Although the sonde data do not cover the entire globe, there have been several well-documented efforts to use varied techniques in order to obtain the temperatures over the entire Northern Hemisphere or the global domains. The sonde data cover primarily the lower stratospheric region (approximately, pressures greater than 10 hPa). The geographical coverage is quite reasonable in the Northern Hemisphere (particularly midlatitudes) but is poor in the extremely high latitudes and tropics, and is seriously deficient in the Southern Hemisphere (Oort and Liu, 1993).

As was the case at the time of the 1988 Assessment, two organizations monitor trends and variations in lower stratospheric temperatures using radiosonde data alone. The “Berlin” group (e.g., Labitzke and van Loon, 1995) prepares daily hand-drawn stratospheric maps based on synoptic analyses of radiosonde data at 100, 50, 30, and, in some months, 10 hPa, beginning from 1964. The Berlin monthly dataset examined by SPARC-STTA is derived from these daily analyses. The National Oceanic and Atmospheric Administration (NOAA) Air Resources Laboratory (e.g., Angell, 1988) uses daily radiosonde

soundings to calculate seasonal layer-mean “virtual temperature” anomalies from long-term means, and uses these to determine trends since 1958 in the 850-300, 300-100, and 100-50 hPa layers (lower stratosphere). (Virtual temperature is the temperature of dry air having the same pressure and density as the actual moist air. Virtual temperature always exceeds temperature, but the difference is negligible in the stratosphere (Elliott *et al.*, 1994).) The layer-mean virtual temperatures are determined from the geopotential heights of the layer endpoints. The Berlin analyses are of the Northern Hemisphere stratosphere and troposphere and are based on all available radiosonde data, whereas the Air Resources Laboratory monitors trends at 63 stations in eight zonal bands covering the globe. Additionally, Angell (1991b) also monitors stratospheric temperature, particularly its response to volcanic eruptions, at four levels between 20 km (50 hPa) and 31 km (10 hPa) using a network of 12 stations ranging from 8°S to 55°N. The “Angell” data used here represent a subset.

Extensive analyses of radiosonde temperature data by the NOAA Geophysical Fluid Dynamics Laboratory (GFDL) (Oort and Liu, 1993) and the U.K. Meteorological Office’s (UKMO) Hadley Centre for Climate Prediction and Research (Parker *et al.*, 1997) have also been used for quantifying stratospheric trends. The GFDL database consists of gridded global objective analyses based on monthly means derived from daily soundings for the period 1958-1989 for the tropospheric levels and the 100-, 70-, 50-, and 30-hPa levels in the lower stratosphere. Layer-mean trends for the 100-50 hPa layer are based on temperature data at the 100-, 70-, and 50-hPa levels. A subset of this dataset, labeled “Oort,” is used here. The UKMO gridded dataset (RAwinsonde OBservations, denoted as “RAOB” or “UK RAOB”) for 1958-1996 is based on monthly mean (CLIMAT TEMP) station reports, adjusted (using MSU Channel 4 data, discussed below, as a reference) to remove some time-varying biases since 1979 for stations in Australia and New Zealand, and interpolated in some data-void regions. The “Russia” set consists of data from the high northern latitudes (70 and 80°N; Koshelkov and Zakharov, 1998). Thus, the Angell, Berlin, Oort, Russia, and RAOB datasets used by SPARC-STTA are compilations of data from various radiosonde stations, grouped, interpolated, and/or averaged in various ways to obtain monthly-mean and latitude-mean, pressure-level or vertical-average temperatures.

Table 5-2. Rocketsonde locations and periods of coverage utilized for the present Assessment. (Based on Dunkerton *et al.*, 1998; Golitsyn *et al.*, 1996; Keckhut *et al.*, 1998; Kokin and Lysenko, 1994; Lysenko *et al.*, 1997; and Komuro, 1989 (updated).)

Station	Latitude, Longitude (degrees)	Period
Heiss Island	81N, 58E	1964-1994
Volgograd	49N, 44E	1965-1994
Balkhash	47N, 75E	1973-1992
Ryori	39N, 141.5E	1970-present
Wallops Island	37.5N, 76W	1965-1990
Point Mugu	34N, 119W	1965-1991
Cape Kennedy	28N, 80W	1965-1993
Barking Sands	22N, 160W	1969-1991
Antigua	17N, 61W	1969-1991
Thumba	08N, 77E	1971-1993
Kwajalein	09N, 167E	1969-1990
Ascension Island	08S, 14W	1965-1993
Molodezhnaya	68S, 46E	1969-1994

5.2.1.2 ROCKETSONDE AND LIDAR DATASETS

Rocketsonde and lidar data cover the altitude range from about the middle stratosphere into the upper stratosphere and mesosphere. Rocketsonde data are available through the early 1990s from some locations, but the activity appears to be virtually terminated except in Japan (see Table 5-2). The lidar measurement, just like the rocketsonde measurement, has a fine vertical resolution. Lidar measurements of stratospheric temperatures are available since 1979 from the Haute Provence Observatory (OHP) in southern France (44°N, 6°E). Specifically, the “lidar” (Table 5-1) temperatures observed at altitudes of 30 to 90 km are obtained from two lidar stations, with data interpolated to pressure levels (Keckhut *et al.*, 1995). Several other lidar sites have initiated operations and could potentially contribute in future temperature trends assessments.

5.2.1.3 MSU AND SSU SATELLITE DATASETS

Satellite instruments of interest have become available since ~1979 (Table 5-1). These fall into two categories: those that remotely sense in the microwave wavelengths (Spencer and Christy, 1993) and those that remotely sense in the thermal infrared wavelengths (Nash and Forrester, 1986). The “MSU” Channel 4 dataset

derives from the lower stratosphere channel (~150-50 hPa) of the Microwave Sounding Unit on NOAA polar-orbiting operational satellites (Figure 5-1, left panel). The “Nash” dataset consists of brightness temperatures from observed (25, 26, and 27) and derived (47X, 36X, 35X, 26X, and 15X) channels of the Stratospheric Sounding Unit (SSU) instrument on these same satellites (Figure 5-1). The SSU data used in this report are extensions (J. Nash, UKMO, UK, personal communication, 1997) of earlier works (e.g., Nash and Forrester, 1986) and have been provided to SPARC and WMO for temperature trends assessment purposes. One complication with satellite data is the fact that there are discontinuities in the time series owing to the measurements being made by different satellites monitoring the stratosphere since 1979. Adjustments have been made in the Nash channel data provided to compensate for radiometric differences, tidal differences between spacecraft, long-term drift in the local time of measurements, and spectroscopic drift in Channels 26 and 27. Adjustments have also been made to MSU data (e.g., Christy *et al.*, 1995).

An important attribute of the satellite instruments is their global coverage. However, in contrast to the ground-based instruments, e.g., radiosondes, which perform measurements at specific pressure levels, the available satellite sensors have response functions that sense the signal from a wide range in altitude. The nadir

STRATOSPHERIC TEMPERATURE TRENDS

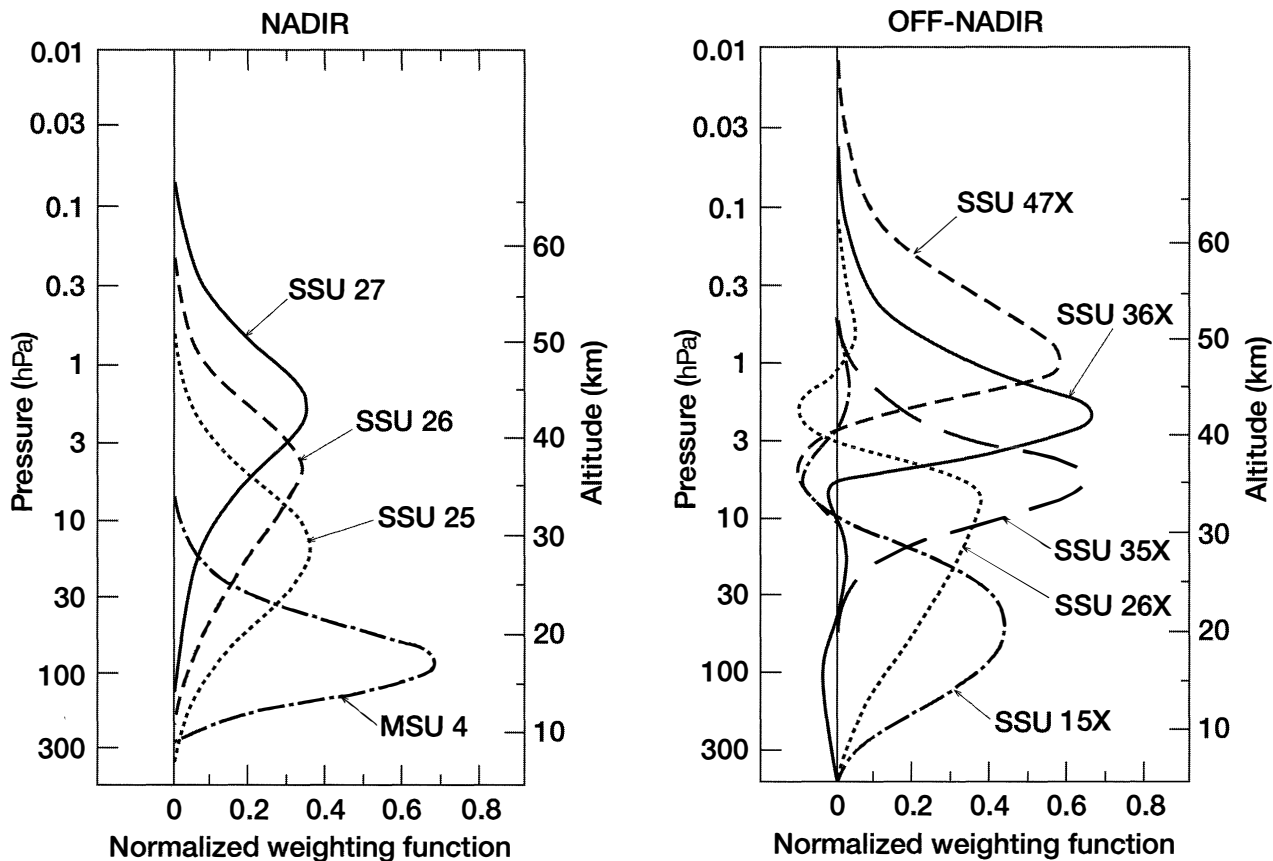


Figure 5-1. Altitude range of the signals “sensed” by the various thermal infrared channels of the Stratospheric Sounding Unit instrument (SSU) and by Channel 4 of the Microwave Sounding Unit (MSU). Nadir (left panel) and off-nadir (right panel) channel weighting functions.

satellite instruments “sense” the emission originating from a layer of the atmosphere approximately 10-15 km thick. Figure 5-1 illustrates the weighting function for the MSU and SSU channels analyzed here, exhibiting the thick-layer nature of the measurements. For example, the emission for microwave MSU Channel 4 comes from the ~12-22 km layer, while, for the thermal infrared SSU Channel 15X, it is from the ~12-28 km layer. In Table 5-1, a nominal center pressure of each satellite channel has been designated, but it is emphasized that the preponderance of energy comes from a vertical layer, ~8-12 km thick, centered around the concerned pressure level, as indicated in Figure 5-1. A perspective into the global-mean anomalies of temperature at various stratospheric altitudes between 1979 and 1995 (deviations with respect to the mean over this period), as derived from different SSU channels, can be obtained from Figure 5-2. The MSU record was discussed in WMO (1995).

5.2.1.4 ANALYZED DATASETS

A number of datasets involve some kind of analyses of the observations. They employ one or more types of observed data, together with the use of some mathematical technique and/or a general circulation assimilation model, to construct the global time series of the temperatures. They are, in essence, more of a derived dataset than the satellite- or the ground-based ones. The “CPC” analyses (from the Climate Prediction Center, formerly Climate Analysis Center) and “UKMO/SSUANAL” stratospheric analyses (Table 5-1) do not involve any numerical atmospheric circulation model. The CPC Northern Hemisphere 70-, 50-, 30- and 10-hPa analyses use radiosonde data. Both the CPC and UKMO/SSUANAL analyses (see also Swinbank and O’Neill, 1994) use Television and InfraRed Observational Satellite (TIROS) Operational Vertical Sounder (TOVS) temperatures, which incorporate data

STRATOSPHERIC TEMPERATURE TRENDS

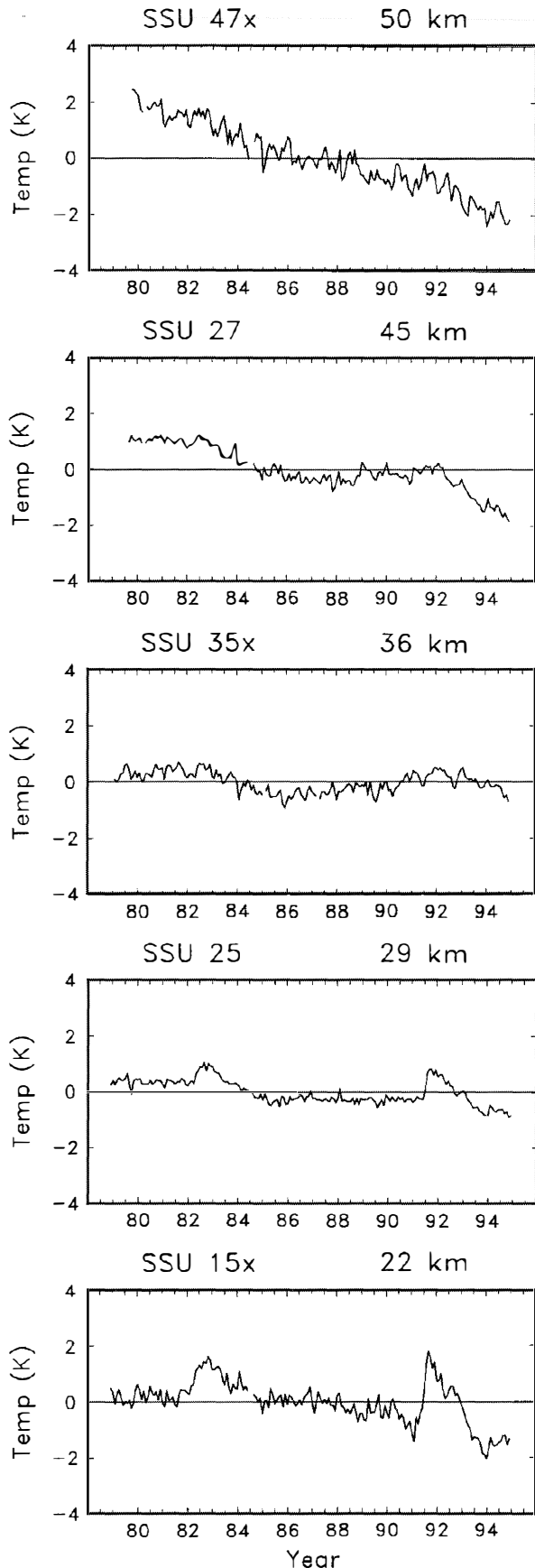


Figure 5-2. Time series of global temperature anomalies from the overlap-adjusted SSU data. These data measure the thermal structure over thick layers (thickness $\sim 10\text{-}15$ km) of the stratosphere; the label of each panel indicates the approximate altitude of the weighting function maximum. (Figure assembled for this chapter in cooperation with the SPARC-Stratospheric Temperature Trends Assessment project.)

from the SSU, High-Resolution Infrared Sounder (HIRS-2), and MSU on the NOAA polar-orbiting satellites. Adjustments based on rocketsonde data (Finger *et al.*, 1993) have been applied to the CPC 5-, 2-, and 1-hPa temperatures for the SPARC dataset. (However, both the CPC data above 10-hPa altitude and the UKMO/SSUANAL datasets may be limited in scope for trend studies, as they have not yet been adjusted for some of the known problems associated with SSU satellite retrievals from many different satellites (see Section 5.2.5.2); hence, they are not considered in this chapter.)

The “Reanal” (viz., the U.S. National Centers for Environmental Prediction (NCEP) reanalyzed) and the “GSFC” (Goddard Space Flight Center, National Aeronautics and Space Administration (NASA)) datasets are derived using numerical atmospheric general circulation models (GCMs) as part of the respective data assimilation systems. These analysis projects provide synoptic meteorological data extending over many years using an unchanged assimilation system. In general, analyzed datasets are dependent on the quality of the data sources, such that a spurious trend in a data source could be inadvertently incorporated in the assimilation. Also, analyses do not necessarily account for longer-term calibration-related problems in the data. Further, the analyzed datasets may not contain adjustments for satellite data discontinuities (Santer *et al.*, 1998).

5.2.2 Summary of Various Radiosonde-Based Investigations of Trends

Radiosonde data show a cooling of the lower stratosphere over the past several decades. Table 5-3 summarizes published temperature trend estimates by various investigators, including those mentioned in Section 5.2.1. The data periods and the analysis techniques vary, as do the levels and layers analyzed. No attempt is made here to critically evaluate these diverse estimation techniques. The reported trends have

STRATOSPHERIC TEMPERATURE TRENDS

Table 5-3. Lower stratospheric temperature trends from published studies of radiosonde data.

Reference	Data Period	Level or Layer	Region	Trend (K/decade)	Comments
Angell (1991a)	1972-1989	50 hPa, 20 km	8°S - 55°N	-0.5 ± 0.3	12 radiosonde stations. Data were adjusted for the El Chichón influence. Greatest cooling in winter.
		30 hPa, 24 km		-0.4 ± 0.3	
		20 hPa, 27 km		-0.3 ± 0.3	
		10 hPa, 31 km		-0.3 ± 0.3	
Angell (1991b)	1970-1988	100-50 hPa layer	NH	-0.2	Trends reported here are based on Angell's presentation of temperature differences between the periods 1980-88 and 1970-78.
			SH	-0.5	
Koshelkov and Zakharov (1998)	1965-1994	50- and 100-hPa levels	65°N - 83°N	0 to -1 (-0.5)	Significant (95% confidence level) trends only from May to October. Significant (95% confidence level) trends only from June to August.
	1979-1994			0 to -1	
Labitzke and van Loon (1995)	1965-1993	100 hPa	NH (10-90°N)	0 to -0.5	Significant (95% confidence level) trends between 60 and 80°N. Significant (95% confidence level) trends between 20 and 90°N. Significant (95% confidence level) trends between 30 and 60°N.
		50 hPa	NH (10-90°N)	0 to -0.5	
		30 hPa	NH (10-90°N)	0 to -0.5	
	1979-1993	100 hPa	NH (10-90°N)	-0.2 to -0.8	Significant (95% confidence level) trends only at about 40°N. Significant (95% confidence level) trends between 35 and 50°N. Significant (95% confidence level) trends between 30 and 50°N.
		50 hPa	NH (10-90°N)	0 to -0.9	
		30 hPa	NH (10-90°N)	0 to -1.0	
Miller <i>et al.</i> (1992)	1964-1986	150-30 hPa	Global (62 stations, as Angell)	-0.2 to -0.4, depending on level	Four stations' data were adjusted for level shifts.

TABLE 5-3, continued.

Reference	Data Period	Level or Layer	Region	Trend (K/decade)	Comments
McCormack and Hood (1994)	1979-1990	100 hPa	NH	0 to -4.5	Data from the FUB analyses. Significant trends only in winter at 30-45°N.
Oort and Liu (1993)	1963-1988	100-50 hPa layer	NH	-0.38 ± 0.14	
			SH	-0.43 ± 0.16	
		Globe	-0.40 ± 0.12		
	1959-1988	NH	-0.40 ± 0.10		
Pawson and Naujokat (1997)	1965-1996	50 hPa	NH (10-90°N)	-1.90 (min) +1.67 (max)	Decrease in daily minimum temperature, increase in daily maximum, for winter season. Increase in the area of T<195 K and T<192 K, although the early data for T<192 are questionable.
		30 hPa		-1.85 (min) +4.07 (max)	
Parker <i>et al.</i> (1997)	1965-1996	150-30 hPa layer	NH	-0.27	Radiosonde data weighted to correspond with MSU4. Adjustments made to Australasia data for 1979-1996. Trends significant at the 95% confidence level or better.
			SH	-0.44	
	1979-1996	NH	-0.63		
			SH	-0.73	
Reid <i>et al.</i> (1989)	1966-1982	100-15 hPa levels	Tropics	-1.2 to +0.8	Five radiosonde stations. Trends vary by station and level.
Taalas and Kyrö (1992)	1965-1988	50 hPa	Sodankylä, Finland, station	-0.2 ± 1.6 (annual) -1.6 ± 0.08 (January) +1.5 ± 0.05 (April)	100, 70, and 30 hPa showed similar results.
Taalas and Kyrö (1994)	1965-1992	50 hPa	Sodankylä, Finland, station	-0.16	Also, an increase in the number of observations of T<195 K in winter.

STRATOSPHERIC TEMPERATURE TRENDS

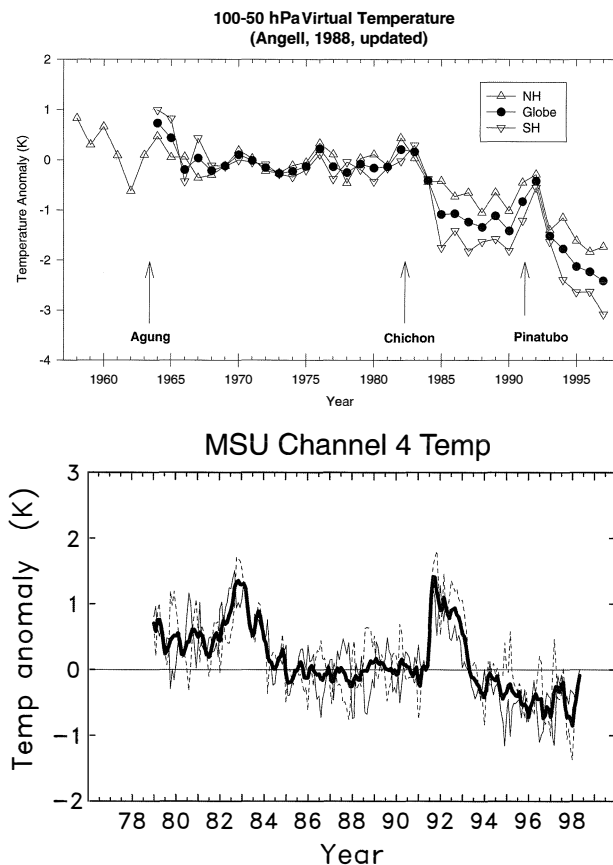


Figure 5-3. Top panel: Global and hemispheric averages of annual anomalies of 100-50 hPa layer-mean virtual temperature, from 63 radiosonde stations (Angell, 1988, updated; Halpert and Bell, 1997). Bottom panel: Same as top panel, except from MSU Channel 4 (see Section 5.1 for stratospheric altitudes “sensed”); the thick, solid line denotes global-mean, the thin, solid line denotes the Northern Hemisphere mean, and the dashed line denotes the Southern Hemisphere mean. (Updated from Randel and Cobb, 1994.)

all been converted to units of degrees Kelvin per decade. Overall, the trends, based on areal averages and all seasons, are negative and range from zero to several tenths of a degree per decade. The few studies with global coverage show more cooling of the Southern Hemisphere (SH) lower stratosphere than the Northern Hemisphere (NH). Large trends evaluated for the decade of the 1980s emphasize the period of ozone loss. Positive trends have been found at a few individual stations in the tropics by

Reid *et al.* (1989) for the period 1966-1982, possibly due to the influence of El Chichón volcano effects. (It may be noted that Labitzke and van Loon (1995) find positive trends (not listed in Table 5-3) at high and low latitudes for the month of January.)

The sensitivity of trend estimates to the period of record considered is evident from the time series of global or hemispheric mean lower stratospheric temperature anomalies (Angell, 1988; Oort and Liu, 1993; Parker *et al.*, 1997). These data (Figure 5-3 (top); Angell, 1988, updated; Halpert and Bell, 1997) show relatively high temperatures (particularly in the Southern Hemisphere) during the early 1960s, fairly steady temperatures till about 1981, and relatively low temperatures since about 1984, with episodic warmings associated with prominent volcanic eruptions. Figure 5-3 (bottom) shows the global temperature anomalies from the MSU satellite. The evolution of the anomalies is qualitatively similar to the radiosonde anomalies (Christy, 1995), including the warming in the wake of the El Chichón and Mt. Pinatubo eruptions (WMO, 1995), followed by a cooling to somewhat below the pre-eruption levels. The long-term cooling tendency of the global stratosphere is discernible in both datasets, although the satellite data exhibit less interhemispheric difference.

The Berlin analysis (Figure 5-4) shows that the radiosonde temperature time series for the 30-hPa region at the northern pole in July acquires a distinct downward trend when the 1955-1997 period is considered, in contrast to the behavior for the 1955-1977 period. The trend estimates are seen to depend on the end years chosen. The summertime temperature decreases in the high northern latitudes have been more substantial and significant when the decade of 1980s and after are considered; note that this does not necessarily imply a sharp downward trend for the other months.

A few studies have examined radiosonde observations of extreme temperatures in the lower stratosphere. At Sodankylä, Finland, Taalas and Kyrö (1994) found an increase in the frequency of occurrence of temperatures below 195 K at 50 hPa during 1965-1992. At both 50 and 30 hPa over the Northern Hemisphere (10-90°N), Pawson and Naujokat (1997) found a decrease in the minimum and an increase in the maximum daily wintertime temperatures during 1965-1996. They also found an increase in the area with temperatures less than 195 K and suggested that extremely low temperatures appear to have occurred more frequently over the past 15 years.

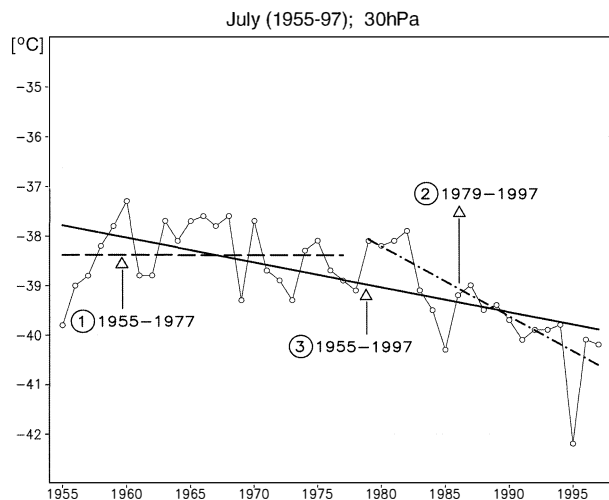


Figure 5-4. Time series of July 30-hPa temperatures for 1955-1997 at high northern latitude (80°N). Trends over the 1955-1977, 1979-1997, and 1955-1997 time periods are -0.01 , -1.41 , and -0.5 K/decade, respectively. Of these, only the 1979-1997 trend is statistically significant. (Updated from Labitzke and van Loon, 1995.)

5.2.3 Zonal, Annual-Mean Trends

5.2.3.1 TRENDS DETERMINATION

There is a wide range in the numerical methods used in the literature to derive trends and their significance. Most studies are based on linear regression analyses, although details of the mathematical models and particularly aspects of the standard error estimates are different. Differences in details of the models include the method of fitting seasonal variability, the number and types of dynamical proxies included, and the method used to account for serial autocorrelation of meteorological data (e.g., the multiple linear regression analysis (MLRA) model of Keckhut *et al.* (1995) and the model used by Randel and Cobb, 1994).

The SPARC-STTA group calculated the temperature trends (K/decade) from each of the datasets using autoregressive time-series analyses (maximum likelihood estimation method; e.g., Efron, 1982). The methodology consists of fitting the time series of monthly-mean values at each latitude with a constant and six variables (annual sine, annual cosine, semiannual sine, semiannual cosine, solar cycle, and linear trend). The derived trend and standard error are the products of

this computation. The t-test for significance at the 95% confidence level is met if the absolute value of the trend divided by the standard error estimate exceeds 2. The results from the statistical technique used by SPARC-STTA have been intercompared with other methods employed in the literature (A.J. Miller, NOAA, U.S., personal communication, 1998) and found to yield similar trend estimates. It is cautioned, however, that the estimates of the statistical uncertainties could be more sensitive to details of the method than the trend results themselves, especially if the time series has lots of missing data.

An important caveat to the interpretation of the significance of the datasets is that the time series analyzed below, in some instances, is only 15 years long or, in the case of the lengthier rocketsonde and radiosonde records, up to ~ 30 years long. In this context, it must be noted that the low-frequency variability in the stratosphere, especially at specific locations, is yet to be fully ascertained and, as such, could have a bearing on the robustness of the derived trend values.

5.2.3.2 TRENDS AT 50 AND 100 hPa

Figure 5-5 illustrates the decadal trends for the different datasets over the 1979-1994 period. For the non-satellite datasets, the trends at 50 and 100 hPa are illustrated in panels (a) and (b), respectively; panel (c) illustrates the satellite-derived trends. The latitudes where the trends are statistically significant for the different datasets are listed in Table 5-4. (The Oort data (Oort and Liu, 1993), which have been used widely (e.g., Hansen *et al.*, 1995; Santer *et al.*, 1996), are not included in this plot owing to the fact that they span a shorter period of time (1979-1989) than the other datasets.) In the case of the MSU and Nash (SSU 15X) satellite data, the trend illustrated in panel (c) is indicative of a response function that spans a wide range in altitude (Figure 5-1); e.g., for MSU, about half of the signal originates from the upper troposphere at the low latitudes. Because of this, caution must be exercised in comparing the magnitudes of the non-satellite trends in Figure 5-5 panels (a) and (b) with those for the satellite in panel (c). This aspect could explain, in part, the lesser cooling obtained by the satellites relative to radiosondes in the tropical regions; however, this argument is contingent upon the trends in the tropical upper troposphere (not investigated in this report). The MSU data indicate less cooling than Nash in the tropics. One reason for this

STRATOSPHERIC TEMPERATURE TRENDS

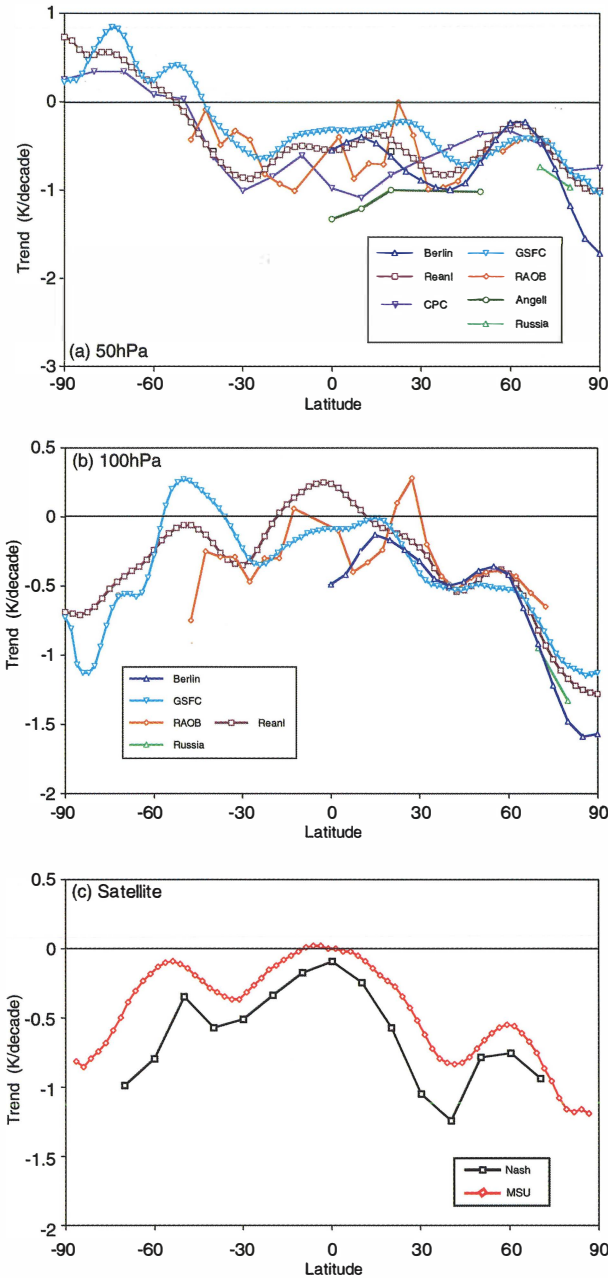


Figure 5-5. Zonal-mean decadal temperature trends for the 1979-1994 period, as obtained from different datasets. These consist of radiosonde (Angell, Berlin, UK/RAOB, and Russia) and satellite (MSU and Nash) observations, and analyzed datasets (CPC, GSFC, and Reanal). See Table 5-1, and Sections 5.2.1 and 5.2.3.2 for details. Panel (a) denotes 50-hPa trends, panel (b) denotes

could be that the Nash peak signal originates from a slightly higher altitude than the MSU; again, though, the extent of the cooling/warming trend in the upper troposphere needs to be considered for a full explanation. The results are statistically insignificant in almost all of the datasets at the low latitudes. This could be in part due to the variable quality of the tropical data. It is conceivable that the radiosonde trends are significant over selected regions where the data are reliable over long time periods, but that the significance aspect is destroyed when reliable and unreliable data are combined to get a zonal mean.

All datasets indicate a cooling of the entire Northern Hemisphere and the entire low- and midlatitude Southern Hemisphere at the 50-hPa level over this period. At the 100-hPa level, there is a cooling over most of the northern and southern latitudes. The midlatitude (30-60°N) trends in the Northern Hemisphere exhibit a statistically significant (Table 5-4) cooling at both 50- and 100-hPa levels, with the magnitude in this region being ~0.5-1 K/decade. This feature is true for the satellite data as well. The similarity of the magnitude and significance in the mid-Northern Hemisphere latitudes from the different datasets is particularly encouraging and suggests a robust trend result for this time period. The trends in the Southern Hemisphere midlatitudes (~15-45°S) range up to ~0.5-1 K/decade but are generally statistically insignificant over most of the area in almost all datasets, except Reanal. Note that the Southern Hemisphere radiosonde data have more uncertainties owing to fewer observing stations and data homogeneity problems (see Section 5.2.5.1). The non-satellite data indicate a warming at 50 hPa but a cooling at 100 hPa at the high southern latitudes, while the satellites indicate a cooling trend. Thus, as for the tropical trends, satellite-radiosonde intercomparisons in this region have to consider carefully the variation of the trends with altitude (Section 5.2.5.3). The lack of

100-hPa trends, and panel (c) denotes trends observed by the satellites for the altitude range “sensed,” which includes the lower stratosphere (see Figure 5-1). Latitude bands where the trends are statistically significant at the 2-sigma level are listed in Table 5-4. (Figure assembled for this chapter in cooperation with the SPARC-Stratospheric Temperature Trends Assessment project.)

Table 5-4. Latitude bands where the observed 50-hPa, 100-hPa, and satellite temperature trends (1979-1994) from various data sources (see Table 5-1 and Figure 5-5) are statistically significant at the 2-sigma level. SH and NH denote Southern and Northern Hemisphere, respectively. A dash denotes either no data or no statistically significant latitude belt in that hemisphere.

Dataset	Latitude Band	
	SH	NH
50 hPa		
Berlin	-	30-55°N
GSFC	-	42-58°N
Reanal	37.5-25°S	32.5-55°N
RAOB	12.5°S	32.5-62.5°N
CPC	30°S	10°N
Angell	-	50°N
Russia	-	-
100 hPa		
Berlin	-	0-5°N; 35-80°N
GSFC	-	38-60°N
Reanal	-	37.5-57.5°N
RAOB	47.5°S	12.5°N; 37.5-72.5°N
Russia	-	70°N
Satellite		
Nash	-	30-60°N
MSU	-	28.75-63.75°N

statistically significant trends in the southern high latitudes need not imply that significant trends do not occur during particular seasons (e.g., Antarctic springtime). The high northern latitudes indicate a strong cooling (1 K/decade or more) in the 50-hPa, 100-hPa, and satellite datasets. However, no trends are significant poleward of $\sim 70^\circ\text{N}$ owing to the large interannual variability there. There is a general consistency of the trends from the analyzed datasets (CPC, GSFC, Reanal) with trends derived directly from the instrumental data. Considering all datasets, the global lower stratospheric cooling trend over the 1979-1994 period is estimated to be ~ 0.6 K/decade. The 50-100 hPa cooling is consistent with earlier WMO results based on shorter records (e.g., Figure 6.17 of WMO, 1990a; Figure 2.4-5 of WMO, 1990b).

Figure 5-6 shows the annual-mean trend over 1966-1994 at 50 hPa and comprises principally the radiosonde record. Note that the Oort time series extends only through 1989. The cooling trends in the northern high latitudes, and in several other latitude belts, are less strong in the radiosonde datasets when the longer period is

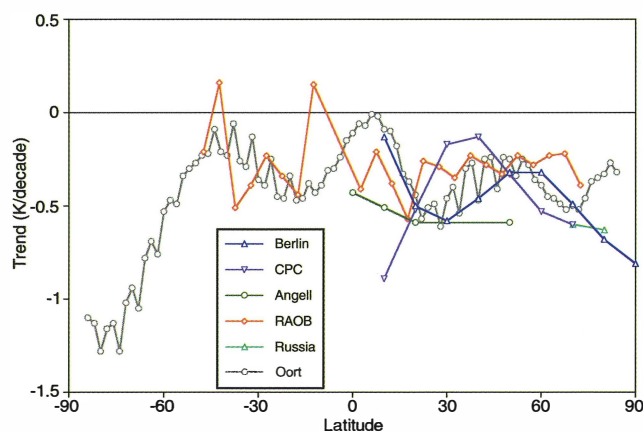


Figure 5-6. Zonal-mean decadal temperature trends at 50 hPa over the 1966-1994 period from different datasets (see Table 5-1 and Sections 5.2.1 and 5.2.3.2 for details). Latitude bands where the trends are statistically significant at the 2-sigma level are listed in Table 5-5. (Figure assembled for this chapter in cooperation with the SPARC-Stratospheric Temperature Trends Assessment project.)

STRATOSPHERIC TEMPERATURE TRENDS

Table 5-5. Latitude bands where the 1966-1994 observed 50-hPa temperature trends from various data sources (see Table 5-1 and Figure 5-6) are statistically significant at the 2-sigma level. SH and NH denote Southern and Northern Hemisphere, respectively. A dash denotes either no data or no statistically significant latitude belt in that hemisphere.

50-hPa Dataset	Latitude Band	
	SH	NH
Berlin	-	20-70°N
CPC	-	10-20°N; 50-60°N
Angell	-	10, 20, 50°N
RAOB	37.5-32.5°S; 22.5-17.5°S	17.5°N; 32.5°N; 42.5-72.5°N
Oort	84-56°S; 30-28°S; 24-22°S; 18-16°S	20-30°N; 34°N; 40°N; 46°N; 52-68°N
Russia	-	70°N

considered (note that the Berlin radiosonde time series for July, Figure 5-4, exhibits a similar feature). The cooling trend in the 30-60°N belt is about 0.3 K/decade. The strong cooling trend in the Oort data in the high southern latitudes is consistent with Oort and Liu (1993), Parker *et al.* (1997), and the Angell data (D. Gaffen, NOAA, U.S., personal communication, 1998). Regions of statistically significant trends in the datasets are listed in Table 5-5. In the Southern Hemisphere, the two global radiosonde datasets indicate a significant cooling over broad belts in the low and midlatitudes, with the Oort data exhibiting this feature at even the higher latitudes. The Oort global-mean trend is -0.33 K/decade over the 1966-1989 period. In the Northern Hemisphere, again, the midlatitude regions stand out in terms of the significance of the estimated trends. Latitudes as low as 10-20° exhibit significant trends over the longer period considered.

5.2.3.3 VERTICAL PROFILES

Figure 5-7 shows the vertical and latitudinal structure of the zonal, annual-mean temperature trend as obtained from the SSU and MSU satellite measurements. The plot is constructed by considering 5-km-thick levels from linear combinations of the weighting functions of the different channels (Figure 5-1). Figure 5-7 shows panels with and without the inclusion of the volcanic periods (i.e., the “no-volcano” calculations omit 2 years of data following the El Chichón and Mt.

Pinatubo eruptions; see Figure 5-2). The omission of the volcano-induced warming period (particularly that due to Mt. Pinatubo near the end of the record) yields an enhanced cooling trend in the lower stratosphere. The vertical profile of the temperature trend in the middle and upper stratosphere between ~60°N and ~60°S shows a strong cooling, particularly in the upper stratosphere (up to 3 K/decade). Cooling at these latitudes in large portions of the middle and upper stratosphere is seen to be statistically significant.

We next focus on 45°N latitude. At this latitude, lidar records from the Haute Provence Observatory (OHP) are available, which afford a high vertical resolution above 30 km, relative to the other instrumental data available. Figure 5-8 displays the annual-mean trend profile for 1979-1998 updated from Keckhut *et al.* (1995) and shows a cooling of ~1-3 K/decade over the entire altitude range 35-70 km, but with statistical significance obtained only around 60 km. The vertical gradient in the profile of cooling between 40 and 50 km differs somewhat from the 1979-1990 summer trend reported in the 1991 WMO Assessment (WMO, 1992, Figure 2-20).

Figure 5-9 compares the vertical pattern of the temperature trend at 45°N obtained from different datasets for the 1979-1994 period. There is a broad agreement in the cooling at the lower stratospheric altitudes, reiterating results in Figure 5-5. The vertical patterns of the trends from the various data are also in qualitative agreement, except for the lidar data (which,

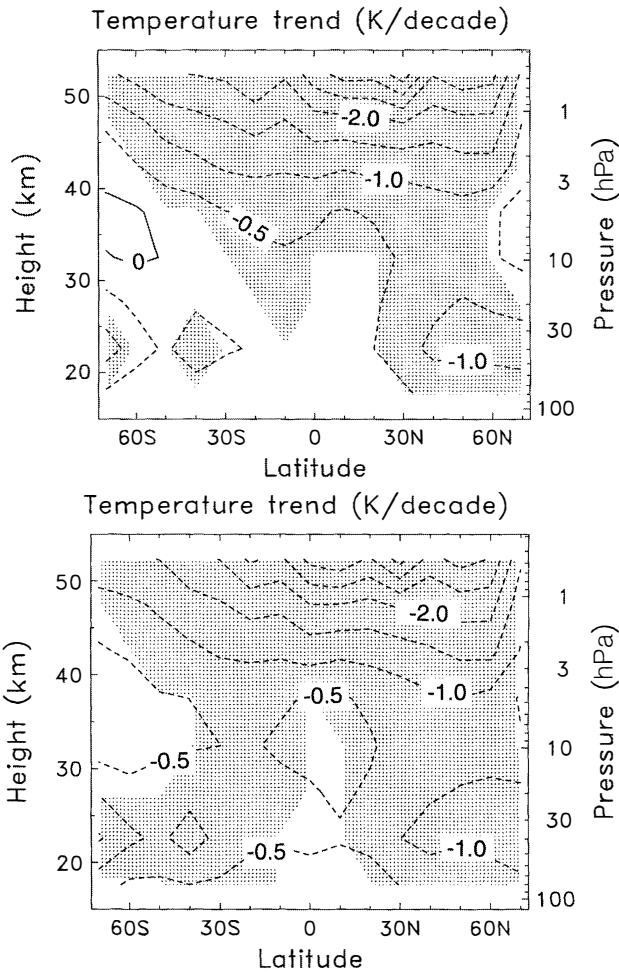


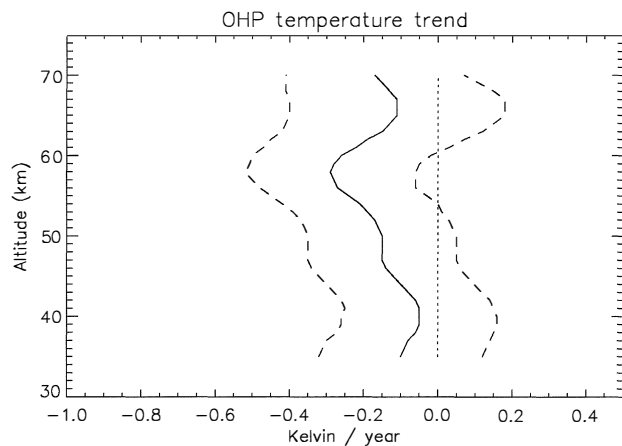
Figure 5-7. Zonal, annual-mean decadal temperature trends versus altitude for the 1979-1994 period, as obtained from the satellite (including MSU and SSU channels) retrievals, with volcanic periods included (top) and with volcanic periods omitted (bottom). Shaded area denotes significance at the 2-sigma level. (Figure assembled for this chapter in cooperation with the SPARC-Stratospheric Temperature Trends Assessment project.)

Figure 5-8. Annual-mean trend (K/yr) from the all-seasons lidar record at Haute Provence, France (44°N, 6°E), over the period 1979-1998. The 2-sigma uncertainties are also indicated. (Updated from Keckhut *et al.*, 1995.)

in any case, are not statistically significant over that height range). Note that the lidar trend for the 1979-1998 period (Figure 5-8) exhibits better agreement with the satellite trend than that in Figure 5-9c, indicating a sensitivity of the decadal trend to the end year considered. Generally speaking, there is an approximately uniform cooling of about 0.8 K/decade between ~50 and 5 hPa (~20-35 km), followed by increasing cooling with height (e.g., ~2.5 K/decade at 1 hPa (~50 km)). The analyzed datasets (Table 5-1), examined here for pressures > 10 hPa, are in approximate agreement with the instrument-based data. Figure 5A (see this chapter's Scientific Summary) illustrates the overall mean vertical profile of the trend and uncertainty at 45°N, taking into account all of the datasets and accounting for the uncertainties of the individual measurements (see also Table 5-6 for numerical values of the trend estimates and the uncertainty at the one-sigma level). The vertical profile of cooling, and especially the large upper stratospheric cooling, are consistent with the global plots in WMO (1990a, e.g., Figure 6.17; 1990b, e.g., Figure 2.4-5) constructed from shorter data records.

5.2.3.4 ROCKET DATA AND TRENDS COMPARISONS

Substantial portions of the three available rocket datasets (comprising data from U.S., Russian, and Japanese rocketsondes; see Table 5-2) have been either reanalyzed or updated since the review by Chanin (1993). Golitsyn *et al.* (1996) and Lysenko *et al.* (1997) updated the data from five different locations over the period 1964-1990 or 1964-1995. Golitsyn *et al.* (1996) conclude a statistically significant cooling from 25 to 75 km, except around 45 km (Figure 5-10a). Lysenko *et al.* (1997)



STRATOSPHERIC TEMPERATURE TRENDS

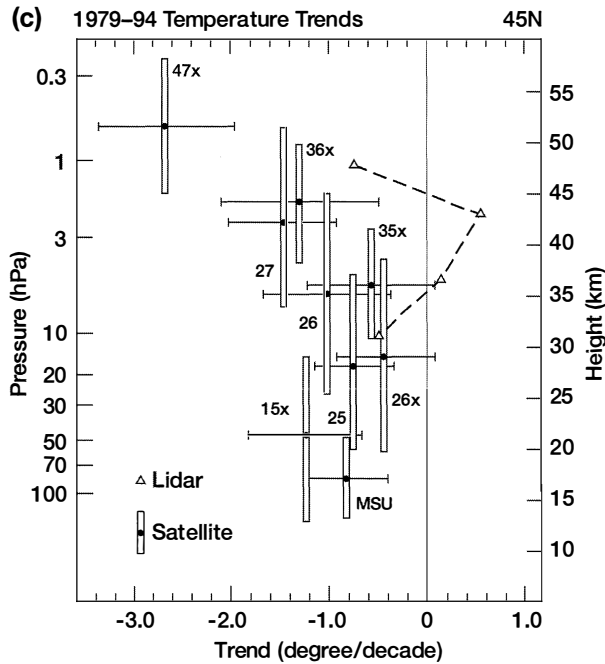
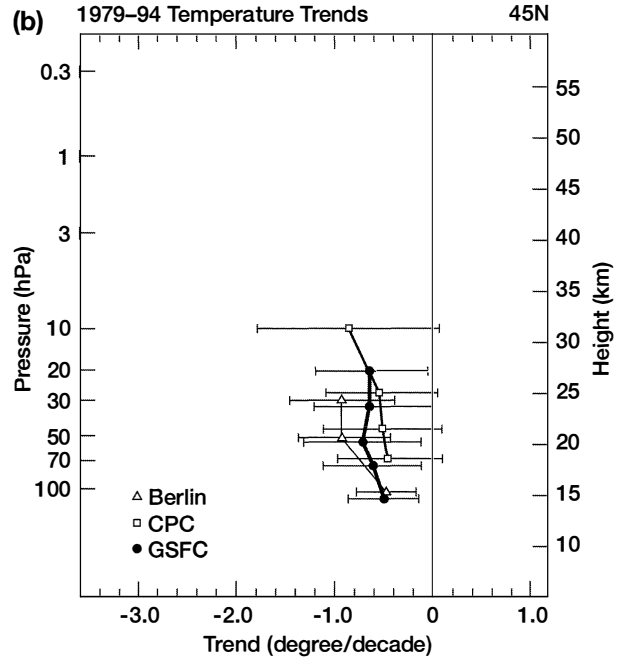
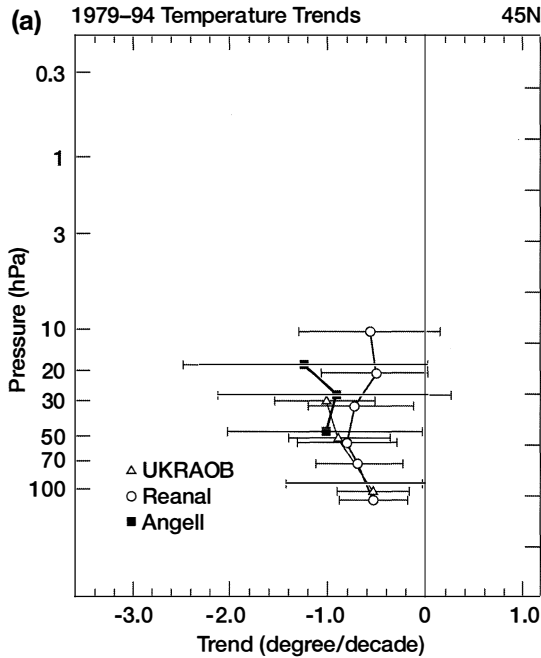


Figure 5-9. Vertical profiles of the zonal, annual-mean decadal stratospheric temperature trend (K/decade) over the 1979-1994 period at 45°N from different datasets (Table 5-1). Horizontal bars denote statistical significance at the 2-sigma level while vertical bars denote the approximate altitude range “sensed” by the MSU and by the different SSU satellite channels (see Figure 5-1). The uncertainty in the lidar trend estimate, which is almost as large as the plot scale employed, is not depicted here. (Figure assembled for this chapter in cooperation with the SPARC-Stratospheric Temperature Trends Assessment project.)

obtain a similar vertical profile of the trend for the individual rocketsonde sites (Figure 5-10b). They find a significant negative trend in the mesosphere particularly at the midlatitude sites.

Out of the 22 stations of the U.S. network, nine have provided data for more than 20 years. Some series have noticeable gaps that prevent them from being used

for trend determination. Independently, two groups have revisited the data: Keckhut *et al.* (1998) selected six low-latitude sites (8°S–28°N), and Dunkerton *et al.* (1998) selected five out of six of the low-latitude sites plus Wallops Islands (37°N). Both accounted for spurious jumps in the data by applying correction techniques.

Keckhut *et al.* (1998) found a significant cooling

Table 5-6. Weighted trend estimates and uncertainty at the 1-sigma level computed from the individual system estimates shown in Figure 5-9. The weighted trend estimates and the uncertainty at the 2-sigma level are illustrated in Figure 5A.

Altitude (km)	Trend (K/decade)	Uncertainty (1-sigma level)
15	-0.49	0.18
20	-0.84	0.18
25	-0.86	0.20
30	-0.80	0.29
35	-0.88	0.30
40	-1.23	0.33
45	-1.81	0.37
50	-2.55	0.40

between 1969 and 1993 of about 1-3 K/decade between 20 and 60 km (Figure 5-11a). A similar result is seen in the data available since 1970 from the single and still operational Japanese rocket station (Figure 5-11b, updated from Komuro, 1989). Dunkerton *et al.* (1998), using data from 1962 to 1991, infer a downward trend of -1.7 K/decade for the altitude range 29-55 km; they also obtain a solar-induced variation of ~1 K in amplitude. It should be noted that the amplitude of the lower-

mesosphere cooling observed in the middle and high latitudes from the Russian rockets (between 3 and 10 K/decade) is somewhat larger than from the U.S. dataset. Nevertheless, all four rocketsonde analyses shown in Figures 5-10 and 5-11, together with the lidar trend at 44°N (Figure 5-8), are consistent in yielding trends of ~-1-2 K/decade between about 30 and 50 km.

Figure 5-12 compares the vertical profiles of trends over the 1979-1994 period from various datasets at

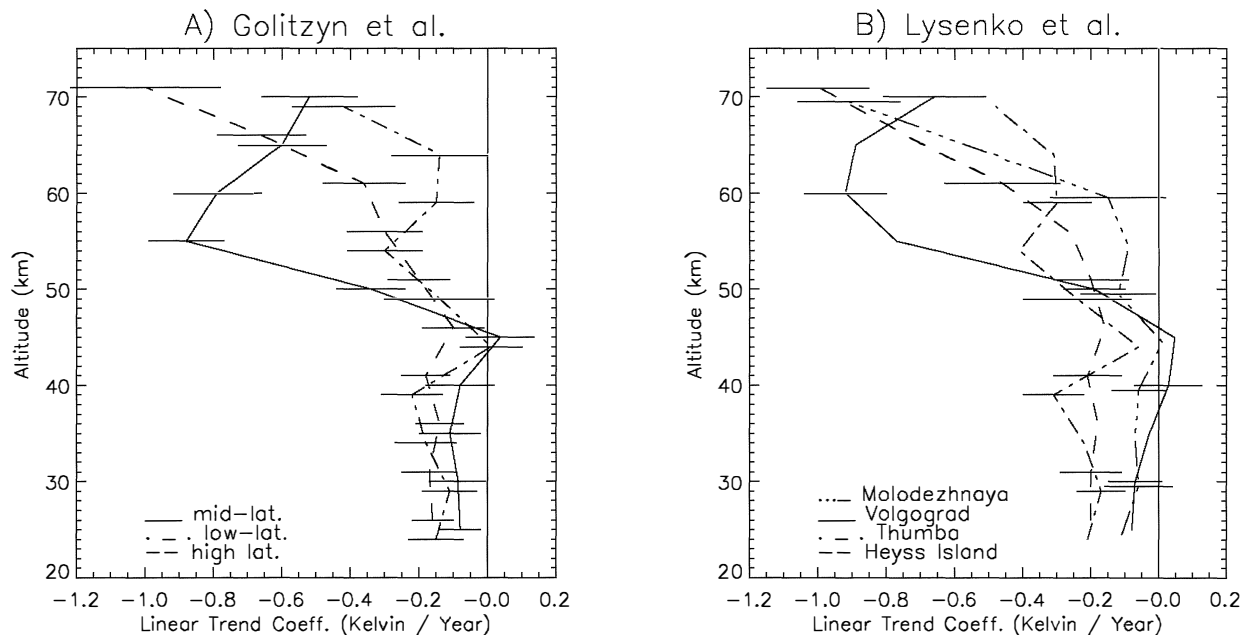


Figure 5-10. Panel A: Trends (K/yr) based on the Former Soviet Union (FSU) rockets (25-70 km) since the mid-1960s (see Table 5-2). (Adapted from Golitsyn *et al.*, 1996.) Panel B: Trends (K/yr) at specific sites based on the same FSU rocket dataset. (Adapted from Lysenko *et al.*, 1997.)

STRATOSPHERIC TEMPERATURE TRENDS

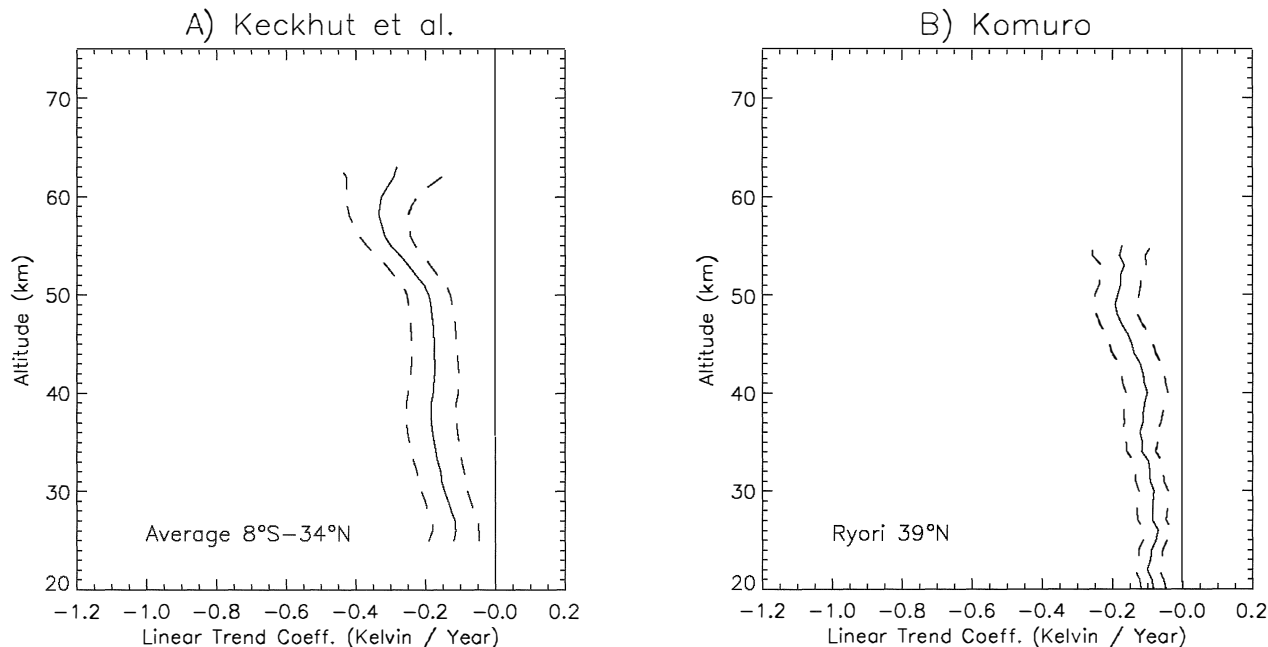


Figure 5-11. Panel A: Trend (K/yr) compiled from U.S. rocket sites in the 8°S–34°N belt (see Table 5-2) over the period 1969–1993 (Keckhut *et al.*, 1998). Panel B: Trend (K/yr) from the Japanese rocket station at Ryori over the period 1970–present. The 2-sigma uncertainties are also indicated. (Updated from Komuro, 1989.)

~30°N, including the rocket stations at 28°N (Cape Kennedy) and 34°N (Point Mugu). As at 45°N (Figure 5-9), almost all the datasets agree in the sign (though not in the precise magnitude) of temperature change below about 20 hPa (~27 km). Above 10 hPa (~30 km), both satellite and rocket trends yield increasing cooling with altitude, with a smaller value at the 28°N rocket site. At 1 hPa, there is considerable divergence in the magnitudes of the two rocket trends. The rocket trends are derived from time series at individual locations, which may explain their greater uncertainty relative to the zonal-mean satellite trends. In a general sense, the vertical profile of the trend follows a pattern similar to that at 45°N (Figure 5-9).

5.2.4 Latitude-Season Trends

The monthly, zonal-mean trends in the lower stratosphere are considered next. Figure 5-13 illustrates the lower stratospheric temperature trends derived from MSU data over the period January 1979–May 1998. This represents an update from the 1994 Assessment (WMO, 1995). Substantial negative trends are observed in the

midlatitudes of both hemispheres during summer (-0.5 K/decade), and in springtime polar regions (up to -3 to -4 K/decade). There is a broad domain of statistical significance in the cooling at the midlatitudes; in the NH, this occurs from ~June through October, whereas in the SH, it occurs from about mid-October to April. Little or no cooling is observed in the tropics in Figure 5-13, although, as already stated, the MSU measurements in the tropics originate from a broad layer of 50–150 hPa and thus implicitly include a trend signal from the upper troposphere (the weighting function maximum is near the tropical tropopause; Figure 5-1). Thus, the tropical MSU result may not be indicative of a purely lower stratospheric trend (Section 5.2.3.2; Figure 5-5). There is some symmetry evident in the observed trends in the two hemispheres, although most of the regions have values not significantly different from zero. Comparison with the MSU trends derived from data for 1979–1991 (Randel and Cobb, 1994; see Figure 8-11 in WMO, 1995) shows similar patterns in the SH, but substantial differences in the NH. The 1979–1991 NH trends peaked in winter midlatitudes, and the springtime polar cooling was not statistically significant. Addition of data through

STRATOSPHERIC TEMPERATURE TRENDS

mid-1998 diminishes the northern midlatitude winter trends and increases those over the pole in spring. Thus, owing to a high degree of interannual variability, especially during polar spring, the MSU trend estimates are dependent on the choice of the end year.

The larger springtime polar trends are strongly influenced by the occurrence of several relatively cold

years since about 1990, as shown in Figure 5-14 (top panel) for 80°N using the NCEP reanalyzed data and MSU observations. Note that the NCEP reanalyzed data have not been adjusted for the discontinuities due to the switchover to satellite temperature retrievals (1976 for SH and 1979 for NH). This leads to a discontinuity in the analyzed temperatures for those years, associated with

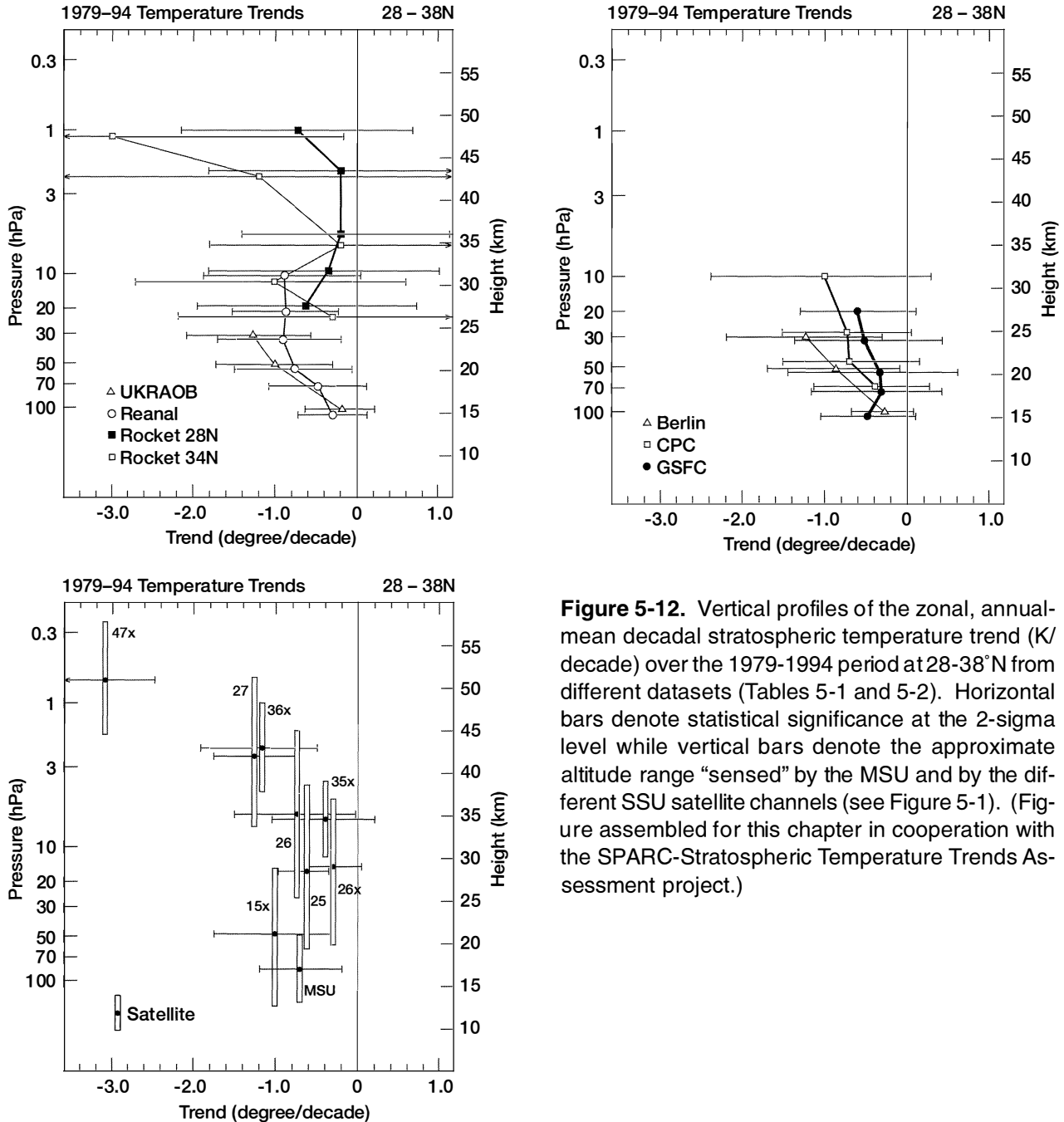


Figure 5-12. Vertical profiles of the zonal, annual-mean decadal stratospheric temperature trend (K/decade) over the 1979-1994 period at 28-38°N from different datasets (Tables 5-1 and 5-2). Horizontal bars denote statistical significance at the 2-sigma level while vertical bars denote the approximate altitude range “sensed” by the MSU and by the different SSU satellite channels (see Figure 5-1). (Figure assembled for this chapter in cooperation with the SPARC-Stratospheric Temperature Trends Assessment project.)

STRATOSPHERIC TEMPERATURE TRENDS

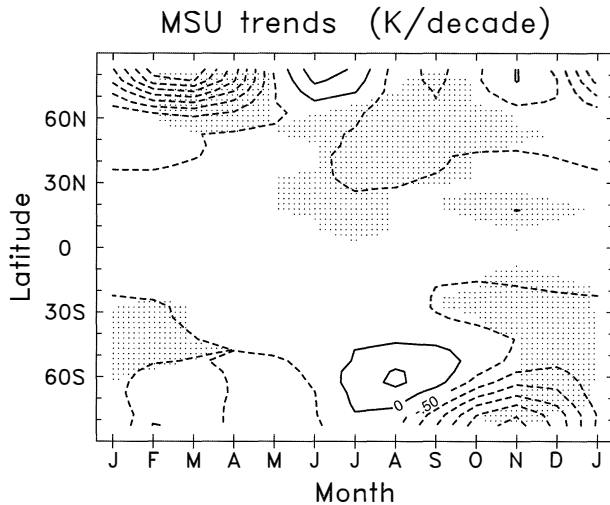


Figure 5-13. Latitude-time section of trends in MSU Channel 4 temperature over January 1979-May 1998. Dashed lines indicate cooling trends. The contour interval is 0.5 K/decade, and shading indicates the trends are significant at the 5% level. (Updated from Randel and Cobb, 1994.)

the model's systematic error. Naujokat and Pawson (1996) also noted the relatively cold 1994/95 and 1995/96 northern polar winters. The 1990s-averaged temperature in March is lower than that for the 1980s. Manney *et al.* (1996) suggest that an unusual circulation pattern (low planetary wave forcing and an intense polar vortex) was primarily responsible for this feature. In particular, March 1997 was very cold, about 18 K below the 1980-1989 decadal average. Indeed, the monthly-mean 30-hPa temperature over the pole in March 1997 may have been one of the coldest years since 1966 ("Monthly Report on Climate System, 1997" by Japan Meteorological Agency). Newman *et al.* (1997) indicate that this coincided with the occurrence of the lowest total ozone amount in the Northern Hemisphere for this season. The extreme low temperatures in March 1997 appear to be associated with record-low planetary wave activity (Coy *et al.*, 1997). There are suggestions that the observed Arctic polar stratospheric conditions in recent years may be linked to changes in tropospheric circulation (see Chapter 12). It is not certain whether these are secular trends or whether they are the consequence of a decadal-scale variability in the climate system. With regard to the frequency of major sudden stratospheric warmings, Labitzke and van Loon (1992) note that, before 1992, the largest lapse of time between

two major warmings was about 4 years. In comparison, no major warming appears to have occurred between 1991 and 1997, i.e., over seven winters. This is broadly consistent with the sense of the temperature trend in the 1990s up to 1997.

In the Antarctic, analyses of long-term records of radiosonde data continue to reveal substantial cooling trends in spring, further endorsing the early study of Newman and Randel (1988). This cooling trend is closely linked to springtime ozone depletion (Angell, 1986; Chubachi, 1986; Trenberth and Olson, 1989; Jones and Shanklin, 1995; Butchart and Austin, 1996). This springtime cooling is an obviously large feature of the MSU temperature trends shown in Figure 5-13. Figure 5-14 (bottom) shows the time series of 100-hPa temperatures in November over Halley Bay, derived from radiosonde data, together with time series from the NCEP reanalysis interpolated to Halley Bay. Both these records reveal a decadal-scale change in temperature beginning in about the early 1980s, together with significant year-to-year variability (see also Chapter 4). The timing of the change in the Antarctic may be compared with that at 80°N (March) around 1990, as illustrated in the top panel of Figure 5-14. It is notable that temperatures in NH springtime polar regions indicate a strong cooling in recent years and an enhancement above natural variability (also, compare Figure 5-13 with Figure 8-11 of WMO, 1995) that is reminiscent of that observed in the Antarctic about a decade ago.

The structure of the decadal-scale temperature change over Antarctica as a function of altitude and month is shown in Figure 5-15, calculated as the difference in decade means (1986-1995 minus 1970-1979), and averaged over seven radiosonde stations (Randel and Wu, 1998). These data show a significant cooling (of ~6 K) in the lower stratosphere in spring (October-December). Significant cooling persists through austral summer (March), while no significant temperature changes are found during winter. These data also show a statistically significant warming trend (3 K or more) at the uppermost data level (30 hPa; 24 km) during spring.

Kokin and Lysenko (1994) have analyzed the seasonal trends in the middle and upper stratosphere from their data for five rocketsonde stations for the 1972-1990 period. Generally, the cooling is evident almost throughout the year at all sites, but there are exceptions. Figure 5-16 indicates a significant positive trend during spring above Molodezhnaya (at ~35 km) and during

winter above Volgograd and Balkhash (at ~40 km). The warming feature for Molodezhnaya is consistent with the springtime warming inferred for lower altitudes in the Antarctic by Randel (1988), and with that shown in Figure 5-15. The warming is located above a domain of cooling in both Figures 5-15 and 5-16. It is interesting that such an effect also takes place during the northern winter over the Volgograd and Balkhash locations.

5.2.5 Uncertainties in Trends Estimated from Observations

Determining stratospheric temperature trends from long-term observations is complicated by the presence of additional, non-trend variability in the data. Two types of phenomena contribute to the uncertainty in trend estimates. The first is true atmospheric variability that is not trend-like in nature. Major sources of such variability include the (quasi-) periodic signals associated with the annual cycle, the quasi-biennial oscillation (QBO), the solar cycle, and the El Niño-Southern Oscillation (ENSO). In addition, stratospheric temperatures vary in response to episodic injections of volcanic aerosols. To first approximation, these atmospheric phenomena have negligible effects on the long-term temperature trend because they are periodic or of relatively short duration. Nevertheless, because current data records are only a few decades long, at most, these phenomena may appear to enhance or reduce an underlying trend. At a minimum, the additional temperature variability associated with these signals reduces the statistical confidence with which long-term trends can be identified. Whereas periodic signals can be removed, the effects of sporadic events are more difficult to model and remove. Furthermore, there may be long-term trends in these cycles and forcings that confound the analysis. A second source of uncertainty is due to spurious signals in the time series that are the result of changes in methods of observation rather than changes in the atmosphere. The problem of detecting

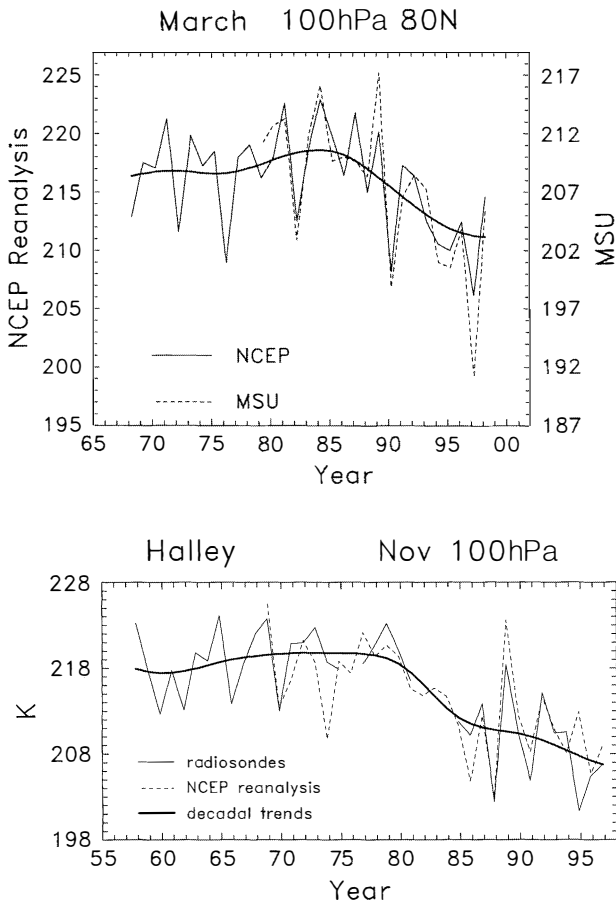


Figure 5-14. Top panel: Time series of 100-hPa zonal-mean temperatures at 80°N in March from NCEP reanalyses (solid lines), together with data from MSU. The smooth curve through the reanalysis data indicates the decadal-scale variation. Bottom panel: Time series of 100-hPa temperature in November at Halley Bay, Antarctica, from radiosonde data (solid lines) and NCEP reanalyses (dashed lines). The smooth curve through radiosonde data indicates the decadal-scale variation. (Randel and Wu, 1998.)

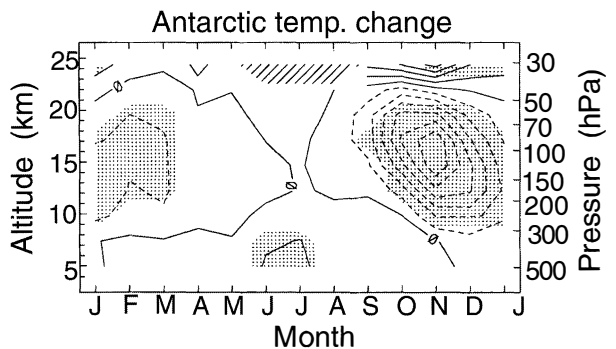


Figure 5-15. Altitude-time section of temperature differences over Antarctica, 1986-1995 minus 1970-1979, derived from an average of seven radiosonde stations. Dashed lines indicate cooling trends. The contour interval is 1 K. Shading denotes that the temperature differences are significantly different from natural variability. (Randel and Wu, 1998.)

STRATOSPHERIC TEMPERATURE TRENDS

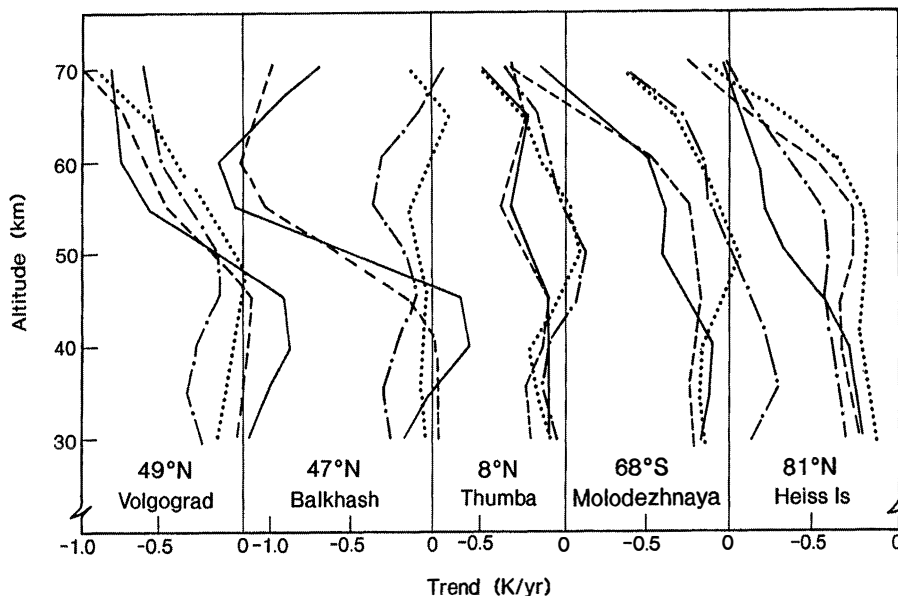


Figure 5-16. Seasonal rocketsonde trends (in K/yr), using Former Soviet Union rocket data from 1972 to 1990 at five sites (see Table 5-2), for winter (solid line), spring (dot-dash line), summer (dotted line), and autumn (dashed line). (Adapted from Kokin and Lysenko, 1994.)

temperature trends in the presence of changes in the bias characteristics of the observations is receiving increased attention (Christy, 1995; Santer *et al.*, 1998). It seems likely that over the next few years, better methods will be employed to quantify and reduce the uncertainty in stratospheric temperature trend estimates attributable to these spurious signals.

5.2.5.1 UNCERTAINTIES ASSOCIATED WITH RADIOSONDE DATA

Although most radiosonde analyses show cooling of the lower stratosphere in recent decades, it is important to recognize that they all rely on subsets of the same basic dataset, the global observing system upper-air network. This network is fundamentally a meteorological one, not a climate monitoring network, not a reference network for satellite observations, and not a network for detection of stratospheric change. When the radiosonde data are used for temperature trends analyses, any difficulties that plague the radiosonde network will also affect the analyses that use those data.

Karl *et al.* (1995) and Christy (1995) have reviewed some of the problems associated with using radiosonde data for the detection of atmospheric temperature trends. These fall into two categories: the uneven spatial distribution of the observations, and temporal discontinuities in station records.

The radiosonde network is predominantly a Northern Hemisphere, midlatitude land network. About half the stations are in the 30-60°N latitude band, and less than 20% are in the Southern Hemisphere (Oort and Liu, 1993). Moreover, the uneven distribution of stations is worse for stratospheric data than for lower tropospheric data, because low-latitude and Southern Hemisphere soundings have a higher probability of taking only one observation daily (other stations make two, and many formerly made four) and because the soundings more often terminate at lower altitudes (Oort and Liu, 1993). Estimates of layer-mean trends, and comparisons of trends at different levels, are less meaningful when data at the top of the layer are fewer than at the bottom.

For trend detection, the temporal homogeneity of the data is the key. As discussed by Parker (1985), Gaffen (1994), Finger *et al.* (1993), and Parker and Cox (1995), numerous changes in operational methods have led to discontinuities in the bias characteristics of upper-air temperature observations, which are particularly severe in the lower stratosphere (Gaffen, 1994). Because radiosondes are essentially expendable probes (although some are recovered and reconditioned), changing methods is much easier than, for example, in surface observations at fixed locations. Effects on data have been shown for changes in instrument manufacturer and replacement of old models with newer ones from the same

manufacturer (Parker, 1985; Gaffen, 1994), changes in time of observation (Elliott and Gaffen, 1991; Zhai and Eskridge, 1996), changes in the lag characteristics of the temperature sensors (Parker, 1985; Huovila and Tuominen, 1990), and even changes in the length of the suspension cord connecting the radiosonde balloon with the instrument package (Suzuki and Asahi, 1978; Gaffen, 1994) and in balloon type (Parker and Cox, 1995).

Daytime stratospheric temperature data in the early years of radiosonde operations were particularly affected by errors due to solar radiation, and substantial changes in both data correction methods (e.g., Scrase, 1956; Teweles and Finger, 1960) and instrument design have been made to address the problem. In general, the result has been a reduction in a high bias over time, leading to an artificial “cooling” in the data (Gaffen, 1994). The example in Figure 5-17, monthly-mean 100-hPa temperatures at Tahiti, shows that a 1976 change from one model of the French Mesural radiosonde to another, each with different temperature sensors, was associated with an artificial temperature drop of several degrees. Given estimated temperature trends on the order of tenths of a degree Kelvin per decade, such inhomogeneities introduce substantial uncertainty regarding the magnitude of the trends in the lower stratosphere. Furthermore,

Luers (1990) has demonstrated that daytime radiosonde temperature errors can exceed 1 K at altitudes above 20 km (50 hPa) and that the magnitude of the error is a strong function of the temperature and radiative environment, which suggests that, as the atmosphere changes, so will the nature of the measurement errors.

A few investigators have attempted to adjust radiosonde temperature time series to account for “change-points,” or level shifts like the one illustrated in Figure 5-17. Miller *et al.* (1992), using data from 1970-1986, made adjustments to lower stratospheric data at four of 62 stations in Angell’s (1988) network on the basis of a statistical regression model that includes a level shift term. However, Gaffen (1994) concluded that, over a longer period, many more of the Angell stations showed data inhomogeneities. Parker *et al.* (1997) have made adjustments to temperature data from Australia and New Zealand for the period 1979-1995 by using MSU data as a reference time series, and station histories (Gaffen, 1994) to identify potential change-points. The adjustments (of earlier data relative to 1995 data) ranged from 0 to -3.3 K and reduced the estimated zonal-mean temperature change between the periods 1965-1974 and 1987-1996 at about 30°S (30 hPa) from -2.5 K/decade to about -1.25 K/decade (Parker *et al.*, 1997).

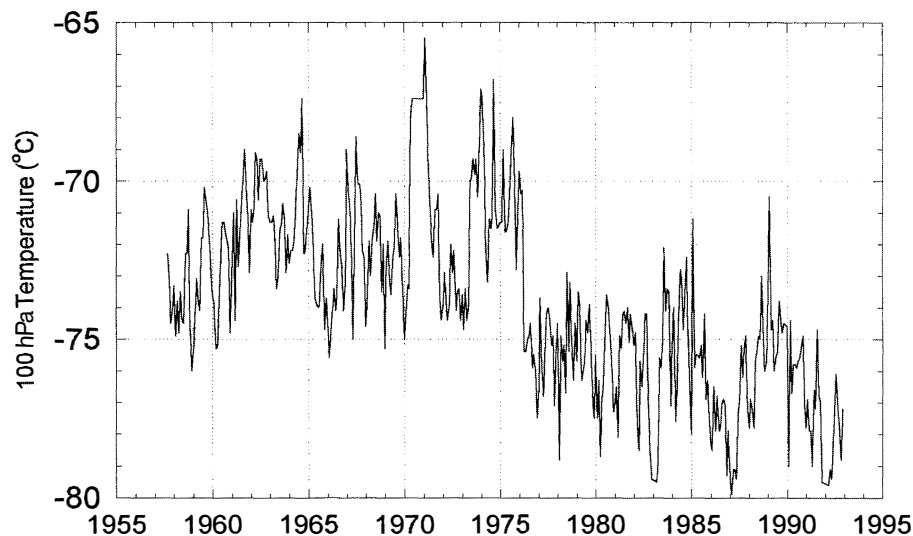


Figure 5-17. Monthly-mean 100-hPa raw temperatures measured by radiosondes at Tahiti. Several instrument changes occurred during this data period, but the 1976 change from the Mesural FMO 1943B, with a bimetal temperature sensor, to the Mesural FMO 1944C, with a thermistor, had the most obvious effect on the time series. (Gaffen, 1996; see also Gaffen, 1994.)

STRATOSPHERIC TEMPERATURE TRENDS

5.2.5.2 UNCERTAINTIES ASSOCIATED WITH ANALYSES OF SSU SATELLITE DATA

The stratospheric temperature analyses from NCEP's Climate Prediction Center (CPC) are an operational product, derived using a combination of satellite and radiosonde temperature measurements. Radiosonde data contribute to the analyses in the NH over the 70-10 hPa levels; satellite data alone are used in the tropics and SH, and over the entire globe above 10 hPa (Gelman *et al.*, 1986; Section 5.2.1). The satellite temperature retrievals are from the TOVS instruments, which have been operational since late 1978. A series of TOVS instruments have been put into orbit aboard a succession of operational satellites; these instruments do not yield identical radiance measurements for a variety of reasons, and derived temperatures may change substantially when a new instrument is introduced (Nash and Forrester, 1986). Finger *et al.* (1993) have compared the operationally derived temperatures with co-located rocketsonde and lidar observations, and find systematic biases of order $\pm(3$ to $6)$ K in the upper stratosphere (due primarily to the low vertical resolution of TOVS). These biases furthermore change with the introduction of new operational satellites, and Finger *et al.* (1993) provide a set of recommended corrections to the temperature data (dependent on the particular satellite instrument for each time period), which have been used by CPC.

In spite of the application of the adjustments recommended by Finger *et al.* (1993), time series of temperature anomalies from the CPC analyses still exhibit significant discontinuity near the times of satellite transitions. Figure 5-18 shows deseasonalized CPC temperature anomalies over the equator at 1 hPa, together with a time series of equatorial anomalies from the overlap-adjusted (i.e., accounting for the discontinuity in satellites) SSU Channel 27 data (whose weighting function peaks near 1.5 hPa; Figure 5-1). These time series show very different characteristics, with apparent discontinuity or "jumps" in the CPC data that are coincident with satellite changes. Two particularly large changes are seen in Figure 5-18 in mid-1984 and late 1988; the specific nature of these discontinuities depends on latitude and altitude. Overall, the presence of such discontinuities in the CPC data limits their reliability for robust estimates of upper stratospheric trends (as in, say, Figure 5-9) and is even problematic for the determination of interannual variability. The overlap-adjusted SSU data (see Figure

5-2) used in Figures 5-7, 5-9, and 5-12 do not exhibit such obvious problems.

5.2.5.3 UNCERTAINTIES IN SATELLITE-RADIOSONDE TREND INTERCOMPARISONS

A distinct advantage of the satellite instruments over in situ ones is their globally extensive coverage. However, as already mentioned, this is tempered by the fact that the signals that they receive originate from a broad range of altitudes (Figure 5-1). This is in contrast to the specific altitudes of measurements in the case of the ground-based instruments located at specific sites. This feature of the satellite trends complicates the interpretation for any particular vertical region of the atmosphere and, more particularly, hampers a rigorous comparison with, say, the radiosonde trends (see Section 5.2.3.2). As an example, consider the problem of the lower stratospheric temperature trends. The MSU's Channel 4 senses the entire extent of the lower part of the stratosphere, and even the upper troposphere at low latitudes. This poses problems in the precise intercomparison of currently available satellite-based trends with those from ground-based instruments. In the tropics, approximately half of the signal originates from the upper troposphere, leading to a potential misinterpretation of the actual lower stratospheric temperature trend based on MSU data alone. This problem can become acute particularly if the tropical upper troposphere and lower stratosphere have temperature trends of opposite signs. A similar comment also applies to the comparison with the stratosphere trends from SSU measurements (Figure 5-1). Further, because of the areal coverage of the low latitudes, the global means from satellite data and those from the in situ instruments may be comparable only after appropriate adjustments are made for the differential sampling by the two kinds of instruments. Therefore, caution must be exercised in the interpretation of satellite-based trends vis-à-vis radiosonde and other ground-based instruments. Besides, satellite data interpretations also have to cope with problems involving temporal discontinuity, instrument calibration, and orbit drift.

5.2.5.4 UNCERTAINTIES ASSOCIATED WITH ROCKET DATA

The rocket data are very useful because they were the only observations of the 30-80 km region before the lidars started operating. However, determining

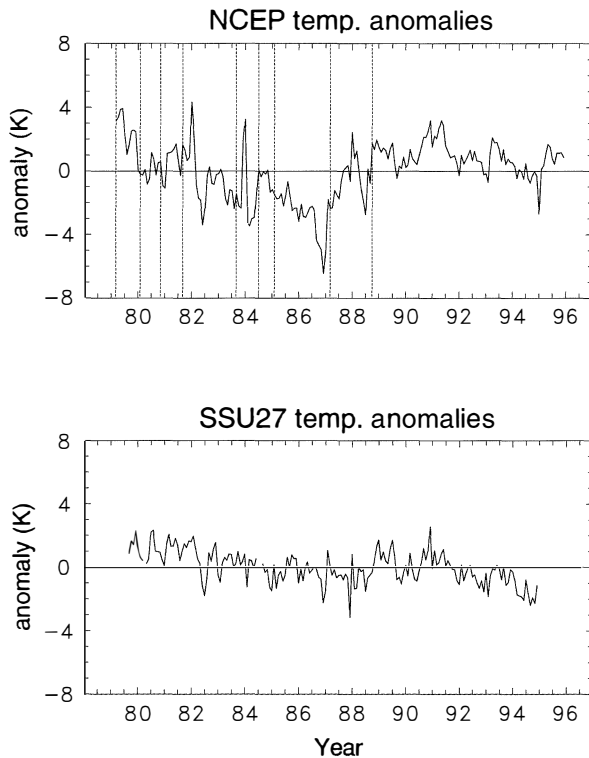


Figure 5-18. Time series of deseasonalized temperature anomalies at the equator for NCEP data at 1 hPa (top panel) and SSU 27 data (bottom panel). Vertical dashed lines in the top panel indicate changes in the operational satellites. Refer to Figures 5-1 and 5-2 concerning SSU 27.

quantitative trends from rocket data is complicated by both physical and measurement issues. A first difficulty with the rocket data is that there have been instrumental changes and the measurements come from different types of sensors (Arcasonde, datasonde, falling spheres). However, Dunkerton *et al.* (1998) have found that these changes were a less important source of error than previously suggested. The major source of error, and the origin of the observed spurious jumps, seems to be due to the change of corrections of the data to take into account aerodynamic heating. Most of the earlier analyses did not take full account of the changes and of the spurious jumps in the data that ensued from the above-mentioned difficulties. These points have been considered in depth by Keckhut *et al.* (1998) and Dunkerton *et al.* (1998), which resulted in a very limited number of U.S. stations that could be used for

determining trends. Yet another source of uncertainty is due to the different times of measurements, as the amplitude of tidal influence may not be negligible at these altitudes (± 2 K around 40-45 km according to Gille *et al.* (1991) and Keckhut *et al.* (1996)). This may explain the small error limit in the Ryori Japanese measurements (Figure 5-11 b), which are always conducted at the same local time. The factor related to the local measurement time was accounted for in the analysis of the U.S. rocket data by Keckhut *et al.* (1998). Because rocket data are available from only a few locations around the globe, there is a difficulty in ascertaining consistency of the trend and its significance when compared against zonal-mean satellite data.

5.2.5.5 UNCERTAINTIES ASSOCIATED WITH THE LIDAR RECORD

Temperatures obtained from Rayleigh lidar are affected by the presence of aerosols. Thus, a measure of the atmospheric scattering ratio is required after major volcanic eruptions. Otherwise, the temperatures are given in absolute value as a function of altitude from 30 km upward, without any need of external calibration. An accuracy of 1% is easily attained, with a principal limit for ascertaining the significance of a trend being the length of the available dataset. Using the actual measurements at the Haute Provence site, France, it was found that the establishment of a significance in the trend at the 95% level in the upper stratosphere required 20.5 years of data for summer and 35 years for winter trends. More years are required for the wintertime owing to the increased variability present in that season (Keckhut *et al.*, 1995). Of course, the length of a period needed to establish statistical significance also depends on the amplitude of the signal. Compared to rocket data, which are made at a specific time (even though it may not be the same local time for different sites), the lidar data can be made at any time during the night. This could constitute a potential source of uncertainty owing to tidal effects and may explain, in part, the large error limits observed in Figure 5-8. This could be improved by selecting data corresponding to the same local time.

5.2.6 Issues Concerning Variability

5.2.6.1 VOLCANIC AEROSOL INFLUENCES

A number of factors influence temperature trends in the stratosphere. Among the most significant as a

STRATOSPHERIC TEMPERATURE TRENDS

short-term phenomenon is the large build-up of stratospheric aerosols following volcanic eruptions (see Chapter 3). The SAGE extinction data and other satellite data (e.g., McCormick *et al.*, 1995) reveal a notable increase in stratospheric aerosol concentrations for 1-2 years following volcanic eruptions. Over the past two decades, such transient enhancements have come about due to volcanic eruptions of different intensities. Data from earlier ground-based observations reveal other episodes of volcanic loading of the stratosphere dating back to the 1960s. It is well understood that aerosols injected into the lower stratosphere by major volcanic eruptions result in a warming of this region of the atmosphere owing to enhanced absorption of solar radiation and the upwelling terrestrial infrared radiation (Pollack and Ackerman, 1983; WMO, 1990a; Labitzke and McCormick, 1992).

Three volcanoes stand out in particular since the 1960s, the period when widespread and routine radiosonde observations began. The three volcanoes of particular importance for climate variations have been Agung (Bali, Indonesia, 1963), El Chichón (Mexico, 1982), and Mt. Pinatubo (Philippines, 1991). In each one of these three cases, well-documented instrumental records indicate that the temperatures increased and stayed elevated until the aerosol concentrations were depleted completely (WMO, 1990a, 1995). All three eruptions produced somewhat similar warming characteristics (Angell, 1993), viz., a warming of the lower stratosphere (~15-25 km) centered in the tropics (~30°N-30°S), with a magnitude of 1-2 K (up to 3 K for Mt. Pinatubo). The warming diminishes in time, but anomalies are observed for approximately 2 years following each eruption (Figures 5-2 (SSU 15X) and 5-3). Because the volcanic effects are episodic and clearly identifiable, their direct effect on calculation of trends is minimal (the volcanic time periods simply need to be omitted prior to trend calculation), except as they possibly overlap with other potentially causal phenomena such as the solar cycle.

The magnitude and evolution of the transient warming agree reasonably well between the radiosonde and satellite datasets (Labitzke and McCormick, 1992; Christy and Drouilhet, 1994; Randel and Cobb, 1994; Figure 5-3). Relative to the analyses in WMO (1995), the temperature of the global-mean lower stratosphere has become progressively colder in both the satellite and radiosonde time series (Figures 5-2 (bottom panel) and 5-3).

In the upper stratosphere and mesospheric regions, an indirect effect could be expected from the change of circulation and/or the upwelling flux arising from the lower stratospheric heating. Such an indirect effect appears to have been observed after the Mt. Pinatubo eruption in the OHP lidar data. A cooling of 1.5 K in the upper stratosphere and a warming of 5 K at 60-80 km were detected (Keckhut *et al.*, 1995). Thus, a trend analysis for these regions also requires the omission or correction of post-volcanic eruption data (e.g., such a correction was applied to the data plotted in Figure 5-8 by adding a term proportional to the aerosol optical thickness in the analysis technique).

5.2.6.2 SOLAR CYCLE

The 11-year modulation of the ultraviolet (UV) solar flux, which is now well documented, is expected to, through photochemistry, influence stratospheric ozone and therefore stratospheric temperature. A number of investigators have attempted to identify a signature of the 11-year solar cycle in the temperature dataset. The solar proxy used in most studies is the 10.7-cm radio flux, which spans the longest period, even though more realistic proxies would be the He I line, Mg II line, or UV irradiance. However, several analyses using these different proxies justify the choice of the 10.7-cm flux (Donnelly *et al.*, 1986; Keckhut *et al.*, 1995).

Satellite data provide a global view of the signature due to solar variations, but the time series is relatively short. The overlap-adjusted SSU and MSU datasets (spanning 1979-1995) exhibit a coherent temperature variation approximately in phase with the solar cycle. Figure 5-19 shows the vertical-latitudinal structure of the solar signal (derived via regression onto the 10.7-cm solar flux time series) using the overlap-adjusted MSU and SSU data. Even though the dataset is limited to 17 years, this shows a statistically significant solar component of order 0.5-1 K throughout most of the low-latitude (30°N-30°S) stratosphere, with a maximum near 40 km. The spatial patterns show maxima in the tropics, with an approximate symmetry about the equator. A small solar response is observed in these data at the high latitudes. The 0.5-1 K solar signal seen in the Nash data is in reasonable agreement with results from the longer records of radiosondes/rocketsondes discussed below. At northern midlatitudes, the satellite-derived signature, which is not statistically significant, goes from slightly positive at ~17 km to slightly negative at ~25 km, with a

STRATOSPHERIC TEMPERATURE TRENDS

null value at 45-50 km. This is similar to the OHP lidar record (Keckhut *et al.*, 1995) and to the Volgograd rocket record (Kokin *et al.*, 1990). At high latitudes, although the satellite data uncertainty is large, there is a hint of a large positive response in the mesosphere, as is observed in the Heiss Island rocket data (Kokin *et al.*, 1990).

The longest time series are provided by radiosondes and rockets; even then, they barely cover at best four solar cycles. There is, thus, in general, some difficulty in establishing a firm relationship with the 11-year solar cycle. Labitzke and van Loon (1989) and van Loon and Labitzke (1990) use the Berlin meteorological analyses, beginning in 1964 and spanning the NH lower stratosphere, to isolate coherent temperature cycles in the subtropics in phase with the solar cycle. Labitzke and van Loon (1997) update their previous analysis and find a correlation of 0.7 with the 30-hPa geopotential height (which can be taken to imply a similar correlation with layer-mean temperature below this level). The maximum correlation occurs over the west Pacific near China. Using the NCEP reanalyzed global dataset, van Loon and Labitzke (1998) show a similar solar signal manifest in the Southern Hemisphere, with higher correlations in the tropical regions.

Angell (1991b) has used radiosonde and rocketsonde data to deduce tropical and NH midlatitude solar cycle variations of approximately 0.4 and 0.8 K in the lower and upper stratosphere, respectively (changes per 100 units of 10.7-cm solar flux, or approximately solar maximum minus solar minimum values). Dunkerton and Baldwin (1992) isolate a weak solar cycle in CPC temperatures in the NH winter lower stratosphere, using data from 1964-1991 (these analyses are based primarily on radiosonde data). Isolation of a solar cycle signal in CPC upper stratospheric temperature data beginning in 1979 is somewhat problematic, due to the spurious discontinuities introduced by satellite changes (see Figure 5-18; Section 5.2.5.2). This suggests that the solar cycle variations derived from these data (e.g., Kodera and Yamazaki, 1990; Hood *et al.*, 1993) should be treated with caution.

In their rocket data analysis, Dunkerton *et al.* (1998) found a 1.1-K response to the solar cycle for the integrated altitude range of 29-55 km (Figure 5-20). Kokin *et al.* (1990), Angell (1991b), and Mohanakumar (1995), using rocket data, and Keckhut *et al.* (1995), using lidar data, infer a clear solar signature in the mesosphere of +4 to 10 K per 100 units of 10.7-cm flux.

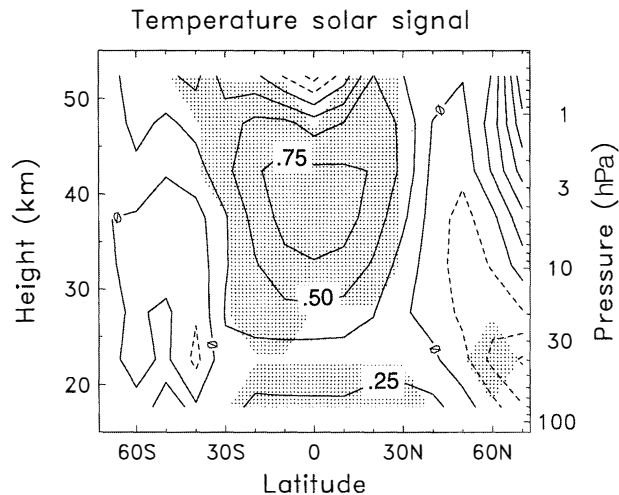


Figure 5-19. Latitude-altitude structure of the solar cycle signal in the satellite temperature (K) dataset, derived from regression analyses. Shaded areas show 95% confidence intervals for the regression estimates. (Figure assembled for this chapter in cooperation with the SPARC-Stratospheric Temperature Trends Assessment project.)

On the other hand, the results obtained in the upper stratosphere and around the stratopause are different in both amplitude and sign for the different sites, and are also variable with season.

From the records, it thus appears that the solar cycle signature in stratospheric temperatures need not be uniform and identical all over the globe and at all altitudes. This has been manifest in Labitzke and van Loon (1997) on the horizontal scale, as well as on the vertical scale in Chanin and Keckhut (1991) and may be attributable to the role of planetary waves. An additional point to note is that the solar-induced temperature changes need not occur at the same latitudes as any changes in ozone.

In the lower stratosphere, the effect of solar variations is found to have a relatively small effect on trend calculations for time series longer than 15 years such as those analyzed here. Regression estimates of trends neglecting a solar cycle term change by only ~10% (this sensitivity was determined by testing several of the time series analyzed here). Elsewhere in the stratosphere, the amplitude of the solar cycle signature has the potential to introduce a bias in trend estimates (especially if the number of cycles involved in the time series is small). The determination of the amplitude and structure of the

STRATOSPHERIC TEMPERATURE TRENDS

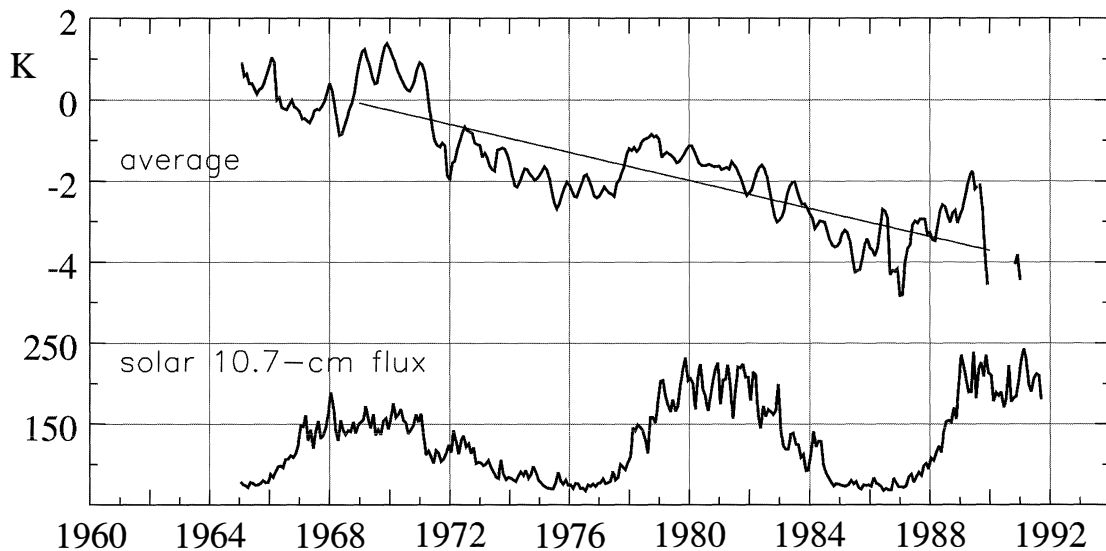


Figure 5-20. Mean temperature trend for six U.S. rocket stations, indicating the influence of the solar cycle (Dunkerton *et al.*, 1998).

solar cycle effect may be disturbed in the two recent cycles by the presence of two major volcanic eruptions spaced about 9 years apart, which is not different enough from 11 years, and so has the potential to be confused with the solar cycle.

5.2.6.3 QBO TEMPERATURE VARIATIONS

Interannual variability of zonal winds and temperature in the tropical stratosphere is dominated by an approximate 2-year periodicity: the quasi-biennial oscillation (QBO). The QBO is most often characterized by downward-propagating zonal wind reversals in the tropics (e.g., Naujokat, 1986; Reid, 1994), but the QBO is also prevalent in tropical temperatures (which are in thermal wind balance with the zonal winds). Aspects of the QBO in global stratospheric temperatures have been derived from radiosonde observations (Dunkerton and Delisi, 1985; Labitzke and van Loon, 1988; Angell, 1997) and satellite-derived datasets (Lait *et al.*, 1989; Randel and Cobb, 1994; Christy and Drouilhet, 1994). Randel *et al.* (1998) have used UKMO assimilated wind and temperature fields (Swinbank and O’Neill, 1994), together with overlap-adjusted SSU data, to isolate global patterns of the QBO. The results of these studies produce the following picture of the QBO in temperature:

1) Tropical QBO temperature anomalies maximize in the lower stratosphere (~20-27 km) over 10°N-10°S, with an

amplitude of $\pm(2$ to 4) K. There is a secondary maximum in the tropical upper stratosphere (~35-45 km) of similar magnitude, approximately out of phase with the lower stratosphere maxima. The structure in temperature is qualitatively similar to the two-cell structure observed in ozone (see Section 4.3 of Chapter 4 of this report).

2) There is a substantial midlatitude component of the QBO in temperature, maximizing over ~20-50° latitude and approximately out of phase with the tropical anomalies. The midlatitude patterns also exhibit maxima in the lower and upper stratosphere, which are vertically out of phase. An intriguing aspect of the midlatitude QBO is that it is seasonally synchronized, occurring only during winter-spring of the respective hemispheres; this produces a highly asymmetric temperature pattern at any given time.

3) There is also evidence for a coupling of the QBO with the lower stratosphere polar vortex in late winter-spring of each hemisphere (Holton and Tan, 1980, 1982; Lait *et al.*, 1989). The polar QBO temperatures are out of phase with those in the tropics. Observational evidence for the polar QBO is less statistically significant than that in the tropics or midlatitudes, at least partly because of the high level of “natural” interannual variability in polar vortex structure. Evidence of a quasi-biennial modulation of the Southern Hemisphere stratospheric polar vortex has been presented by Baldwin and

Dunkerton (1998b). An interesting question arising from recent studies (Salby *et al.*, 1997; Baldwin and Dunkerton, 1998a) is whether the interactions between the QBO and a so-called biennial oscillation could be a factor in the observed signature of the solar cycle.

Because the available satellite and radiosonde data records span many observed QBO cycles, it is possible to empirically model and isolate QBO variations in temperature with a good degree of confidence. The QBO has little effect on calculated trends, although trend significance levels are increased by accurate characterization of QBO variability.

5.2.6.4 PLANETARY WAVE EFFECTS

The trend, solar cycle, volcanic, and QBO variations account for the majority of observed interannual temperature variability in the tropics and low latitudes. Over middle and high latitudes there is a substantial amount of residual interannual variance, particularly during winter (e.g., Dunkerton and Baldwin, 1992). This additional variance is due to “natural” meteorological fluctuations, in particular the presence or absence of stratospheric warming (or planetary wave) events during a particular month (a large wave event corresponds to a warm month, and vice versa). This relatively high level of natural variability of the polar vortex means that somewhat larger natural or anthropogenic signals (e.g., trends due to changes in radiative species, or solar or QBO variations) are required for statistical significance.

5.2.6.5 EL NIÑO-SOUTHERN OSCILLATION (ENSO)

El Niño events are known to have a major impact on lower stratospheric temperature anomalies in the tropics, with a warming of the sea surface temperature (SST) and the increase in moist convection being accompanied by a cooling of the lower stratosphere (Pan and Oort, 1983; Reid, 1994). This inverse relationship between tropical surface and lower stratosphere temperatures is also manifest in the long-term record (Sun and Oort, 1995). Because tropical SSTs are known to have been increasing in recent decades (e.g., Graham, 1995), this suggests a potential contribution toward a tropical lower stratospheric cooling trend. It remains to be determined how the secular trends in the upper troposphere and lower stratosphere are quantitatively related to SST variations and trends, both in the tropics and extratropics.

5.2.7 Changes in Tropopause Height

Temperature changes in the upper troposphere and lower stratosphere may induce a change in the tropopause height, which may complicate the determination of temperature trends in the tropopause region. This was first suggested by Fortuin and Kelder (1996) in the context of radiative cooling caused by the trends in ozone and other greenhouse gases. To date, most models would be unable to represent such changes, as they are much smaller than the typical vertical spacing in models. Therefore, inferences have to rely entirely on the review of the available observations. Several results obtained at northern midlatitudes provide some indication of such changes, even though there is a lack of agreement on the amplitude of the effect.

An increase of the tropopause height by 150 ± 70 m (2-sigma) has been found at Hohenpeissenberg over the last 30 years (Steinbrecht *et al.*, 1998). This increase is correlated with the decrease in the ozone mixing ratio in the lower stratosphere and with a tropospheric warming at 5 km of 0.7 ± 0.3 K/decade (2-sigma) since 1967 (Figure 5-21). Bojkov and Fioletov (1997) indicate that the tropopause over Central Europe has increased by about 300 m over the last 20 years. For the tropics, Reid (G. Reid, NOAA, U.S., personal communication, 1998) has carried out a preliminary analysis of data from Truk (7.5°N , 151.8°E) for the period 1965-1994 and has found no detectable change in the temperature but a significant change in height, consistent with a warming of the troposphere (7.7 m/yr, or 230 m in 30 years). These results have yet to be extended to include other stations and have not yet accounted for ENSO and volcanic influences. On a global scale, Hoinka (1998a) has made a study of the tropopause surfaces based on European Centre for Medium-Range Weather Forecasts (ECMWF) reanalyses data, but for a shorter time period. His results indicate that the sign of the trend could vary depending on the latitude and longitude. A more recent work (Hoinka, 1998b) analyzes the trends for tropopause height, potential temperature, and water vapor mixing ratio. Clearly, this subject warrants more scrutiny on all spatial scales in order to quantify more rigorously the increase in the height of the tropopause, particularly over the past decade.

STRATOSPHERIC TEMPERATURE TRENDS

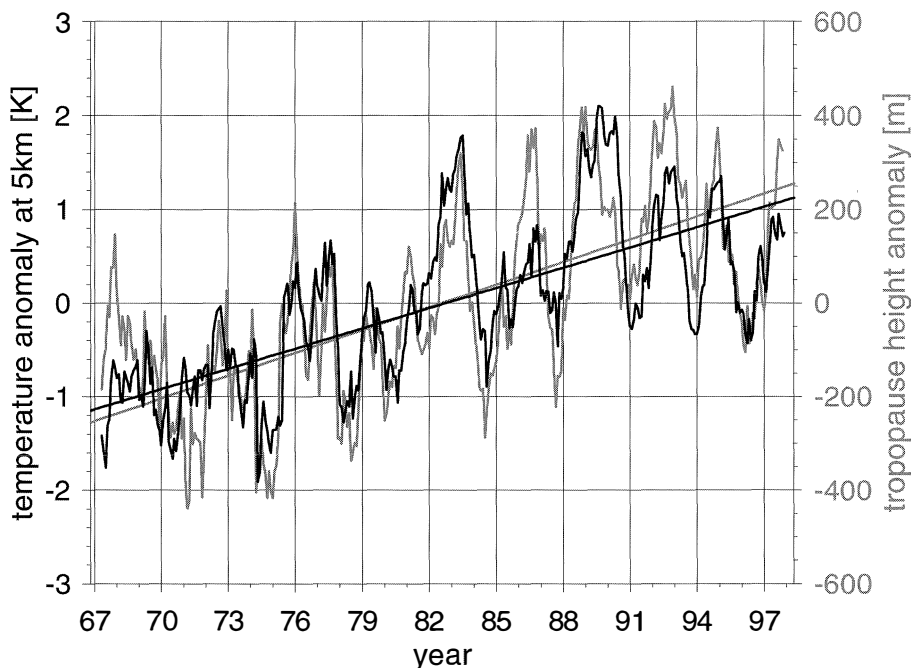


Figure 5-21. Change in tropopause height compared with the change in the 5-km temperature at Hohenpeissenberg. The 5-km temperature (dark line) shows a trend of 0.7 K/decade while the tropopause height (grey line) shows a trend of 150 m/decade (Steinbrecht *et al.*, 1998).

5.3 MODEL SIMULATIONS

5.3.1 Background

In this section, we discuss results from model investigations that have analyzed the effects of various natural and anthropogenic factors, notably changes in trace species, upon stratospheric temperature trends and variations. We focus in particular on the changes in the lower stratospheric region and also discuss the vertical profile of the modeled trends from the lower to upper stratosphere. Where possible and relevant, available model results are compared with observations.

Numerical models based on fundamental understanding of radiative, dynamical, and chemical processes constitute essential tools for understanding the effects of specific mechanisms on temperature trends and variability in the stratosphere, and for interpreting observed temperature changes in terms of specific mechanisms. The numerical models used thus far have attempted to include, to varying degrees, the relevant components of the climate system that could influence stratospheric temperatures. These include interactions among radiative, chemical, and dynamical processes.

The models also attempt to capture the important links between the stratosphere, troposphere, and mesosphere.

It is well recognized that the global, annual-mean thermal profile in the stratosphere represents a balance between solar radiative heating and longwave radiative cooling, involving mainly ozone, carbon dioxide, water vapor, methane, nitrous oxide, halocarbons, and aerosols (see Chapter 9 of Goody and Yung (1989) and references therein). In the context of the general global stratosphere, dynamical effects also become a factor in determining the thermal profile. Since the late 1950s, with increasing knowledge of trace species' concentration changes and their optical properties, numerical models have played a significant role in highlighting the potential roles of various constituents and the different mechanisms operating in the stratosphere. For example, WMO (1986, 1990a) concluded that changes in the concentrations of trace gases and aerosols could substantially perturb the radiative balance of the contemporary stratosphere and thereby affect its thermal state.

Early numerical models were developed as one-dimensional ones on the basis that the global, annual-mean stratosphere is in radiative equilibrium. Together with the assumption of a radiative-convective

equilibrium in the troposphere, this led to the so-called one-dimensional radiative-convective models (1-D RCMs), which have been widely employed to study effects due to trace-gas perturbations (WMO, 1986). The radiative-convective models represent the atmosphere as a single global-mean vertical column (Manabe and Wetherald, 1967; Ramanathan, 1981). The temperatures at the surface and in the troposphere are determined both by radiation and by some representation of the processes that determine the vertical advection of heat by the fluid motions (normally via a convection scheme). In the stratosphere, the thermal state determined is a balance between absorbed solar radiation, and absorbed and emitted thermal infrared radiation. Radiative-convective models can also include chemical processes to represent feedbacks between temperature and chemical constituents (e.g., Brühl and Crutzen, 1988).

A variation of the RCMs is the so-called Fixed Dynamical Heating (FDH) model (Fels and Kaplan, 1975; Ramanathan and Dickinson, 1979; Fels *et al.*, 1980). The contemporary FDH models (e.g., WMO, 1992) hold the tropospheric temperature, humidity, and cloud fields fixed and allow for changes in the stratospheric temperature in response to changes in radiatively active species. It is assumed that, in the unperturbed state, the radiative heating is exactly balanced by the dynamical heating at each height. If the concentration of a radiatively active constituent is altered, then the radiative heating field is altered. It is assumed that the dynamical heating remains unchanged and that the temperature field adjusts in response to the perturbation. In turn, this alters the radiative heating field such that it again exactly balances the dynamical field. The time scale for adjustment to a specific perturbation typically varies on the order of a few months in the lower stratosphere to a few days in the upper stratosphere.

The application of the RCM and FDH model concepts for understanding stratospheric temperature changes has evolved with time (see WMO, 1990b, 1992, 1995). Both types of models have been extensively used for gaining perspectives into the thermal effects due to the observed and projected changes in radiatively active trace gases. These simple models, though, have important limitations. In particular, the FDH models can only predict temperature changes at any location due to constituent changes occurring there; i.e., the response is entirely localized within that particular stratospheric column. As will be seen in Section 5.3.3.1, changes in

the circulation as a consequence of a radiative perturbation at any latitude can influence temperature changes at other latitudes. Hence, it should not be expected that FDH or FDH-like models can realistically simulate features such as the latitudinal and monthly variation of trends. Nonetheless, these simple models remain useful in revealing reasonable, first-order solutions of the problem.

There has been a steady progression from the simple RCMs and FDH models to the three-dimensional (3-D) general circulation model (GCM; see WMO (1986) for an early discussion of models used for studying the stratosphere), which seeks to represent the radiative-dynamical (and even chemical in some instances) interactions in their entirety. Such models have representations of radiative processes that may be less complete and accurate than in the 1-D models, but provide the best means of mimicking the physical processes in the real atmosphere. It may be noted that one useful aspect of the FDH simulations is that their comparison vis-à-vis a GCM simulation enables a quantitative distinction to be made between the radiative and radiative-dynamical responses of the stratosphere to a specific perturbation.

5.3.2 Well-Mixed Greenhouse Gases

While increases in well-mixed greenhouse gases (carbon dioxide (CO₂), methane (CH₄), nitrous oxide (N₂O), halocarbons) warm the Earth surface, their effects on the lower stratospheric temperature vary, primarily because of the location of the absorption bands of each of the species and the radiative characteristics of the atmosphere in those bands. The essential radiative processes are that, first, an increase in greenhouse gas concentration enhances the thermal infrared emissivity of a layer in the stratosphere; hence, if the radiation absorbed by this layer remains fixed and other factors remain the same, then, to achieve equilibrium, the same amount of energy has to be emitted at a lower temperature and the layer cools. Second, an increase in emissivity due to increased concentration also implies an increase in the thermal infrared absorptivity; a larger amount of the radiation emitted by the troposphere will be absorbed in the stratosphere, leading to a warming tendency. Note that the upwelling/downwelling radiation reaching the lower stratosphere is itself dependent on the infrared opacity and the thermal state of the troposphere/middle- and-upper stratosphere. The net result is a balance

STRATOSPHERIC TEMPERATURE TRENDS

involving these processes (Ramanathan *et al.*, 1985; Ramaswamy and Bowen, 1994; Pinnock *et al.*, 1995).

For carbon dioxide, the main 15- μm band is saturated over quite short distances. Hence the upwelling radiation reaching the lower stratosphere originates from the cold upper troposphere. When the CO_2 concentration is increased, the increase in absorbed radiation is quite small and the effect of the increased emission dominates, leading to a cooling at all heights in the stratosphere. For gases such as the chlorofluorocarbons (CFCs), their absorption bands are generally in the 8-13 μm "atmospheric window" (WMO, 1986); hence much of the upwelling radiation is originating from the warm lower troposphere. In this case the increase in the absorbed energy is generally greater than the increase in emitted energy and a warming of the lower stratosphere results (although there are exceptions to this case if the halocarbon absorption is in a region of already large atmospheric absorption; see Pinnock *et al.*, 1995). Methane and nitrous oxide are midway between these two regimes, so that an increase in concentration has little effect on the lower stratospheric temperature because the increased absorption and increased emission almost balance. In the upper stratosphere, increases in all well-mixed gases lead to a cooling because the increased emission effect becomes greater than that due to the increased absorption.

One significant consequence of this differing behavior concerns the common use of "equivalent CO_2 " in climate simulations. Equivalent CO_2 is the amount of CO_2 used in a model calculation that results in the same radiative forcing of the surface-troposphere system as a mixture of greenhouse gases (see, e.g., IPCC, 1995). Although the equivalence concept works reasonably well for tropospheric climate change (IPCC, 1995), it does not work well for stratospheric temperature changes because increases in different greenhouse gases cause different stratospheric temperature responses, thus requiring the consideration of each gas explicitly. In fact, some trace gases warm, not cool like CO_2 , the lower stratospheric region near the tropopause (WMO, 1986). Even if all gases were to cause an effect of the same sign in the stratosphere, an equivalence with respect to CO_2 that holds for the troposphere need not be true for the stratosphere. In general, the use of an equivalent CO_2 concentration, such as used for estimating tropospheric climate change, overestimates the actual stratospheric cooling by the non- CO_2 well-mixed greenhouse gases. For realistic mixtures of greenhouse gases, the strat-

ospheric cooling is found to be about half of that obtained using equivalent CO_2 (Wang *et al.*, 1991; Shine, 1993).

The mechanism by which temperatures change in the stratosphere as a result of constituent changes is twofold. First, the change in the constituent leads to a change in the radiative heating field, even if all other conditions are kept fixed. Second, in considering the response of the climate system, the time scale for the adjustment of stratospheric temperatures is less than about 100 days, which is much faster than the decadal (or multi-decadal) time-scale response of surface and lower tropospheric temperatures. This "fast" process of stratospheric temperature change is then modified as the troposphere comes into a new equilibrium with the forcing. Thus, for example, an increase in CO_2 leads to an initial cooling of the stratosphere. As the surface and troposphere warm up due to CO_2 increase, the increased emission from the surface-troposphere system contributes a warming tendency in the lower stratosphere. Forster *et al.* (1997) have shown that this process leads to a significant reduction of the initial cooling in the very lower stratosphere for CO_2 ; in the case of CFCs, it leads to a significant heating. When increases in all the well-mixed gases over the last century are considered in a 1-D RCM, the overall result for the lower stratosphere is one of an initial radiative cooling, arising due to increase in tropospheric opacity, which reduces the upwelling longwave flux reaching the stratosphere and its absorption there. There is also an increased emission from the stratosphere. The equilibrium result is a decrease in lower stratospheric temperatures, with an increased flux divergence of the downward longwave beam in the now colder lower stratosphere balancing the increase in the flux convergence of the upward beam due to tropospheric warming (Ramaswamy and Bowen, 1994). Thus, the actual temperature change in the lower stratosphere depends on the degree to which the surface-troposphere system equilibrates to the changes in the radiative constituents.

GCMs have been used to determine the changes in stratospheric climate due to changes in the well-mixed greenhouse gases. Fels *et al.* (1980) obtained a cooling of ~ 10 K at 50 km for a doubling of CO_2 . This study also found that FDH results for CO_2 doubling agreed reasonably well with the GCM simulations. Subsequently, other GCM experiments of a similar nature (e.g., Wang *et al.*, 1991; Rind *et al.*, 1990) also obtain a substantial cooling of the stratosphere. However, the

degree of cooling, especially in the polar stratospheres, is model dependent because of differences in the manner in which physical processes are parameterized in the models (Mahlman, 1992; Shindell *et al.*, 1998). GCMs that are used to determine changes in surface and tropospheric climates also simulate the stratospheric changes (e.g., those discussed in Chapter 8 of IPCC, 1996). However, several such models have a coarse vertical resolution in the stratosphere, which inhibits performing a reliable trends assessment using their results at those altitudes. Nonetheless, all models predict a general cooling of the stratosphere due to CO₂ increases. WMO (1990a) estimated a cooling of 0.2-0.3 K at 2 hPa and 0.15 K at 10 hPa between 1979/80 and 1985/86 due to CO₂ increases alone.

A number of 1-D radiative-photochemical model predictions of the cooling due to increased concentrations of greenhouse gases (CO₂, N₂O, CH₄, and the CFCs) were reviewed in WMO (1990a). These models included the effects of the temperature changes caused by increases in the well-mixed greenhouse gases upon the ozone concentrations. Our understanding of the chemistry at that time was such that the important feedbacks were deemed to occur in the upper stratosphere. Briefly, the features of these calculations were that peak coolings were estimated to occur between 40 and 50 km. Simulations for the period since 1960 indicated that the mean cooling rate was about 1.5 K/decade, for the period since 1940 it was about 1 K/decade, and for the period from 1850 it was about 0.4 K/decade. There was more spread in model results at 24 km, ranging from almost zero to -0.3 K/decade for the period since 1960.

Both 1-D RCMs (e.g., Ramanathan *et al.*, 1985) and 3-D GCMs (e.g., Wang *et al.*, 1991) indicate that the presence of the well-mixed non-CO₂ trace gases can be expected to yield a slight warming of the lower stratosphere. Ramaswamy *et al.* (1996) have compared the 50-100 hPa temperature change for different time periods for CO₂ alone, and for a realistic mixture of gases (Figure 5-22) using a 1-D RCM. For the period 1765-1990, the temperature change due to all gases is less than 50% of the effect due to CO₂ alone. For more recent periods, e.g., since ~1960, when the relative importance of other gases, and in particular that of the CFCs, has grown (Ramanathan *et al.*, 1985), the temperature change due to all well-mixed greenhouse gases is not only less than that due to CO₂ alone, but becomes quite small in absolute value. The overall cooling effect in the lower stratosphere due to increases in the well-mixed

greenhouse gases is to be contrasted with their warming effect on the surface.

The vertical profile of the computed temperature change in the stratosphere due to recent changes in the well-mixed gases is discussed in WMO (1992; see Figure 7-7 of that report). There is a general increase of the cooling with height. This is further exemplified by Forster and Shine (1997), who show that the FDH-computed increases in the well-mixed greenhouse gases over the decade of the 1980s would yield an increasing cooling with height at 40°N (~0.7 K/decade at 35 km; Figure 5-23). The FDH model of Ramaswamy *et al.* (1992) considered the well-mixed greenhouse gas increases over the 1979-1990 period. The model calculations yield an annual-mean cooling that increases with height between ~20 and 50 km and is fairly uniform throughout the globe (Figure 5-24), with a peak cooling of ~1 K/decade occurring in the tropics at ~50 km. This figure also illustrates that the combined effect of the well-mixed greenhouse gases is a slight but characteristic warming near the tropopause at low latitudes.

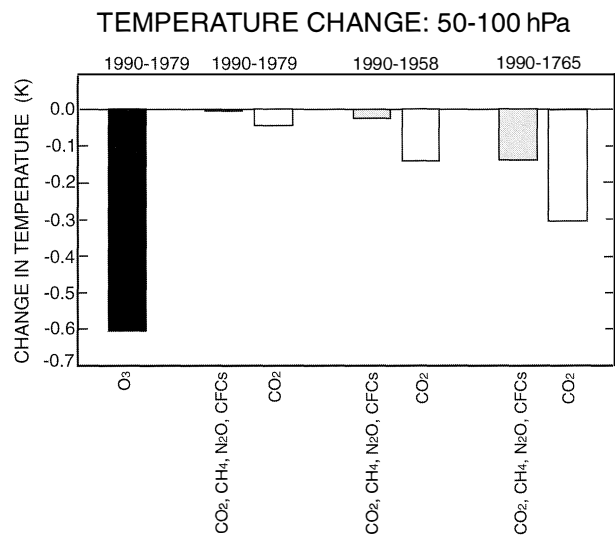


Figure 5-22. Computed global- and annual-mean temperature changes in the ~50-100 hPa (~16-21 km) lower stratospheric region. The result for the ozone depletion corresponds to the 1979 to 1990 losses and is computed using a GCM. The results for CO₂ alone, and for all the well-mixed greenhouse gases together (viz., CO₂, CH₄, N₂O, and CFCs) are computed using a 1-D RCM for three different periods. (Reprinted by permission from *Nature* (Ramaswamy *et al.*, *Nature*, 382, 616-618, 1996) Copyright (1996) Macmillan Magazines Ltd.)

STRATOSPHERIC TEMPERATURE TRENDS

5.3.3 Stratospheric Ozone

5.3.3.1 LOWER STRATOSPHERE

Over the past decade or so, much of the work on stratospheric temperature trends has focused on the effects due to lower stratospheric ozone change, following the realization of the large ozone loss trends in this region, as well as the accumulating evidence for substantial temperature changes in this region (WMO, 1990b, 1992, 1995). In particular, the large Antarctic springtime ozone losses were the first to be examined for their potential temperature effects. Subsequently, investigations have been extended to examine the changes initiated by ozone depletion in the global lower stratosphere.

As a general demonstration of the sensitivity of the global lower stratosphere to changes in ozone, Figure 5-25 shows the change in lower stratospheric and tropospheric temperatures when the entire ozone in the 70-250 hPa region is removed. Temperature decreases of up to about 4 K are obtained. Note that the region in the vicinity of the tropopause is most substantially affected, consistent with the known radiative sensitivity and large radiative damping time of this region (Fels, 1982; Kiehl and Solomon, 1986). A warming is seen above the cooling, which is in part due to more upwelling thermal infrared radiation reaching this region in the absence of ozone in the 70-250 hPa layer, and in part due to dynamical changes; these will be elaborated upon later in this section.

With regard to actual decadal trends, Miller *et al.* (1992) estimated a cooling of the lower stratosphere by about 0.3 K/decade over the 1970-1986 period, based on radiosonde observations. By performing a calculation of temperature changes using observed ozone trends, they inferred a substantial role due to ozone losses in the observed temperature trend. Because ozone changes vary greatly with latitude, there is a need to proceed beyond global means and perform model calculations that resolve the latitudinal variations. Locally, the stratosphere is not in radiative equilibrium, and the temperature is determined by both radiative and dynamical processes. However, by considering the stratosphere to be in a local radiative-dynamical equilibrium, with the dynamical heating rates fixed over some specific time scale (e.g., season), the FDH concept in effect has been extended to derive the local columnar temperature changes. Shine (1986) demonstrated that a large cooling would occur in

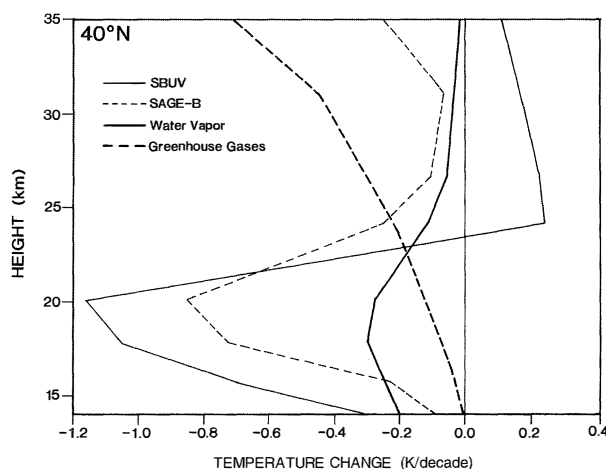


Figure 5-23. Vertical profile (~ 15 -35 km) of the FDH-computed annually averaged temperature change during the 1980s at 40°N due to changes in the concentrations of various stratospheric species. “Greenhouse gases” denotes well-mixed greenhouse gases; the “SBUV” ozone refers to a calculation that considers the column loss using SBUV satellite trends; the “SAGE-B” calculation uses the vertical profile of ozone change observed by the SAGE satellite; “water vapor” refers to the decadal change in water vapor reported by Oltmans and Hofmann (1995). (Adapted from Forster and Shine, 1997.)

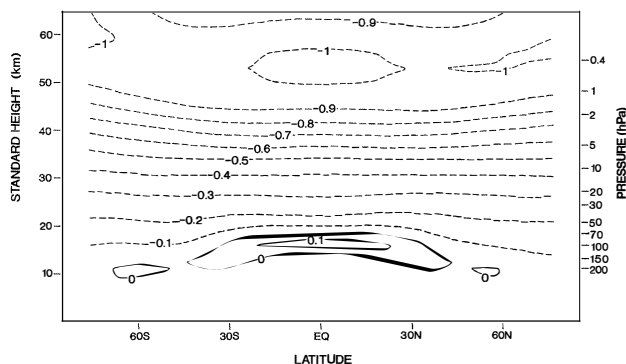


Figure 5-24. Vertical profile of the zonal, annual-mean temperature change from the lower to upper stratosphere resulting from the 1979-1990 changes in the well-mixed greenhouse gases. (The results are from the FDH model used in Ramaswamy *et al.*, 1992.)

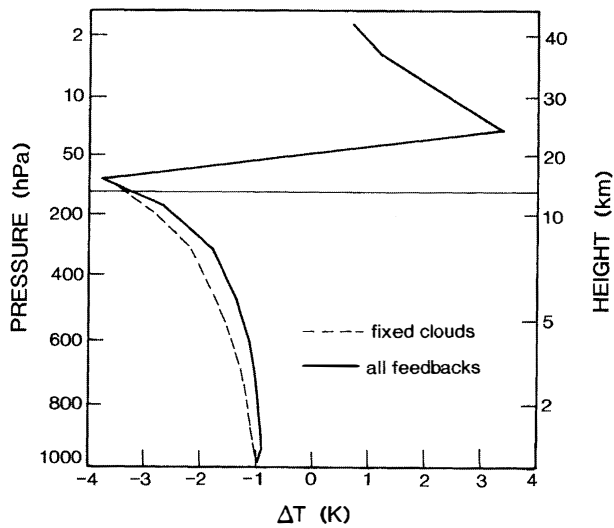


Figure 5-25. GCM-computed temperature change in the atmosphere due to a total loss of ozone between 70 and 250 hPa. Results are shown for the case with fixed clouds (dashed line), and with consideration of all feedbacks including cloud feedback effects (solid line). (Adapted from Hansen *et al.*, 1997a.)

the Antarctic winter/spring lower stratosphere owing to the ozone hole.

McCormack and Hood (1994) presented the first attempt to match the observed seasonal and latitudinal variation of lower stratospheric temperature with that predicted by an FDH model using imposed ozone changes based on observations. The resemblance between the size and pattern of the model temperature changes (with peak changes in the winter/spring of northern midlatitudes and spring of southern high latitudes) and MSU satellite observations (Randel and Cobb, 1994) was found to be encouraging. As discussed below, this work has been taken further by using GCMs, which strengthens the model-observation comparisons.

One particular item of interest in the case of FDH calculations (e.g., McCormack and Hood, 1994) is that the peak cooling in the Antarctic springtime tends to occur about one month earlier than in the observations. This occurs because the standard FDH approximation does not account for the time period during which the perturbation in the constituent (in this case ozone) persists. In the Antarctic springtime, typical radiative time scales are in excess of a month and yet the time

scale of the most marked ozone change is only one month. Hence, the atmosphere does not have time to fully equilibrate to the ozone-induced radiative perturbation (Shine, 1986). The standard FDH approximation does not account for this and assumes that the temperature adjustment occurs essentially instantaneously. Figure 5-26, from Forster *et al.* (1997), shows the temperature change at 80°S and 18.5 km using seasonally varying ozone changes in the context of the standard FDH approach, and a modified FDH approach (termed the Seasonally Evolving FDH (SEFDH)) that accounts for the time scale of the perturbation. The SEFDH result is obtained by time-marching the radiation calculations through the seasons. As can be seen, the maximum cooling in the FDH occurs earlier in the austral spring and is significantly larger than the SEFDH-derived maximum cooling. Also notable is that the FDH model does not retain a “memory” of perturbations at other times of year. An ozone loss only in October would have no effect on temperatures at other times of year. The SEFDH model does retain a memory of the radiative perturbations, and the increased cooling that persists from late spring to late summer in the SEFDH calculations is because the model temperatures have not yet recovered from the large loss of ozone in the springtime.

Early GCM works investigating the effects of ozone depletion did so assuming uniform stratospheric ozone losses, with a view toward diagnosing in a simple manner the radiative-dynamical response of the stratosphere (e.g., Fels *et al.*, 1980; Kiehl and Boville, 1988). Although the depletion profiles employed did not quite represent those observed subsequently in the lower stratosphere, these studies have provided insights on the mechanism of the stratospheric response to ozone changes there. Recently, Christiansen *et al.* (1997) have further examined the nature of the stratospheric response to different types of idealized ozone perturbations.

With the steady build-up of knowledge since the early to middle 1980s about the spatial and temporal distribution of ozone losses in the lower stratosphere, GCM experiments of two types have been carried out to determine the resulting temperature changes in the stratosphere. One type of investigation concerns attempts to simulate the interactive radiative-chemistry-dynamical changes due to ozone losses in the Antarctic polar region during springtime; e.g., Cariolle *et al.* (1990) and Prather *et al.* (1990) found a substantial lower stratospheric cooling during the duration of the ozone hole. Mahlman

STRATOSPHERIC TEMPERATURE TRENDS

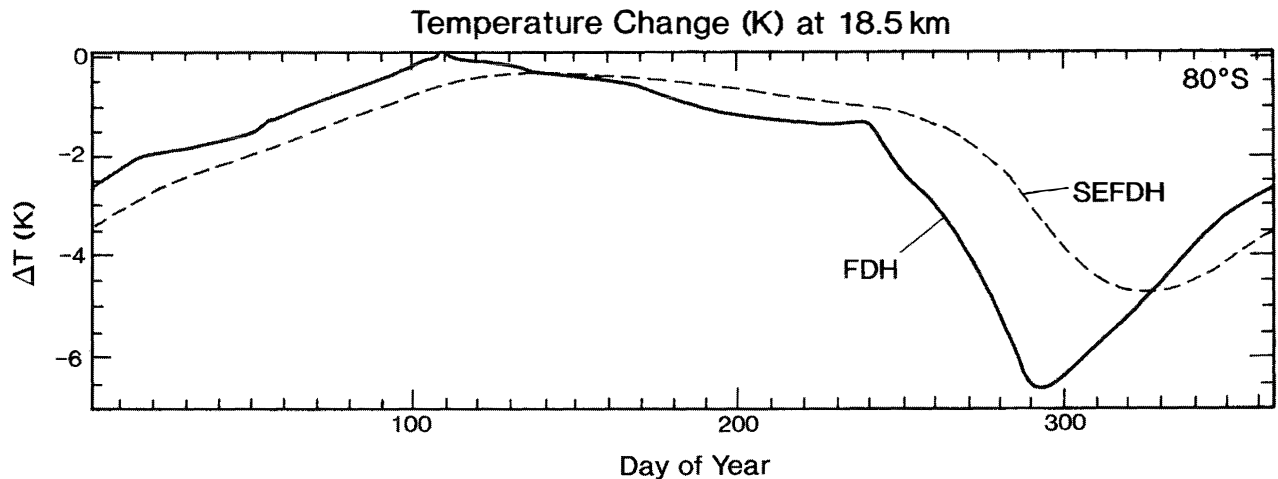


Figure 5-26. Modeled evolution of temperature changes in the lower stratosphere (18.5 km; 80°S) using two different assumptions. FDH denotes the usual Fixed Dynamical Heating while SEFDH denotes a Seasonally Evolving Fixed Dynamical Heating. (Adapted from Forster *et al.*, 1997.)

et al. (1994) found a statistically significant cooling in the Antarctic spring due to the ozone loss. They also found a significant warming of the altitude region above the altitudes of ozone loss, consistent with the observations (Randel, 1988; Figures 5-15 and 5-16). Recent studies have extended the interactive simulations to the Arctic region as well. Austin *et al.* (1992) concluded from their investigation that the stratosphere can be expected to be cooler owing to both long-term CO₂ increases and ozone decreases, which raises the possibility in the future of Arctic “ozone holes” and a strong positive feedback effect involving ozone depletion and lower stratospheric cooling. Shindell *et al.* (1998) have also examined the effects of increased well-mixed greenhouse gases and ozone changes upon the global stratospheric temperatures over the next few decades (see Chapter 12). Their results reiterate the sensitivity of the polar springtime temperatures to greenhouse gas increases and the feedback effect caused by ozone losses, with the actual magnitudes subject to details of model representations of various physical processes.

Another type of GCM investigation has consisted of imposing the observed ozone losses and then determining the GCM response, without any considerations of the chemical and dynamical processes affecting ozone distributions. Again, early studies began with investigations of the Antarctic springtime lower stratosphere owing to the large observed losses there. A substantial lead-in to the 3-D aspects was provided by the 2-D study of Chipperfield and Pyle (1988). They found a large

cooling (>9 K) at ~70 hPa during October, just like the earlier FDH result (Shine, 1986). In addition, they found a warming (up to ~6 K) in the upper stratosphere. The GCM simulation of Kiehl *et al.* (1988) yielded a large cooling (~5 K) by the end of October, which further substantiated the FDH inference. This GCM study also found a warming in the upper stratosphere (up to ~4 K at 10 hPa).

Employing the observed global lower stratospheric ozone depletion, Hansen *et al.* (1995) demonstrate a good agreement in the magnitude of the GCM-simulated cooling of the global, annual-mean lower stratosphere with the observed MSU satellite and radiosonde temperature trends (Figure 5-27). This study, along with others, also indicates that the cooling due to ozone loss overwhelms the temperature change resulting from changes in concentration of the well-mixed greenhouse gases in the 50-100 hPa (~16-21 km) region (see Figures 5-22, 5-23, and 5-27).

The differences between FDH and GCM simulations of the effects of ozone losses have been investigated by Fels *et al.* (1980) and Kiehl and Boville (1988) using idealized stratospheric ozone perturbations. For annual-mean model simulations, Fels *et al.* (1980) concluded that the FDH response to uniform percentage reductions tended to be comparable to the GCM solutions, except at the tropical tropopause and tropical mesosphere. For “perpetual January” simulations, Kiehl and Boville (1988) found that the uniform reduction experiments were not well represented by the FDH

STRATOSPHERIC TEMPERATURE TRENDS

calculations. However, more realistic ozone scenarios in which the losses increase from equator to the poles yielded FDH results comparable to the GCM. This point is substantiated by the “perpetual January” simulations of Christiansen *et al.* (1997), who performed uniform ozone reduction and large lower stratospheric depletion experiments. The main dynamical effect in their perturbation experiments was a weakening of the diabatic meridional circulation accompanied by a latitudinal smoothing of the temperature response.

The satellite-observed global lower stratospheric ozone losses over the ~1979-1991 period (i.e., just prior to the Mt. Pinatubo volcanic eruption) can be used to obtain a comparison of the resulting radiative and radiative-dynamical solutions for the stratospheric temperature changes. This is illustrated here by comparing the results of the FDH and GCM simulations performed, respectively, by Ramaswamy *et al.* (1992) and (1996) using an identical model framework (Figure 5-28). This comparison enables a delineation of the role of dynamical influences on the temperature changes caused by the observed ozone depletion. The GCM result, like the FDH, indicates a cooling of the lower stratosphere, but there are distinct differences due to dynamical changes. In the middle to high southern latitudes, there is less cooling in the GCM. In the Northern Hemisphere, the midlatitudes are less cold in the GCM, but the high latitudes are more so relative to the FDH result, again a consequence of the dynamical changes in the model. In the GCM, there is a cooling even in those regions where there are no ozone losses imposed, e.g., the lower stratosphere equatorward of 15°. A warming occurs above the region of cooling, particularly noticeable in the Southern Hemisphere, similar to the results obtained by other GCM studies (Kiehl *et al.*, 1988; Mahlman *et al.*, 1994; Shindell *et al.*, 1998). The dynamical changes (see also Mahlman *et al.*, 1994) consist of an induced net rising motion in the tropics and a compressional heating of the middle stratosphere at the higher latitudes. The annual-mean response is statistically significant between ~13 and 21 km in the ~20 to 50° latitude belt (Ramaswamy *et al.*, 1996). The changes at high latitudes (>60°) fail the significance test because of large interannual variability in those regions. The warming above the lower stratospheric regions in both hemispheres is reasonably similar to observations (Randel, 1988; Figures 5-15 and 5-16). On the basis of the GCMs-observations comparisons, a principal factor for the observed warming

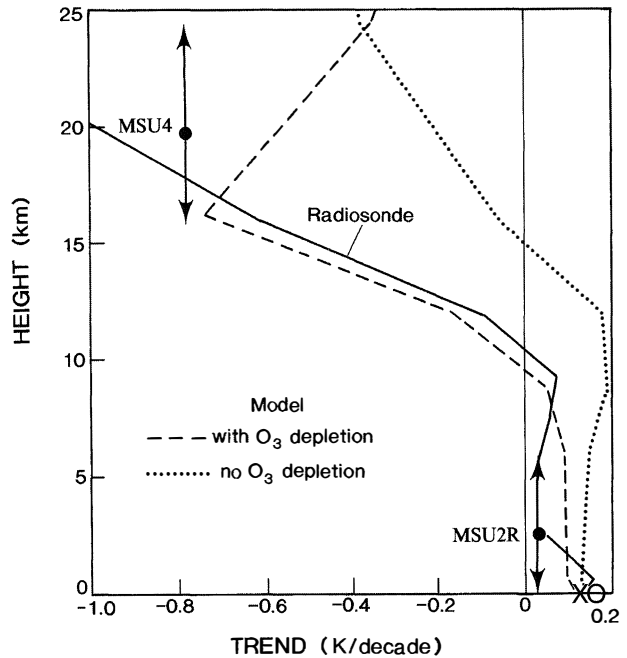


Figure 5-27. Comparison of GCM-simulated vertical profiles of temperature change (K) over the 1979-1990 period with radiosonde and MSU satellite observations. The simulations were performed considering well-mixed greenhouse gas increases, and with or without consideration of the lower stratospheric ozone depletion. The “O” and the “X” symbols denote the surface temperature changes from the Jones (1994) and Hansen and Wilson (1993) observational datasets, respectively. (Adapted from Hansen *et al.*, 1995.)

could be the radiative-dynamical feedbacks involving ozone depletion in the lower stratosphere.

Hansen *et al.* (1993) show that the zonal-mean patterns of GCM-simulated lower stratospheric temperature change due to imposed ozone losses correspond well with observed changes. In a study analogous to the FDH model-observation comparison discussed earlier, Ramaswamy *et al.* (1996) have compared the latitude-month trend pattern of the decadal (period: ~1979-1990) temperature change and its statistical significance, as simulated by a GCM (Figure 5-29a) in the altitude region of the observed lower stratospheric ozone change (tropopause to ~7 km above), with that derived from satellite observations (Figure 5-29b) of the lower stratosphere for the same period (Randel and Cobb, 1994). The match of the latitudinal-

STRATOSPHERIC TEMPERATURE TRENDS

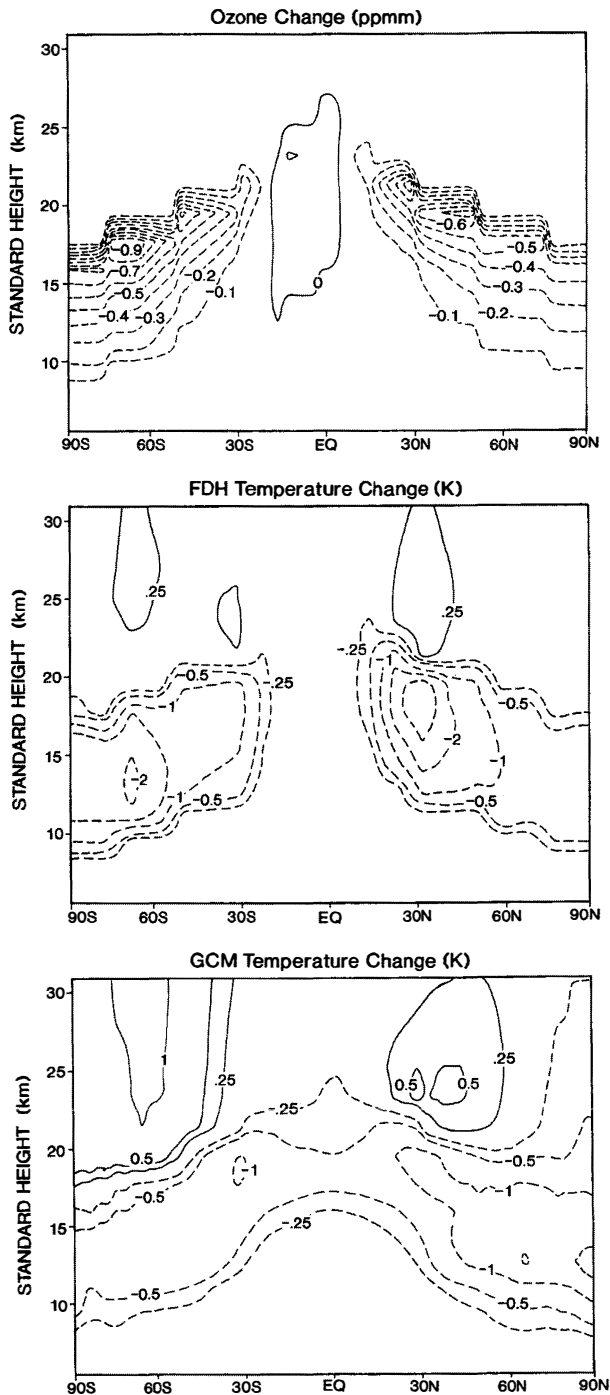


Figure 5-28. Idealized, annual-mean stratospheric ozone loss profile based on TOMS and SAGE satellite-observed ozone trends (top panel), and the corresponding temperature changes, as obtained using a FDH model (middle panel) and GCM (bottom panel). (Adapted from the model simulations of Ramaswamy *et al.*, 1992, 1996).

month pattern of cooling with observations bears a fair resemblance to the FDH-based study of McCormack and Hood (1994). In the midlatitudes, both panels illustrate a cooling from ~January to October in the Northern Hemisphere and from ~September to July in the Southern Hemisphere. The cooling in the midlatitudes of the Northern Hemisphere from ~December to July, and in the Southern Hemisphere from ~December to May, are statistically significant in both model and observation. Comparing Figure 5-29 with Figure 5-13, it is apparent that the observed space-time domain of statistically significant cooling is also dependent on the end year chosen for the analysis. Near the poles, both the simulation and observation exhibit a relatively large magnitude of cooling during winter and spring. The simulated cooling in the Antarctic is highly significant during the austral spring (period of the ozone hole), consistent with observation. The springtime cooling in the Arctic does not show a high significance owing to a large dynamical variability there. The simulated cooling in the tropics, which arises as a result of changes in circulation and is absent in FDH, is not significant for most of the year owing to small temperature changes there. There exist some quantitative differences between the simulated and observed trends. In addition, there is less variability in the model compared to observations.

In general, the observed ozone losses introduce a nonuniform space-time cooling. This is in contrast to well-mixed greenhouse gas effects that tend to yield a more uniform lower stratospheric cooling with season (not shown). Thus, the observed seasonal trend (Figure 5-29b), which exhibits a spatial dependence, is unlikely to be due solely to increases in well-mixed greenhouse gases. Note that, in the context of the GCM results, it is not possible to associate specific seasonal cooling at any location with the corresponding seasonal ozone loss.

Some models that have been principally used to study tropospheric climate changes due to greenhouse gases (e.g., IPCC, 1996) have also considered the lower stratospheric ozone depletion. However, as noted earlier, several of these climate models have a poor vertical resolution in the stratosphere that affects the accuracy of the calculated temperature changes. Nevertheless, the cooling predicted by these models using observed ozone loss in the lower stratosphere is generally consistent with the observed global-mean cooling trend, typically 0.5 K/decade.

Model calculations illustrate that, in addition to lower stratospheric ozone change, tropospheric ozone

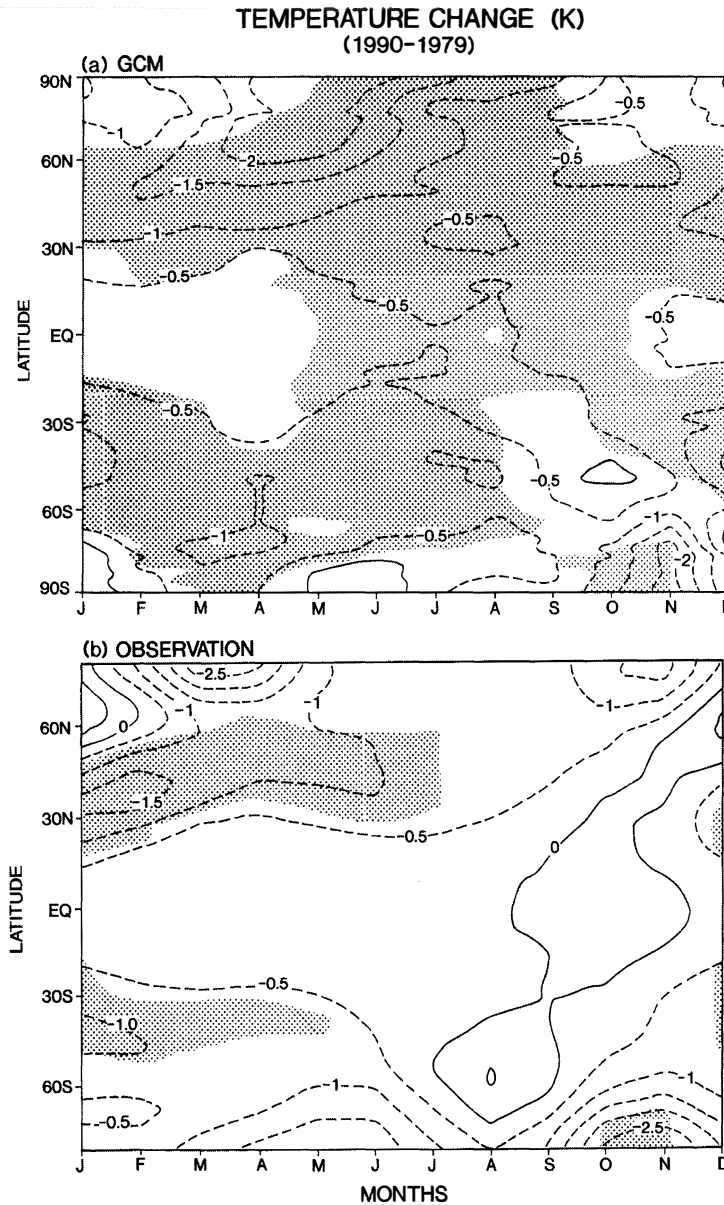


Figure 5-29. Zonally-averaged, monthly-mean, lower stratospheric temperature change for ~1979-1991: (a) as simulated by the general circulation model (90°S to 90°N) due to the observed global ozone depletion, and (b) as inferred (Randel and Cobb, 1994) from satellite observations (82.5°S to 82.5°N). Shaded areas show statistical significance at the 95% confidence level. (Reprinted by permission from *Nature* (Ramaswamy *et al.*, *Nature*, 382, 616-618, 1996) Copyright (1996) Macmillan Magazines Ltd.).

change could also have a smaller but non-negligible effect on stratospheric temperatures (Ramaswamy and Bowen, 1994). Since preindustrial times, tropospheric ozone may have increased by ~50% or more in some regions in the Northern Hemisphere (IPCC, 1995; Berntsen *et al.*, 1997). As a result, this may have contributed to a substantial cooling tendency in the lower stratosphere in specific regions.

In a diagnostic study, Fortuin and Kelder (1996) discuss relationships between ozone and temperature changes by analyzing concurrent measurements of these two quantities made at eight stations over the past two decades. They find that both vertical displacement and radiative adjustment to trace gas concentrations need to be considered in order to explain the observed ozone and temperature variations at the various locations.

STRATOSPHERIC TEMPERATURE TRENDS

5.3.3.2 SENSITIVITIES RELATED TO OZONE CHANGE

One of the most important factors affecting the temperature change due to ozone is the precise vertical profile of the ozone changes in the stratosphere, especially the region near the tropopause, a problem that has been reiterated for a number of years now (WMO, 1986, 1992, 1995). Additionally, there are some uncertainties about the middle and upper stratospheric ozone changes that, too, impact in a non-negligible manner upon the temperature changes in those regions.

The sensitivity of the temperature change to the details of the vertical profile of ozone change has been discussed by Forster and Shine (1997). Figure 5-30 shows the latitude-height profile of the FDH-derived temperature change using a simplified vertical profile of ozone change (where a constant percentage of ozone is removed within 7 km of the tropopause, with the total column ozone change derived from the SBUV trends reported in WMO, 1995), and one where the vertical profile of trends derived from SAGE data is used. The calculations are for the period since 1979. The vertical profile of the cooling obtained due to the two ozone profiles at 40°N is compared with other species in Figure 5-23. Generally speaking, the cooling in the lower stratosphere due to either profile is strong and outweighs contributions estimated due to other possible species' changes. Although the general vertical profile of the ozone-induced coolings remains the same, peaking at ~1 K/decade in some regions, the latitudinal variation is quite different. The SBUV trends give only small ozone changes in low latitudes, and the cooling is concentrated in the extratropical lower stratosphere. The SAGE trends show large changes in the tropical lower stratosphere (despite modest total column changes), and these result in the peak cooling in the tropics. It is noted that the SPARC Ozone Trends Panel has recently assessed the status of knowledge about the vertical trends of ozone changes (WMO, 1998). According to that panel and Cunnold *et al.* (1996a,b), the large trends of SAGE I/II at 15-20 km are unrealistic, with these data being most reliable above 20 km.

One further important aspect of Figure 5-30 concerns the trends in the middle stratosphere. Using the simplified ozone change profile, there is only heating at ~30 km, most marked in southern high latitudes where the increase in the upwelling thermal infrared radiation, as a result of the removal of ozone in the lower

stratosphere, leads to an increase in the absorbed radiation. Using the SAGE vertical profiles, which are probably more reliable at these heights, there are coolings at almost all latitudes, reaching 0.4 K/decade. Hence, whilst the ozone loss is probably most important in the lower stratosphere, the losses at these stratospheric altitudes (~30 km) remain substantial and could lead to trends that are of the same magnitude approximately as the temperature trends, over the same period, due to increases in well-mixed greenhouse gases (see Figure 5-24).

Hansen *et al.* (1997a) have examined the sensitivity of the lower stratospheric temperature changes due to ozone depletion by conducting various GCM experiments with varying profiles and amounts of ozone losses (their result for the specific case when depletion of ozone occurs over the 70-250 hPa region is illustrated by Figure 5-25). They find that the magnitude of temperature change near the tropopause is strongly dependent on the vertical profile of the ozone loss. The degree to which the temperature change is affected is also dependent on the latitude under consideration.

The GCM sensitivity experiments by Hansen *et al.* (1997a) mentioned above also demonstrate that the observed ozone losses not only cool the lower stratosphere but also affect the vertical profile of temperature change below the region of ozone losses. The crossover of temperature change from a warming in the troposphere to a cooling in the stratosphere occurs at a lower altitude when stratospheric ozone depletion is considered in the models, in contrast to when only the changes in the well-mixed gases are considered. Santer *et al.* (1996) have shown how the inclusion of the ozone loss in the lower stratosphere not only alters the modeled vertical profile of the atmospheric temperature change due to anthropogenic species, but is a critical element in the attribution of the observed temperature profile change to human activity. Tett *et al.* (1996) and Folland *et al.* (1998) further point out that the inclusion of the lower stratospheric ozone depletion is an important anthropogenic factor for the vertical profile of temperature changes near the tropopause, and thereby could affect the lower altitudes and surface.

Ozone changes also affect higher regions of the stratosphere. Fels *et al.* (1980) and Rind *et al.* (1990, 1998) point out that, while the stratosphere generally cools in response to the carbon dioxide increases, the cooling in the middle and upper stratosphere is reduced (by ~10% at 50 km) when ozone is allowed to respond

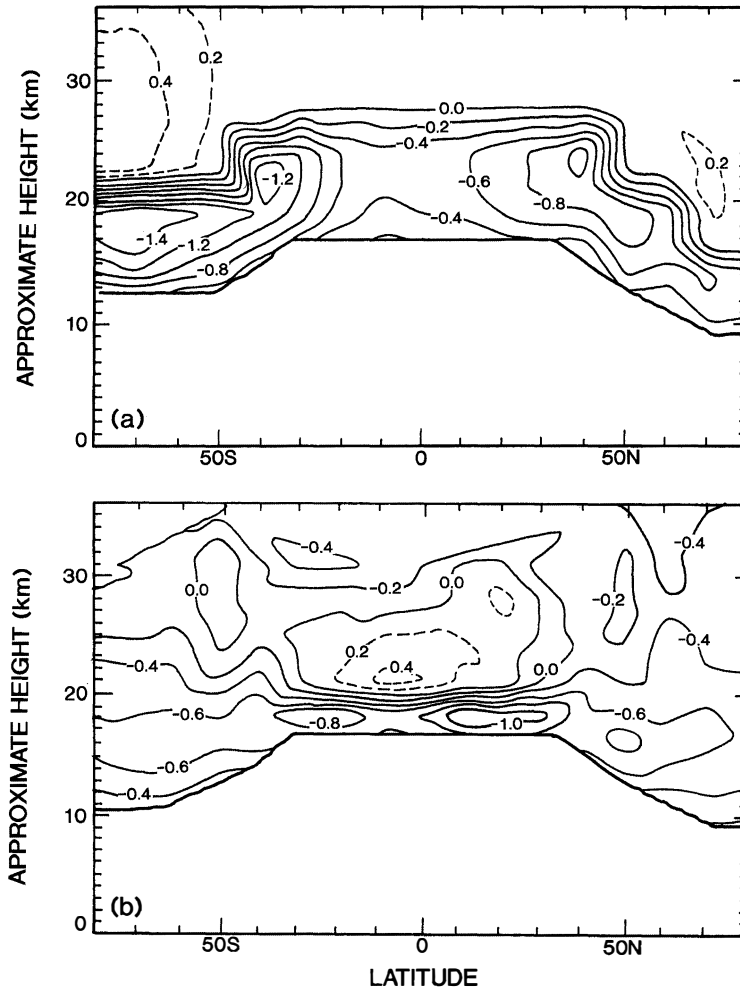


Figure 5-30. FDH-computed annually averaged global stratospheric temperature change during the 1980s versus latitude due to (a) SBUV column depletion with ozone loss between local tropopause and 7 km above it, and (b) assumption of the SAGE vertical profile. (Adapted from Forster and Shine, 1997.)

photochemically. FDH estimates using the SAGE vertical profile of temperature change indicate that the positive (or negative) temperature change generally follows the positive (or negative) changes in ozone. Thus, the result from the calculations performed by Schwarzkopf and Ramaswamy (1993) suggests that ozone losses over the 1980-1990 period have caused a cooling of ~ 0.3 K/decade at ~ 40 km. This is to be contrasted with the well-mixed greenhouse gas-induced cooling of about 0.7 K/decade at these altitudes (Figures 5-23 and 5-24).

As mentioned in Section 5.3.3.1, Shindell *et al.* (1998) simulate the changes in the stratosphere due to

secular trends in greenhouse gases and ozone changes using an interactive radiative-dynamical-chemical GCM (see also Chapter 12). Their results indicate that the cooling of the entire stratosphere due to the trace-gas changes leads to a significant expansion of the area of ozone loss in the polar regions. Besides the expansion of the Antarctic polar ozone loss area, there also occurs a pronounced depletion of the Arctic springtime ozone. The rather dramatic modeled cooling is attributed to changes in planetary wave characteristics. In general, the quantitative nature of such changes in GCMs depends crucially on the model parameterizations.

STRATOSPHERIC TEMPERATURE TRENDS

5.3.4 Aerosols

As stated in Section 5.2.6.1, major volcanic eruptions result in temporary increases of stratospheric aerosol concentrations which, in turn, cause transient warmings of the lower stratosphere (WMO, 1990a, 1992). One-dimensional radiative-convective, two-dimensional, and three-dimensional models have all been used to estimate the effects on stratospheric temperatures (e.g., Hansen *et al.*, 1978, 1997b; Harshvardhan, 1979; Pitari *et al.*, 1987). An important research outcome in recent years has been the fact that simulations of the climatic effect of the Mt. Pinatubo eruption (Hansen *et al.*, 1993, 1997b) reproduce the observed lower stratospheric warming (refer to Section 5.2.6.1; Christy, 1995; Randel *et al.*, 1995; Angell, 1997; also Figures 5-2 (bottom panel) and 5-3), the peak and its duration, remarkably well (IPCC, 1995). Although temporary, the volcanic aerosol-induced lower stratospheric warming is in the opposite sense of the cooling due to ozone depletion and the cooling due to the combined well-mixed greenhouse gas increases (Figures 5-23, 5-24, and 5-27).

Rind *et al.* (1992) investigated the role of volcanic effects on the stratosphere in GCM experiments with and without sea surface temperature changes. Their results show that, in response to the volcanic injections, the lower stratosphere warmed, while the upper stratosphere cooled and the mesosphere warmed at middle and high latitudes. These responses are similar qualitatively to the OHP lidar observations. The occurrence of mesospheric warming is indirectly supported by a decrease in the occurrence of noctilucent clouds in the summer of 1992 (Zalcik, 1993).

Several 2-D radiative-dynamical-photochemical models (Brasseur and Granier, 1992; Tie *et al.*, 1994; Rosenfield *et al.*, 1997), with different degrees of complexity in the representation of physical and chemical processes, have been deployed to study the temperature, circulation, and ozone changes due to the increase in stratospheric aerosol concentrations following the Mt. Pinatubo volcanic eruption. Additionally, Eluszkiewicz *et al.* (1997) have used Upper Atmosphere Research Satellite (UARS) measurements to investigate the stratospheric heating rate sensitivity and the resulting residual circulation. These studies indicate a warming of the tropical lower stratosphere that is approximately

consistent with observations. This heating is found to be sensitive to the presence of tropospheric clouds and to the aerosol vertical extinction profiles, which corroborates the sensitivity results of WMO (1990a). The perturbed heating in the tropics results in an upwelling and an altered circulation, a feature seen in model simulations and diagnosed from observations. Thus, the transient volcanic aerosol-induced warming has the potential to alter atmospheric dynamics and could thereby affect the surface-troposphere system (Hansen *et al.*, 1997b). Ozone depletions are obtained by the 2-D model as a result of the heterogeneous processes involving aerosols, changes in photolysis rates, and changes in the meridional circulation (Tie *et al.*, 1994). The ozone loss at high latitudes yields a cooling there (Rosenfield *et al.*, 1997), which could have contributed to the prolonged duration of the colder-than-normal temperatures in the Arctic region (Section 5.2.4; Figures 5-4 and 5-14 (top)).

Although both the El Chichón and Mt. Pinatubo eruptions have resulted in a large transient warming, these are estimated to have only a small direct effect on the decadal temperature trends in the lower stratosphere, with even smaller effects higher up. However, an indirect effect through aerosol-induced, chemically catalyzed ozone loss, and the subsequent ozone radiative feedback, can yield an enhanced global cooling trend (Solomon *et al.*, 1996). Figures 5-2 (bottom panel) and 5-3 illustrate the colder global-mean lower stratospheric temperatures now than in the pre-Pinatubo period (see also Chapter 7). Thus, the volcanic events could have had an important bearing on the lower stratospheric temperature trend observed over the decade of the 1980s and early 1990s.

Ramaswamy and Bowen (1994) show that changes in tropospheric aerosols can affect lower stratospheric temperatures. While the tropospheric aerosols assumed in that study acted to oppose the greenhouse warming in the troposphere, they enhanced the cooling in the stratosphere by reducing the upwelling thermal infrared radiation coming from a cooler troposphere. It should be noted that there is considerable uncertainty in the distribution and optical properties of aerosols; in addition, they may have a substantial effect on the optical properties of clouds (see IPCC, 1995, 1996), which would also affect the upwelling longwave flux from the troposphere. Thus, it is not possible as yet to be quantitative about the present-day tropospheric aerosols' effect on stratospheric temperatures.

5.3.5 Water Vapor

Stratospheric water vapor is an important radiatively active constituent, and it is expected to increase in concentration due to increased methane oxidation. It could also be influenced by changes in tropospheric water vapor concentration and changes in the transport of water vapor across the tropopause. Oltmans and Hofmann (1995) reported significant trends of 0.5%/yr in water vapor over Boulder, Colorado, from balloonsonde observations between 1981 and 1994. It is not clear whether these changes are occurring at other locations and, more important, on a global scale. Forster and Shine (1997) have used a FDH model to calculate the possible impact of these changes. At 40°N and between 15 and 20 km, the cooling due to water vapor changes exceeds 0.2 K/decade (Figure 5-23). This is much larger than the effect of changes in the well-mixed greenhouse gases at the same altitude (typically 0.1 K/decade; Figures 5-23 and 5-24); depending on the vertical profile of ozone loss adopted, the water vapor change causes a cooling of about 20-30% of the effect of the ozone change. Recent observational analyses (Nedoluha *et al.*, 1998) suggest an increase in H₂O of 1-2% or more per year (between 1991 and 1996) in the middle and upper stratosphere and mesosphere. If sustained for a decade, the heating rate change would be about 0.05 K/day. Combining this with a radiative damping time of ~10 days (Fels, 1982; Kiehl and Solomon, 1986) would yield a cooling of 0.5 K/decade at 50 km. This value would be about half of that for the well-mixed greenhouse gases (Section 5.3.2; Figure 5-24), and could exceed that due to ozone change at that altitude (Section 5.3.3.2).

5.3.6 Other (Solar Cycle, QBO)

All the above constituent changes are essentially ones that have taken place in the stratosphere itself. External changes, such as changes in the incoming solar radiation, reflected solar radiation from the troposphere, and emitted thermal infrared radiation, can also impact stratospheric temperatures.

Changes in the output of the Sun can clearly influence the amount of UV and visible radiation absorbed by the stratosphere. In the absence of changes in ozone, WMO (1990a) radiative-convective model calculations showed that, over the course of a solar cycle, the temperature at the stratopause can vary by about 1 K, but by 20 km, the changes are less than 0.1 K. If planetary wave propagation plays a role in the way the

solar cycle influences the stratosphere, as observations appear to indicate, then model simulations need to adequately account for these dynamical processes. Several numerical model simulations (Garcia *et al.*, 1984; Brasseur, 1993; Fleming *et al.* 1995; McCormack and Hood, 1996) indicate that the maximum of the solar effect should be situated at the stratopause at all latitudes, with a value of about 1.5-2 K/cycle in the tropics. Figure 5-31 illustrates results from two models for the equatorial latitudes and compares them with rocket and satellite (see also Figure 5-19) observations. The models yield amplitudes of ~2 K at the tropical stratopause. The modeled temperature change is roughly consistent with observations, although the maximum at the stratopause is not manifest in the satellite data; the same models are less successful when compared with observations at middle and high latitudes. In fact, any potential dynamical effects associated with the observed solar cycle signature (Section 5.2.6.2) are likely not being captured adequately by interactive radiative-chemical-dynamical models as yet.

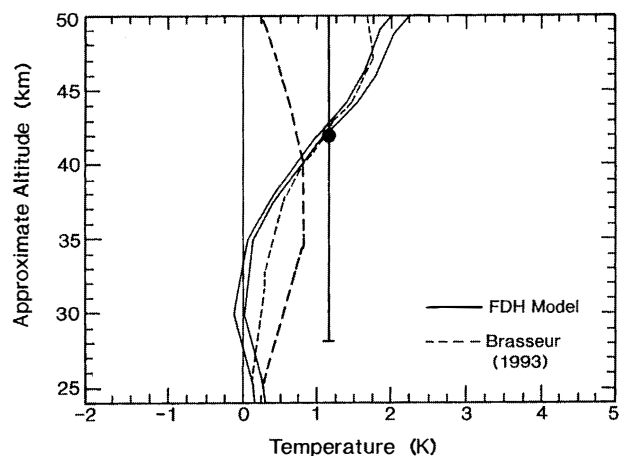


Figure 5-31. Comparison of low-latitude (5°N) temperature response due to solar cycle variation, as computed by two models (Brasseur, 1993; McCormack and Hood, 1996), with SSU satellite observations (thick, dashed line), and rocket data (Dunkerton *et al.*, 1998) for the altitude range ~28-55 km (vertical bar). McCormack and Hood (1996) performed two FDH calculations using the range of the observed ozone values; their model results (solid curves) are quite similar to the result of Brasseur, 1993 (thin dashed curve). (Adapted from McCormack and Hood, 1996.)

STRATOSPHERIC TEMPERATURE TRENDS

Haigh (1996) has simulated the possible effect of solar-induced stratospheric ozone and temperature variations on the tropospheric Hadley circulation and jet streams using a GCM. The results suggest that changes in stratospheric ozone may provide a mechanism whereby small changes in solar irradiance can cause a measurable impact on climate. Haigh (1996) proposed that changes in the thermal structure of the lower stratosphere could cause a strengthening of the low-latitude upper tropospheric easterly winds. Haigh (1998) further suggests that this easterly acceleration can come about as a result of a lowering of the tropopause and deceleration of the poleward meridional winds in the upper portions of the Hadley cells. More observational diagnostics work and model investigations are needed to confirm these hypotheses.

Balachandran and Rind (1995) studied the influence of UV variability and QBO using a GCM that emphasizes the middle atmosphere. They found that changes in UV tended to alter the radiative heating, with an accompanying influence on the winter polar jet, though it must be noted that the large variability in this quantity inhibits a statistically significant and robust determination. The high-latitude response to UV is affected by alteration in planetary wave activity, with the QBO exerting a modulating effect. The influence of solar change on the temperature yielded changes of opposite sign at the stratopause between latitudes above and below 60°N. Such changes are quite similar to those seen in the overall stratosphere from the satellite data analyses (Figure 5-19).

5.4 CHANGES IN TRACE SPECIES AND OBSERVED TEMPERATURE TRENDS

5.4.1 Lower Stratosphere

As far as the global lower stratosphere is concerned, there is now a firm documentation of the changes in ozone and greenhouse gases. With regard to temperature trends, the importance of ozone depletion relative to that due to changes in other greenhouse gases that are well-mixed (CO₂, CH₄, N₂O, CFCs) has been evaluated by several studies with various types of models (1-D to 3-D). Miller *et al.* (1992) and Hansen *et al.* (1995) demonstrate that the global-mean lower stratospheric temperature change in the 1980s can be explained only when ozone changes are considered (Figure 5-27). Ramaswamy *et al.* (1996) show that the

global, annual-mean GCM temperature change due to the decadal ozone losses in the ~50-100 hPa (~16-21 km) lower stratospheric region is much greater than that due to increases in CO₂ only and all well-mixed greenhouse gases taken together (Figure 5-22). It is thus encouraging that all model studies, ranging from FDH and RCMs to GCMs, yield similar findings (Section 5.3.3.1). The global-mean decadal cooling in the 1980s due to ozone is estimated to be ~0.5 to 0.6 K, which is comparable to the reported decadal trends from observations (Section 5.2.3.2; Figure 5-27). The well-mixed gases' effect is less than one-fourth that due to ozone depletion. The increase in CO₂ alone since 1765 yields a cooling of ~0.3 K; inclusion of the other well-mixed gases, which together tend to warm the tropopause region, yields ~0.15 K. It is thus clear that the computed 1979 to 1990 ozone effect on lower stratospheric temperature outweighs the effects of changes in other gases not only over the last 10 to 30 years, but also over the past two centuries. In the global, annual mean, it can be strongly declared that the observed ozone depletion in the lower stratosphere is the dominant radiative cause of the observed global-mean cooling. Section 7.3 presents a theoretical basis for how a long-term global, annual-mean trend in the stratosphere must necessarily be associated with radiative perturbations.

As discussed in Section 5.3.3.2, uncertainties arise in the simulation owing to incomplete observational knowledge of the vertical profile of global ozone loss near the tropopause, including that in the tropical areas. While more thorough altitudinal measurements of ozone loss would lead to more precise simulation of temperature change, with cooling extending to perhaps even higher altitudes (e.g., springtime southern polar latitudes), the lower stratosphere region, taken as a whole, can be expected to cool notably given the magnitude of the ozone losses observed. A principal conclusion from all investigations thus far is that, whether ozone changes are prescribed or determined self-consistently within a model, the global lower stratospheric region (especially the mid to high latitudes) cools in a significant manner in simulations for the decades of the 1980s and 1990s.

In addition to the above, a principal feature from especially the GCM studies is the reasonably good correspondence of the zonal-mean lower stratospheric cooling trends since ~1979 with satellite and radiosonde records (e.g., Hansen *et al.*, 1993). It is concluded that the reasonable consistency of the simulated cooling pattern and magnitudes with those observed, including

the regimes of statistically significant changes, coupled with the high correlations noted between observed temperature changes and ozone losses (Section 5.3.3.1), confirm the notion that ozone depletion has caused a substantial spatially and seasonally dependent effect in the lower stratosphere over the past decade. For example, Figure 5-29 highlights the model-observation consistency with regard to magnitude and statistical significance in the midlatitudes of both hemispheres during the first half of the year, and during the Antarctic springtime. Although the attribution of the observed temperature trends to the observed ozone depletion in the lower stratosphere is strong in the global, annual-mean sense, the spatial and temporal aspects demand more circumspection. However, no other cause besides ozone depletion has been shown as yet to yield a latitude-month fingerprint such as that seen in the observations (Figure 5-29b). Thus, in the zonal-mean, seasonal sense, it can be stated that ozone is identified as an important causal factor of lower stratospheric temperature change.

Possible secular changes in other radiatively active species are estimated to contribute smaller decadal effects than the stratospheric ozone loss. Information on decadal changes in global water vapor (Section 5.3.5) and clouds is insufficient to estimate their influence precisely; there is no information at present to suggest that their effects could be as dominant as that due to the stratospheric ozone loss. Although volcanic aerosols can have substantial impact over the 1-2 years that they are present in the lower stratosphere, their direct effect on the past decade's temperature trend has probably been small compared with that of ozone (Sections 5.2.6.1, 5.3.4). There is little evidence to suggest that forcings from the troposphere (e.g., sea surface temperature changes; Section 5.2.6.5) or natural climate variability or solar cycle (Sections 5.2.6.2, 5.3.6) have significantly influenced the global lower stratospheric temperature change over the past 1.5 decades, although, in the absence of rigorous long-term observations, a precise estimate of their contributions cannot be obtained. It is noted that some ozone loss has been reported for the 1970s, too (Lacis *et al.*, 1990), which would have contributed to the small observed cooling during that decade (e.g., Figures 5-3(top) and 5-4). However, this contribution is not likely to have been as much as in the 1980s and 1990s, because the ozone losses for the earlier decades are concluded to have been never as high as those in recent ones (Bojkov and Fioletov, 1995).

There is a scarcity of knowledge on the low-frequency variability of the stratosphere and its causes, from either observations or models. Unlike surface temperature measurements that span multi-decades, those for the stratosphere are available only from about the late 1950s, and the continuous record is available only at a few locations in the NH. This makes it difficult to assess accurately the low-frequency variability. Although global coverage has become possible with the MSU and SSU satellites since 1979, the time period available to date is too short to assess anything beyond interannual variability; certainly, rigorous decadal-scale variability analysis will not be possible until data for a few more decades become available. The model simulations to date suggest an interannual variability in some features that bears some resemblance to that observed, but there are also features that the existing models either cannot reproduce or that fail to mimic the observations (e.g., Hamilton *et al.*, 1995). A prominent uncertainty arises due to the lack of a proper simulation of the polar wintertime and winter-to-spring transitional temperatures (including sudden warmings) from first principles. The usual method to reproduce observations is to "tune" the model in some manner, e.g., gravity-wave drag. The quantitative effect that this has on the fidelity of the simulation of trends and variability remains to be determined.

The cold winters/springs occurring in the lower stratosphere of the Arctic in recent times (Section 5.2.4) have drawn considerable attention, including a search for the possible cause(s). The Arctic temperatures can vary substantially in magnitude on interannual time scales (see Figure 5-14(top)), thus demanding caution in the inference and attribution of long-term trends there. Baldwin *et al.* (1994) and Perlwitz and Graf (1995) document the existence of a coupling between the winter polar vortex and middle troposphere. Thompson and Wallace (1998) show coherence between hemispheric wintertime surface air temperature and pressure, and 50-hPa temperatures. The studies of Manney *et al.* (1996) and Coy *et al.* (1997) indicate that extreme low temperatures in spring are associated with record-low planetary wave activity and an intense vortex. The above studies suggest a possible shift in Arctic meteorological conditions in the early to middle 1990s, one that is linked to tropospheric circulation and variability in planetary wave forcing. The notion that this could be related in some manner to greenhouse gas-induced warming of the lower atmosphere (Chapter 12) remains to be conclusively demonstrated.

STRATOSPHERIC TEMPERATURE TRENDS

Indeed, the effect of tropospheric climate change due to changes in trace gases and aerosols, equator-to-pole tropospheric temperature gradient, waves propagating into the stratosphere, and the ensuing effects on the radiative-dynamical-chemical stratospheric equilibrium are not well understood in a quantitative manner. For example, different GCMs suggest a substantially different manner of changes in the characteristics of the planetary wave activity due to increase of CO₂, which would, in turn, impact the radiative-dynamical interactions and the magnitude of stratospheric temperature changes (Fels *et al.*, 1980; Fels, 1985; Rind *et al.*, 1990; Mahlman *et al.*, 1992; Graf *et al.*, 1995; Shindell *et al.*, 1998; Rind *et al.*, 1998).

5.4.2 Middle and Upper Stratosphere

Unlike the case for the lower stratosphere, the trends estimated from the different observational platforms for the middle and upper stratosphere are not as robust. The satellite, lidar, and rocket data, although having a consistency of pattern above ~50 hPa (e.g., Figures 5-9 and 5-12), do not exhibit the same degree of coherency that exists with respect to both magnitude and statistical significance for the different datasets of the lower stratosphere (Figures 5-5 and 5-6).

In the middle and upper stratosphere, model results suggest that the increases in the well-mixed greenhouse gases and changes in ozone will contribute to temperature changes. Figure 5-24 shows the zonal, annual-mean temperature trend due to the well-mixed greenhouse gas increases in the 1980s. The overall picture in the annual mean is one of cooling from the lower to the upper stratosphere (see also Figure 5-23). This cooling in the middle stratosphere due to the well-mixed gases can be expected to be enhanced in FDH calculations that also consider ozone losses in the middle stratosphere; the latter is estimated to yield about a 0.3 K/decade cooling using the SAGE depletion for the 1980s period (Section 5.3.3.2). The computed vertical profile bears a qualitative similarity to the observations (e.g., Figures 5-7 and 5-9) with regard to the cooling of the entire stratosphere. This reaffirms the secular cooling trend due to greenhouse gas increases inferred for the stratosphere from shorter records (WMO, 1990a,b).

However, at altitudes above the lower stratosphere, there are major quantitative differences between the

modeled and observed cooling. The FDH simulated cooling increases with height when only the well-mixed gases are considered (Figure 5-24), whereas the observations indicate a rather uniform trend between 20 and 35 km (with perhaps even a slight reduction at ~30-35 km; see Figure 5A and Figures 5-7 to 5-12). It must be noted here that the GCM's simulation of the effects due to ozone loss involve a dynamical change (not evident in FDH) that causes some warming above the location of the cooling in the lower stratosphere (Section 5.3.3.1 and Figure 5-28). This GCM-simulated warming, which may not be statistically significant, occurs mainly in winter/spring and is qualitatively consistent with observations during that season (Figures 5-15 and 5-16). Consideration of this warming could retard somewhat the rapid increase of the well-mixed greenhouse gas-induced cooling with height seen in Figure 5-24 (e.g., above 25 km) and enable a full radiative-dynamical (i.e., GCM) computation to become more consistent with observations than the FDH results.

Additionally, the magnitude of the modeled cooling in the upper stratosphere is less than that observed; e.g., at ~45 km, the modeled cooling is about 1 K/decade due to the well-mixed greenhouse gases and about 0.3 K/decade due to ozone, while the observed cooling is greater than 1.5 K/decade (e.g., at 45 km in Figure 5A). Some of this bias could be due to water vapor, whose decadal trend in the 1980s globally is not known. Recent satellite data suggest an upward trend over the past 5 years, which would add to the cooling trend computed for the upper stratosphere (Section 5.3.5) and reduce the present discrepancy.

The vertical and latitudinal magnitude of the cooling, and likewise the location of the warming region above the cooling in the lower stratosphere, are very sensitive to the vertical profile of ozone depletion imposed in the model. The models invariably locate the cooling at exactly the region of the imposed ozone loss, with a warming immediately above it at the higher latitudes. Thus, any shift of the altitude extent of ozone depletion in the model has the potential to shift the peak cooling, and thus alter the vertical profile of the computed cooling trend. In turn, this affects the quantitative inferences about the consistency between computed and observed temperature trends in the middle and upper stratosphere.

5.4.3 Upper Troposphere

The cooling of the lower stratosphere in response to ozone losses there also leads to a cooling below the ozone loss region in the global upper troposphere (~10-14 km), in part due to reduced infrared emission from the stratosphere (Ramanathan and Dickinson, 1979). The cooling of the lower stratosphere also impacts the forcing of the troposphere (WMO, 1992, 1995; Chapter 10). Specifically, an ozone-induced cooling of the lower stratosphere implies a reduction in the longwave radiative emission from the stratosphere into the troposphere. This leads to a negative radiative forcing of the surface-troposphere system (Hansen *et al.*, 1997a). In general, GCMs simulating the effects of stratospheric ozone loss indicate a cooling of the upper troposphere (see Figures 5-25, 5-27, and 5-28).

All modeling efforts that have considered appropriate changes in trace gases yield a cooling of the tropopause region (e.g., Hansen *et al.*, 1995; see also Figure 5-27; Vinnikov *et al.*, 1996; Santer *et al.*, 1996; Hansen *et al.*, 1997a). Here, again, the lower stratospheric ozone depletion effects dominate over all other gases including CO₂. Further, the vertical profile of changes in ozone critically determines the profile of the temperature change in the upper troposphere.

A difficulty arises in comparing simulated upper tropospheric temperature changes due to ozone losses with observations over the past decade, as the “signal” from models (see Figures 5-27, and 5-28) is quite small, less so than that in the lower stratosphere (say, at 50 hPa or ~20 km). It may be noted that the modeled upper tropospheric changes, even for as large a forcing as a doubling of CO₂, are generally small compared with those in the lower troposphere or higher in the stratosphere (Vinnikov *et al.*, 1996). It is difficult at present to interpret the small change in the upper tropospheric temperatures inferred from observations in terms of a change originating primarily from the stratosphere (e.g., lower stratospheric ozone loss) or one arising in the troposphere (e.g., tropospheric ozone chemistry). Further, the halocarbon-induced depletion of ozone in the lower stratosphere can also be expected to affect upper tropospheric ozone through a downward transport of the anomalies, thereby contributing to a cooling of the upper troposphere.

In general, the temperature changes near the tropopause have the potential to affect the water vapor

distribution and cloudiness, especially cirrus clouds, which in turn can cause feedback effects in the climate system. One example available from observations of the effects in the upper troposphere due to a stratospheric perturbation concerns the aftermath of the Mt. Pinatubo eruption. Lidar and other observations (Sassen *et al.*, 1995) suggest that the aerosols from this volcanic eruption affected cirrus (ice) cloud formations near the tropopause.

The interactions between trace species’ changes and the associated chemistry, microphysics, radiation, and dynamics remain to be more thoroughly explored, both from modeling and observational perspectives, taking into account the three-dimensional nature of the problem (Holton *et al.*, 1995). Meteorological parameters such as tropopause location (Schubert and Munteanu, 1988; Hoinka *et al.*, 1998a), temperature, and geopotential height (Ohring and Muench, 1960; Spankuch and Schulz, 1995) tend to be highly correlated to total ozone. They can, therefore, be expected to exhibit changes owing to trends in ozone. At this time, such changes are not well documented (Section 5.2.7). There is growing evidence of a connection between variability and trends in the stratosphere with those in the troposphere (e.g., Kodera *et al.*, 1990; Kitoh *et al.*, 1996; Perlwitz and Graf, 1995). As noted earlier, Thompson and Wallace (1998) show a connection between the trend in winter-mean NH surface temperature and pressure and the trend in polar vortex strength. Such linkages inferred from observations emphasize that the radiative-chemical-dynamical interactions, which couple the stratospheric and tropospheric processes, need to be fully accounted for in order to attribute the observed temperature variations and trends to well-defined mechanisms that include changes in trace species.

REFERENCES

- Angell, J.K., The close relation between Antarctic total-ozone depletion and cooling of the Antarctic low stratosphere, *Geophys. Res. Lett.*, 13, 1240-1243, 1986.
- Angell, J.K., Variations and trends in tropospheric and stratospheric global temperatures, *J. Clim.*, 1, 1296-1313, 1988.

STRATOSPHERIC TEMPERATURE TRENDS

- Angell, J.K., Changes in tropospheric and stratospheric global temperatures, 1958-1988, in *Greenhouse-Gas-Induced Climatic Change: A Critical Appraisal of Simulations and Observations*, edited by M. E. Schlesinger, pp. 231-247, Elsevier, Amsterdam, 1991a.
- Angell, J.K., Stratospheric temperature change as a function of height and sunspot number during 1972-89 based on rocketsonde and radiosonde data, *J. Clim.*, 4, 1170-1180, 1991b.
- Angell, J.K., Comparisons of stratospheric warming following Agung, El Chichón, and Pinatubo volcanic eruptions, *Geophys. Res. Lett.*, 20, 715-718, 1993.
- Angell, J.K., Stratospheric warming due to Agung, El Chichón, and Pinatubo taking into account the quasi-biennial oscillation, *J. Geophys. Res.*, 102, 9479-9485, 1997.
- Austin, J., N. Butchart, and K.P. Shine, Probability of an Arctic ozone hole in a doubled CO₂ climate, *Nature*, 360, 221-225, 1992.
- Bailey, M.J., A. O'Neill, and V.D. Pope, Stratospheric analyses produced by the United Kingdom Meteorological Office, *J. Appl. Meteorol.*, 32, 1472-1483, 1993.
- Balachandran, N.K., and D. Rind, Modeling the effects of solar variability and the QBO on the troposphere/stratosphere system: Part I, The middle atmosphere, *J. Clim.*, 8, 2058-2079, 1995.
- Baldwin, M.P., and T.J. Dunkerton, Biennial, quasi-biennial, and decadal oscillations of potential vorticity in the northern stratosphere, *J. Geophys. Res.*, 103, 3919-3928, 1998a.
- Baldwin, M.P., and T.J. Dunkerton, Quasi-biennial modulation of the southern hemisphere stratospheric polar vortex, *Geophys. Res. Lett.*, in press, 1998b.
- Baldwin, M.P., X. Cheng, and T.J. Dunkerton, Observed correlation between winter-mean tropospheric and stratospheric anomalies, *Geophys. Res. Lett.*, 21, 1141-1144, 1994.
- Berntsen, T., I.S.A. Isaksen, G. Myrhe, J.S. Fuglestedt, F. Stordal, T.A. Larsen, R.S. Freckleton, and K.P. Shine, Effects of anthropogenic emissions on tropospheric ozone and its radiative forcing, *J. Geophys. Res.*, 102, 28101-28126, 1997.
- Bojkov, R., and V.E. Fioletov, Estimating the global ozone characteristics during the last 30 years, *J. Geophys. Res.*, 100, 16537-16551, 1995.
- Bojkov, R., and V.E. Fioletov, Changes of the lower stratospheric ozone over Europe and Canada, *J. Geophys. Res.*, 102, 1337-1347, 1997.
- Brasseur, G., The response of the middle atmosphere to long-term and short-term solar variability: A two-dimensional model, *J. Geophys. Res.*, 98, 23079-23090, 1993.
- Brasseur, G., and C. Granier, Mt. Pinatubo aerosols, chlorofluorocarbons and ozone depletion, *Science*, 258, 1239-1242, 1992.
- Brühl, C., and P. Crutzen, Scenarios of possible changes in atmospheric temperatures and ozone concentrations due to man's activities, estimated with a one-dimensional coupled photochemical climate model, *Clim. Dyn.*, 2, 173-203, 1988.
- Butchart, N., and J. Austin, On the relationship between the quasi-biennial oscillation, total chlorine and the severity of the Antarctic ozone hole, *Quart. J. Roy. Meteorol. Soc.*, 122, 183-217, 1996.
- Cariolle, D., A. Lasserre-Bigorry, J.-F. Royer, and J.F. Geleyn, A GCM simulation of the springtime Antarctic decrease and its impact on midlatitudes, *J. Geophys. Res.*, 95, 1883-1898, 1990.
- Chanin, M.-L., Long term trend in the middle atmosphere temperature, in *The Role of the Stratosphere in Global Change*, NATO ASI Series I, Vol. 8, edited by M.-L. Chanin, pp. 301-317, Springer-Verlag, Berlin, 1993.
- Chanin, M.-L., and P. Keckhut, Influence on the middle atmosphere of the 27-day and 11-year solar cycles: Radiative and/or dynamical forcing? *J. Geomagn. Geoelectr.*, 43, 647-655, 1991.
- Chipperfield, M.P., and J.A. Pyle, Two-dimensional modelling of the Antarctic lower stratosphere, *Geophys. Res. Lett.*, 15, 875-878, 1988.
- Christiansen, B., A. Guldborg, A.W. Hansen, and L.P. Riishojgaard, On the response of a three-dimensional general circulation model to imposed changes in the ozone distribution, *J. Geophys. Res.*, 102, 13051-13077, 1997.
- Christy, J.R., Temperature above the surface layer, *Clim. Change*, 31, 455-474, 1995.
- Christy, J.R., and S.J. Drouilhet, Variability in daily, zonal-mean lower stratospheric temperatures, *J. Clim.*, 7, 106-120, 1994.
- Christy, J.R., R.W. Spencer, and R.T. McNider, Reducing noise in the daily MSU lower tropospheric temperature dataset, *J. Clim.*, 8, 888-896, 1995.

- Chubachi, S., On the cooling of stratospheric temperatures at Syowa, Antarctica, *Geophys. Res. Lett.*, *13*, 1221-1223, 1986.
- Coy, L., E.R. Nash, and P.A. Newman, Meteorology of the polar vortex: Spring 1997, *Geophys. Res. Lett.*, *24*, 2693-2696, 1997.
- Cunnold, D.M., H. Wang, W. Chu, and L. Froidevaux, Comparisons between SAGE II and MLS ozone measurements and aliasing of SAGE II ozone trends in the lower stratosphere, *J. Geophys. Res.*, *101*, 10061-10075, 1996a.
- Cunnold, D.M., L. Froidevaux, J. Russell, B. Connor, and A. Roche, An overview of UARS ozone validation based primarily on intercomparisons among UARS and SAGE II measurements, *J. Geophys. Res.*, *101*, 10335-10350, 1996b.
- Donnelly, R.F., H.E. Hintnerger, and D.F. Heath, Temporal variation of solar EUV, UV, and 10830-Å radiations, *J. Geophys. Res.*, *91*, 5567-5578, 1986.
- Dunkerton, T.J., and M.P. Baldwin, Modes of interannual variability in the stratosphere, *Geophys. Res. Lett.*, *19*, 49-52, 1992.
- Dunkerton T.J., and D.P. Delisi, Climatology of the equatorial lower stratosphere: An observational study, *J. Atmos. Sci.*, *42*, 376-396, 1985.
- Dunkerton, T., D. Delisi, and M. Baldwin, Examination of middle atmosphere cooling trend in historical rocketsonde data, *Geophys. Res. Lett.*, submitted, 1998.
- Efron, B., *The Jackknife, The Bootstrap, and Other Resampling Plans*, 92 pp., Society for Industrial and Applied Mathematics (SIAM), Philadelphia, Pa., 1982.
- Elliott, W.P., and D.J. Gaffen, On the utility of radiosonde humidity archives for climate studies, *Bull. Amer. Meteorol. Soc.*, *72*, 1507-1520, 1991.
- Elliott, W.P., D.J. Gaffen, J.D. Kahl, and J.K. Angell, The effect of moisture on layer thicknesses used to monitor global temperatures, *J. Clim.*, *7*, 304-308, 1994.
- Eluszkiewicz, J., D. Crisp, R.G. Grainger, A. Lambert, A.E. Roche, J. B. Kumer, and J.L. Mergenthaler, Sensitivity of the residual circulation diagnosed from UARS data to the uncertainties in the input fields and to the inclusion of aerosols, *J. Atmos. Sci.*, *54*, 1739-1757, 1997.
- Fels, S.B., A parameterization of scale-dependent radiative damping rates in the middle atmosphere, *J. Atmos. Sci.*, *39*, 1141-1152, 1982.
- Fels, S.B., Radiative-dynamical interactions in the middle atmosphere, *Adv. Geophys.*, *28A*, 277-300, 1985.
- Fels, S.B., and L.D. Kaplan, A test of the role of longwave radiative transfer in a general circulation model, *J. Atmos. Sci.*, *33*, 779-789, 1975.
- Fels, S.B., J.D. Mahlman, M.D. Schwarzkopf, and R.W. Sinclair, Stratospheric sensitivity to perturbations in ozone and carbon dioxide: Radiative and dynamical response, *J. Atmos. Sci.*, *37*, 2265-2297, 1980.
- Finger, F.G., M.E. Gelman, J.D. Wild, M.-L. Chanin, A. Hauchecorne, and A.J. Miller, Evaluation of NMC upper-stratospheric temperature analyses using rocketsonde and lidar data, *Bull. Amer. Meteorol. Soc.*, *74*, 789-799, 1993.
- Fleming, E., S. Chandra, C.H. Jackman, D.B. Considine, and A.R. Douglass, The middle atmosphere response to short and long term solar UV variations: Analysis of observations and 2D model results, *J. Atmos. Terr. Phys.*, *57*, 333-365, 1995.
- Folland, C.K., D.M.H. Sexton, D.J. Karoly, C.E. Johnson, D.P. Rowell, and D.E. Parker, Influence of anthropogenic and oceanic forcing on recent climate change, *Geophys. Res. Lett.*, *25*, 353-356, 1998.
- Forster, P., and K.P. Shine, Radiative forcing and temperature trends from stratospheric ozone changes, *J. Geophys. Res.*, *102*, 10841-10855, 1997.
- Forster, P., R.S. Freckleton, and K.P. Shine, On aspects of the concept of radiative forcing, *Clim. Dyn.*, *13*, 547-560, 1997.
- Fortuin, J.P.F., and H. Kelder, Possible links between ozone and temperature profiles, *Geophys. Res. Lett.*, *23*, 1517-1520, 1996.
- Gaffen, D.J., Temporal inhomogeneities in radiosonde temperature records, *J. Geophys. Res.*, *99*, 3667-3676, 1994.
- Gaffen, D.J., *A Digitized Metadata Set of Global Upper-Air Station Histories*, NOAA Tech. Memo. ERL-ARL 211, 38 pp., National Oceanic and Atmospheric Administration, Silver Spring, Md., 1996.
- Garcia, R.R., S. Solomon, R.G. Roble, and D.W. Rusch, A numerical study of the response of the middle atmosphere to the 11-year solar cycle, *Planet. Space Sci.*, *32*, 411-423, 1984.
- Gelman, M.E., A.J. Miller, K.W. Johnson, and R.M. Nagatani, Detection of long-term trends in global stratospheric temperature from NMC analyses derived from NOAA satellite data, *Adv. Space Res.*, *6*, 17-26, 1986.

STRATOSPHERIC TEMPERATURE TRENDS

- Gelman, M.E., A.J. Miller, R.M. Nagatani, and H.D. Bowman III, Use of UARS data in the NOAA stratospheric monitoring program, *Adv. Space Res.*, 14, 21-31, 1994.
- Gille, S.T., A. Hauchecorne, and M.-L. Chanin, Semi-diurnal and diurnal tide effects in the middle atmosphere as seen by Rayleigh lidar, *J. Geophys. Res.*, 96, 7579-7587, 1991.
- Golitsyn, G.S., A.I. Semenov, N.N. Shefov, L.M. Fishkova, E.V. Lysenko, and S.P. Perov, Long-term temperature trends in the middle and upper atmosphere, *Geophys. Res. Lett.*, 23, 1741-1744, 1996.
- Goody, R.M., and Y.L. Yung, *Atmospheric Radiation*, pp. 388-425, Oxford University Press, Oxford, U.K., 1989.
- Graf, H.-F., J. Perlwitz, I. Kirchner, and I. Schult, Recent northern winter climate trends, ozone changes and increased greenhouse gas forcing, *Contrib. Atmos. Phys.*, 68, 233-248, 1995.
- Graham, N.E., Simulation of recent global temperature trends, *Science*, 267, 666-671, 1995.
- Haigh, J., The impact of solar variability on climate, *Science*, 272, 981-984, 1996.
- Haigh, J., A GCM study of climate change in response to the 11-year solar cycle, *Quart. J. Roy. Meteorol. Soc.*, in press, 1998.
- Halpert, M.S., and G.D. Bell, Climate assessment for 1996, *Bull. Amer. Meteorol. Soc.*, 78, S1-S49, 1997.
- Hamilton, K., R.J. Wilson, J.D. Mahlman, and L.J. Umscheid, Climatology of the GFDL SKYHI troposphere-stratosphere-mesosphere general circulation model, *J. Atmos. Sci.*, 52, 5-43, 1995.
- Hansen, J., and H. Wilson, Commentary on the significance of global temperature records, *Clim. Change*, 25, 185-191, 1993.
- Hansen, J.E., W.-C. Wang, and A.A. Lacis, Mt. Agung provides test of a global climate perturbation, *Science*, 199, 1065-1068, 1978.
- Hansen, J., A. Lacis, R. Ruedy, M. Sato, and H. Wilson, How sensitive is the world's climate? *Natl. Geogr. Res. Explor.*, 9, 142-158, 1993.
- Hansen, J.E., H. Wilson, M. Sato, R. Ruedy, K. Shah, and E. Hansen, Satellite and surface temperature data at odds? *Clim. Change*, 30, 103-117, 1995.
- Hansen, J.E., M. Sato, and R. Ruedy, Radiative forcing and climate response, *J. Geophys. Res.*, 102, 6831-6864, 1997a.
- Hansen, J., M. Sato, R. Ruedy, A. Lacis, K. Asamoah, K. Beckford, S. Borenstein, E. Brown, B. Cairns, B. Carlson, B. Curran, S. de Castro, L. Druyan, P. Etwarrow, T. Ferede, M. Fox, D. Gaffen, J. Glascoe, H. Gordon, S. Hollandsworth, X. Jiang, C. Johnson, N. Lawrence, J. Lean, J. Lerner, K. Lo, J. Logan, A. Lueckert, M.P. McCormick, R. McPeters, R. Miller, P. Minnis, I. Rambaran, G. Russell, P. Russell, P. Stone, I. Tegen, S. Thomas, L. Thomason, A. Thompson, J. Wilder, R. Willson, and J. Zawodny, Forcings and chaos in interannual to decadal climate change, *J. Geophys. Res.*, 102, 25679-25720, 1997b.
- Harshvardhan, Perturbation of the zonal radiation balance by a stratospheric aerosol layer, *J. Atmos. Sci.*, 36, 1274-1285, 1979.
- Hauchecorne, A., M.-L. Chanin, and P. Keckhut, Climatology and trends of the middle atmospheric temperature (33-87 km) as seen by Rayleigh lidar over the south of France, *J. Geophys. Res.*, 96, 15297-15309, 1991.
- Hoinka, K.P., Statistics of the global tropopause, *Mon. Wea. Rev.*, in press, 1998a.
- Hoinka, K.P., Temperature, humidity and wind at the global tropopause, *Mon. Wea. Rev.*, submitted, 1998b.
- Holton, J.R., and H.-C. Tan, The influence of the equatorial quasi-biennial oscillation on the global circulation at 50 mb, *J. Atmos. Sci.*, 37, 2200-2208, 1980.
- Holton, J.R., and H.-C. Tan, The quasi-biennial oscillation in the Northern Hemisphere lower stratosphere, *J. Meteorol. Soc. Japan*, 60, 140-148, 1982.
- Holton, J.R., P.H. Haynes, M.E. McIntyre, A.R. Douglass, R.B. Rood, and L. Pfister, Stratosphere-troposphere exchange, *Rev. Geophys.*, 33, 403-439, 1995.
- Hood, L.L., J. L. Jirikowic, and J.P. McCormack, Quasi-decadal variability of the stratosphere: Influence of long-term solar ultraviolet variations, *J. Atmos. Sci.*, 50, 3941-3958, 1993.
- Huovila, S., and A. Tuominen, *On the Influence of Radiosonde Lag Error on Upper-Air Climatological Data in Finland 1951-1988*, Meteorological Publications, No. 14, 29 pp., Finnish Meteorological Institute, Helsinki, 1990.

- IPCC (Intergovernmental Panel on Climate Change), *Climate Change 1994: Radiative Forcing of Climate Change and An Evaluation of the IPCC IS92 Emission Scenarios*, edited by J.T. Houghton, L.G. Meira Filho, J. Bruce, H. Lee, B.A. Callander, E. Haites, N. Harris, and K. Maskell, 339 pp., Cambridge University Press, Cambridge, U.K., 1995.
- IPCC (Intergovernmental Panel on Climate Change), *Climate Change 1995: The Science of Climate Change*, edited by J.T. Houghton, L.G. Meira Filho, B.A. Callander, N. Harris, A. Kattenberg, and K. Maskell, 572 pp., Cambridge University Press, Cambridge, U.K., 1996.
- Jones, A.E., and J.D. Shanklin, Continued decline of total ozone over Halley, Antarctica, since 1985, *Nature*, 376, 409-411, 1995.
- Jones, P.D., Recent warming in global temperature series, *Geophys. Res. Lett.*, 21, 1149-1152, 1994.
- Kalnay, E., M. Kanamitsu, R. Kistler, W. Collins, D. Deaven, L. Gandin, M. Iredell, S. Saha, G. White, J. Woollen, Y. Zhu, M. Chelliah, W. Ebisuzaki, W. Higgins, J. Janowiak, K.C. Mo, C. Ropelewski, J. Wang, A. Leetmaa, R. Reynolds, R. Jenne, and D. Joseph, The NCEP/NCAR 40-year reanalysis project, *Bull. Amer. Meteorol. Soc.*, 77, 437-471, 1996.
- Karl, T.R., V.E. Derr, D.R. Easterling, C.K. Folland, D.J. Hofmann, S. Levitus, N. Nicholls, D.E. Parker, and G.W. Withee, Critical issues for long-term climate monitoring, *Clim. Change*, 31, 185-221, 1995.
- Keckhut, P., A. Hauchecorne, and M.-L. Chanin, Midlatitude long-term variability of the middle atmosphere: Trends and cyclic and episodic changes, *J. Geophys. Res.*, 100, 18887-18897, 1995.
- Keckhut, P., M.E. Gelman, J.D. Wild, F. Tissot, A.J. Miller, A. Hauchecorne, M.-L. Chanin, E.F. Fishbein, J. Gille, J.M. Russell III, and F.W. Taylor, Semidiurnal and diurnal temperature tides (30-55 km): Climatology and effect on UARS lidar data comparisons, *J. Geophys. Res.*, 101, 10299-10310, 1996.
- Keckhut P., F.J. Schmidlin, A. Hauchecorne, and M.-L. Chanin, Trend estimates from rocketsondes at low latitude station (8S-34N), taking into account instrumental changes and natural variability, *J. Atmos. Solar-Terr. Phys.*, in press, 1998.
- Kiehl, J.T., and B.A. Boville, The radiative-dynamical response of a stratospheric-tropospheric general circulation model to changes in ozone, *J. Atmos. Sci.*, 45, 1798-1817, 1988.
- Kiehl, J.T., and S. Solomon, On the radiative balance of the stratosphere, *J. Atmos. Sci.*, 43, 1525-1534, 1986.
- Kiehl, J.T., B.A. Boville, and B.P. Briegleb, Response of a general circulation model to a prescribed Antarctic ozone hole, *Nature*, 332, 501-504, 1988.
- Kitoh, A., H. Koide, K. Kodera, S. Yukimoto, and A. Noda, Interannual variability in the stratospheric-tropospheric circulation in a coupled ocean-atmosphere GCM, *Geophys. Res. Lett.*, 23, 543-546, 1996.
- Kodera, K., and K. Yamazaki, Long-term variation of upper stratospheric circulation in the Northern Hemisphere in December, *J. Meteorol. Soc. Japan*, 68, 101-105, 1990.
- Kodera, K., K. Yamazaki, M. Chiba, and K. Shibata, Downward propagation of upper stratospheric mean zonal wind perturbation to the troposphere, *Geophys. Res. Lett.*, 17, 1263-1266, 1990.
- Kokin, G.A., and E.V. Lysenko, On temperature trends of the atmosphere from rocket and radiosonde data, *J. Atmos. Terr. Phys.*, 56, 1035-1044, 1994.
- Kokin, G.A., E.V. Lysenko, and S.K. Rozenfeld, Temperature changes in the stratosphere and mesosphere in 1964-1988 based on rocket sounding data, *Izv. Atmos. Oceanic Phys.*, 26, 518-523, 1990.
- Komuro, H., Long-term cooling in the stratosphere observed by aerological rockets at Ryori, Japan, *J. Meteorol. Soc. Japan*, 67, 1081-1082, 1989.
- Koshelkov, Yu P., and G.R. Zakharov, On temperature trends in the Arctic lower stratosphere, *Meteorol. Gidrol.*, in press, 1998.
- Labitzke, K., and M.P. McCormick, Stratospheric temperature increases due to Pinatubo aerosols, *Geophys. Res. Lett.*, 19, 207-210, 1992.
- Labitzke, K., and H. van Loon, Association between the 11-year solar cycle, the QBO and the atmosphere: Part I, The troposphere and stratosphere in the northern hemisphere in winter, *J. Atmos. Terr. Phys.*, 50, 197-206, 1988.
- Labitzke, K., and H. van Loon, The 11-year solar cycle in the stratosphere in the northern summer, *Ann. Geophys.*, 7, 595-598, 1989.

STRATOSPHERIC TEMPERATURE TRENDS

- Labitzke, K., and H. van Loon, On the association between the QBO and the extratropical stratosphere, *J. Atmos. Terr. Phys.*, *54*, 1453-1463, 1992.
- Labitzke, K., and H. van Loon, Trends of temperature and geopotential height between 100 and 10 hPa in the Northern Hemisphere, *J. Meteorol. Soc. Japan*, *72*, 643-652, 1994.
- Labitzke, K., and H. van Loon, A note on the distribution of trends below 10hPa: The extratropical northern hemisphere, *J. Meteorol. Soc. Japan*, *73*, 883-889, 1995.
- Labitzke, K., and H. van Loon, The signal of the 11-year sunspot cycle in the upper troposphere-lower stratosphere, *Space Sci. Rev.*, *80*, 393-410, 1997.
- Lacis, A.A., D.J. Wuebbles, and J.A. Logan, Radiative forcing of climate by changes in the vertical distribution of ozone, *J. Geophys. Res.*, *95*, 9971-9981, 1990.
- Lait, L.R., M.R. Schoeberl, and P.A. Newman, Quasi-biennial modulation of Antarctic ozone depletion, *J. Geophys. Res.*, *94*, 11559-11571, 1989.
- Luers, J.K., Estimating the temperature error of the radiosonde rod thermistor under different environments, *J. Atmos. Oceanic Technol.*, *7*, 882-895, 1990.
- Lysenko, E.V., G. Nelidova, and A. Prostova, Changes in the stratospheric and mesospheric thermal conditions during the last 3 decades: 1, The evolution of a temperature trend, *Izv. Atmos. Oceanic Phys.*, *33*, 218-225, 1997.
- Mahlman, J.D., A looming Arctic ozone hole? *Nature*, *360*, 209, 1992.
- Mahlman, J.D., J.P. Pinto, and L.J. Umscheid, Transport, radiative, and dynamical effects of the Antarctic ozone hole: A GFDL "SKYHI" model experiment, *J. Atmos. Sci.*, *51*, 489-508, 1994.
- Manabe, S., and R.T. Wetherald, Thermal equilibrium of the atmosphere with a given distribution of relative humidity, *J. Atmos. Sci.*, *24*, 241-259, 1967.
- Manney, G.L., R. Swinbank, S.T. Massie, M.E. Gelman, A.J. Miller, R. Nagatani, A. O'Neill, and R.W. Zurek, Comparison of U.K. Meteorological Office and U.S. National Meteorological Center stratospheric analyses during northern and southern winter, *J. Geophys. Res.*, *101*, 10311-10334, 1996.
- McCormack, J.P., and L.L. Hood, Relationship between ozone and temperature trends in the lower stratosphere: Latitude and seasonal dependencies, *Geophys. Res. Lett.*, *21*, 1615-1618, 1994.
- McCormack, J.P., and L.L. Hood, Apparent solar cycle variations of upper stratospheric ozone and temperature: Latitudinal and seasonal dependencies, *J. Geophys. Res.*, *101*, 20933-20944, 1996.
- McCormick, M.P., L.W. Thomason, and C.R. Trepte, Atmospheric effects of the Mt. Pinatubo eruption, *Nature*, *373*, 399-404, 1995.
- Miller, A.J., R.M. Nagatani, G.C. Tiao, X.F. Niu, G.C. Reinsel, D. Wuebbles, and K. Grant, Comparisons of observed ozone and temperature trends in the lower stratosphere, *Geophys. Res. Lett.*, *19*, 929-932, 1992.
- Mohanakumar, K., Solar activity forcing of the middle atmosphere, *Ann. Geophys.*, *13*, 879-885, 1995.
- Nash, J., and G.F. Forrester, Long-term monitoring of stratospheric temperature trends using radiance measurements obtained by the TIROS-N series of NOAA spacecraft, *Adv. Space Res.*, *6*, 37-44, 1986.
- Naujokat, B., An update of the observed quasi-biennial oscillation of the stratospheric winds over the tropics, *J. Atmos. Sci.*, *43*, 1873-1877, 1986.
- Naujokat, B., and S. Pawson, The cold stratospheric winters 1994/95 and 1995/96, *Geophys. Res. Lett.*, *23*, 3703-3706, 1996.
- Nedoluha, G.E., R.M. Bevilacqua, R.M. Gomez, D.E. Siskind, and B.C. Hicks, Increases in middle atmospheric water vapor as observed by the Halogen Occultation Experiment and the ground-based water vapor millimeter-wave spectrometer from 1991 to 1997, *J. Geophys. Res.*, *103*, 3531-3543, 1998.
- Newman, P.A., and W.J. Randel, Coherent, ozone-dynamical changes during the Southern Hemisphere spring, 1979-1986, *J. Geophys. Res.*, *93*, 12585-12606, 1988.
- Newman, P., J. Gleason, R.D. McPeters, and R. Stolarski, Anomalous low ozone over the Arctic, *Geophys. Res. Lett.*, *24*, 2689-2692, 1997.
- Ohring, G., and H.S. Muench, Relationship between ozone and meteorological parameters in the lower stratosphere, *J. Meteorol.*, *17*, 195-206, 1960.
- Oltmans, S., and D. Hofmann, Increase in lower stratospheric water vapor at midlatitude northern hemisphere, *Nature*, *374*, 146-149, 1995.
- Oort, A.H., and H. Liu, Upper-air temperature trends over the globe, 1956-1989, *J. Clim.*, *6*, 292-307, 1993.

- Pan, Y.H., and A.H. Oort, Global climate variations connected with sea surface temperature anomalies in the eastern equatorial Pacific Ocean for the 1958-1973 period, *Mon. Wea. Rev.*, *111*, 1244-1258, 1983.
- Parker, D.E., On the detection of temperature changes induced by increasing atmospheric carbon dioxide, *Quart. J. Roy. Meteorol. Soc.*, *111*, 587-601, 1985.
- Parker, D.E., and D.I. Cox, Towards a consistent global climatological rawinsonde data-base, *Intl. J. Climatol.*, *15*, 473-496, 1995.
- Parker, D.E., M. Gordon, D.P.N. Cullum, D.M.H. Sexton, C.K. Folland, and N. Rayner, A new global gridded radiosonde temperature data base and recalculated temperature trends, *Geophys. Res. Lett.*, *24*, 1499-1502, 1997.
- Pawson, S., and B. Naujokat, Trends in daily wintertime temperatures in the northern stratosphere, *Geophys. Res. Lett.*, *24*, 575-578, 1997.
- Perlwitz, J., and H.F. Graf, The statistical connection between tropospheric and stratospheric circulation of the northern hemisphere in winter, *J. Clim.*, *8*, 2281-2295, 1995.
- Pinnock, S., M.D. Hurley, K.P. Shine, T.J. Wallington, and T.J. Smyth, Radiative forcing by hydrochlorofluorocarbons and hydrofluorocarbons, *J. Geophys. Res.*, *100*, 23227-23238, 1995.
- Pitari, G., M. Verdecchia, and G. Visconti, A transformed Eulerian model to study possible effects of the El Chichón eruption on stratospheric circulation, *J. Geophys. Res.*, *92*, 10961-10975, 1987.
- Pollack, J., and T. Ackerman, Possible effects of the El Chichón cloud on the radiation budget of the northern tropics, *Geophys. Res. Lett.*, *10*, 1057-1060, 1983.
- Prather, M.J., M.M. Garcia, R. Suozzo, and D. Rind, Global impact of the Antarctic ozone hole: Dynamical dilution with a three-dimensional chemical transport model, *J. Geophys. Res.*, *95*, 3449-3471, 1990.
- Ramanathan, V., The role of ocean-atmosphere interactions in the CO₂ climate problem, *J. Atmos. Sci.*, *38*, 918-930, 1981.
- Ramanathan, V., and R.E. Dickinson, The role of stratospheric ozone in the zonal and seasonal radiative energy balance of the Earth-troposphere system, *J. Atmos. Sci.*, *36*, 1084-1104, 1979.
- Ramanathan, V., R.J. Cicerone, H.B. Singh, and J.T. Kiehl, Trace gas trends and their potential role in climate change, *J. Geophys. Res.*, *90*, 5547-5566, 1985.
- Ramaswamy, V., and M.M. Bowen, Effect of changes in radiatively active species upon the lower stratospheric temperatures, *J. Geophys. Res.*, *99*, 18909-18921, 1994.
- Ramaswamy, V., M.D. Schwarzkopf, and K.P. Shine, Radiative forcing of climate from halocarbon-induced global stratospheric ozone loss, *Nature*, *355*, 810-812, 1992.
- Ramaswamy, V., M.D. Schwarzkopf, and W. Randel, Fingerprint of ozone depletion in the spatial and temporal pattern of recent lower-stratospheric cooling, *Nature*, *382*, 616-618, 1996.
- Randel, W.J., The anomalous circulation in the Southern Hemisphere stratosphere during spring 1987, *Geophys. Res. Lett.*, *15*, 911-914, 1988.
- Randel, W.J., and J.B. Cobb, Coherent variations of monthly mean total ozone and lower stratospheric temperature, *J. Geophys. Res.*, *99*, 5433-5447, 1994.
- Randel, W.J., and F. Wu, Cooling of the Arctic and Antarctic polar stratospheres due to ozone depletion, *J. Clim.*, in press, 1998.
- Randel, W.J., F. Wu, J.M. Russell III, J.W. Waters, and L. Froidevaux, Ozone and temperature changes in the stratosphere following the eruption of Mt. Pinatubo, *J. Geophys. Res.*, *100*, 16753-16764, 1995.
- Randel, W.J., F. Wu, R. Swinbank, J. Nash, and A. O'Neill, Global QBO circulation derived from UKMO stratospheric analyses, *J. Atmos. Sci.*, in press, 1998.
- Reid, G.C., Seasonal and interannual temperature variations in the tropical stratosphere, *J. Geophys. Res.*, *99*, 18923-18932, 1994.
- Reid, G.C., K.S. Gage, and J.R. McAfee, The thermal response of the tropical atmosphere to variations in equatorial Pacific sea surface temperature, *J. Geophys. Res.*, *94*, 14705-14716, 1989.
- Rind, D., R. Suozzo, N. Balachandran, and M. Prather, Climate change and the middle atmosphere: Part I, The doubled CO₂ climate, *J. Atmos. Sci.*, *4*, 475-494, 1990.

STRATOSPHERIC TEMPERATURE TRENDS

- Rind, D., N. Balachandran, and R. Suozzo, Climate change and the middle atmosphere: Part II, The impact of volcanic aerosols, *J. Clim.*, 5, 189-207, 1992.
- Rind, D., D. Shindell, P. Lonergan, and N.K. Balachandran, Climate change and the middle atmosphere: Part III, The doubled CO₂ climate revisited, *J. Clim.*, in press, 1998.
- Rosenfield, J., D.B. Considine, P.E. Meade, J.T. Bacmeister, C.H. Jackman, and M.R. Schoeberl, Stratospheric effects of Mt. Pinatubo aerosol studied with a coupled two-dimensional model, *J. Geophys. Res.*, 102, 3649-3670, 1997.
- Salby, M., P. Callaghan, and D. Shea, Interdependence of the tropical and extratropical QBO: Relationship to the solar cycle versus a biennial oscillation of the stratosphere, *J. Geophys. Res.*, 102, 789-798, 1997.
- Santer, B.D., K.E. Taylor, T.M.L. Wigley, T.C. Johns, P.D. Jones, D.J. Karoly, J.F.B. Mitchell, A.H. Oort, J.E. Penner, V. Ramaswamy, M.D. Schwarzkopf, R.J. Stouffer, and S. Tett, A search for human influences on the thermal structure of the atmosphere, *Nature*, 382, 39-46, 1996.
- Santer, B.D., J.J. Hnilo, T.M.L. Wigley, J.S. Boyle, C. Doutriaux, M. Fiorino, D.E. Parker, and K.E. Taylor, Uncertainties in 'Observational' estimates of temperature change in the free atmosphere, *J. Geophys. Res.*, submitted, 1998.
- Sassen, K., D.O. Starr, G.G. Mace, M.R. Poellot, S.H. Melfi, W.L. Eberhard, J.D. Spinhirne, E.W. Eloranta, D.E. Hagen, and J. Hallett, The 5-6 December 1991 FIRE IFO II jet stream cirrus case study: Possible influences of volcanic aerosols, *J. Atmos. Sci.*, 52, 97-123, 1995.
- Schubert, S., and M. Munteanu, An analysis of tropopause pressure and total ozone, *Mon. Wea. Rev.*, 116, 569-582, 1988.
- Schubert, S.R., R. Rood, and J. Pfaendtner, An assimilated dataset for earth science applications, *Bull. Amer. Meteorol. Soc.*, 74, 2331-2342, 1993.
- Schwarzkopf, M.D., and V. Ramaswamy, Radiative forcing due to ozone in the 1980s: Dependence on altitude of ozone change, *Geophys. Res. Lett.*, 20, 205-208, 1993.
- Scrase, F.J., Application of radiation and lag corrections to temperatures measured with Meteorological Office radiosonde, *Meteorol. Mag.*, 85, 65-75, 1956.
- Shindell, D.T., D. Rind, and P. Lonergan, Increased polar stratospheric ozone losses and delayed eventual recovery owing to increasing greenhouse-gas concentrations, *Nature*, 392, 598-592, 1998.
- Shine, K.P., On the modelled thermal response of the Antarctic stratosphere to a depletion of ozone, *Geophys. Res. Lett.*, 13, 1331-1334, 1986.
- Shine, K.P., The greenhouse effect and stratospheric change, in *The Role of the Stratosphere in Global Change*, NATO ASI Series I, Vol. 8, edited by M.-L. Chanin, pp. 285-300, Springer-Verlag, Berlin, 1993.
- Solomon, S., R.W. Portmann, R.R. Garcia, L.W. Thomason, L.R. Poole, and M.P. McCormick, The role of aerosol variations in anthropogenic ozone depletion at northern midlatitudes, *J. Geophys. Res.*, 101, 6713-6727, 1996.
- Spankuch, D., and E. Schulz, Diagnosing and forecasting total column ozone by statistical relations, *J. Geophys. Res.*, 100, 18873-18885, 1995.
- Spencer, R.W., and J.R. Christy, Precision lower stratospheric temperature monitoring with the MSU technique, validation and results 1979-1991, *J. Clim.*, 6, 1194-1204, 1993.
- Steinbrecht, W., H. Claude, U. Koehler, and K. Hoinka, Correlations between tropopause height and total ozone: Implications for long-term changes, *J. Geophys. Res.*, in press, 1998.
- Sun, D.-Z., and A.H. Oort, Humidity-temperature relationships in the tropical troposphere, *J. Clim.*, 8, 1974-1987, 1995.
- Suzuki, S., and M. Asahi, Influence of solar radiation on the temperature measurement before and after the change of the length of suspension used for the Japanese radiosonde observation, *J. Meteorol. Soc. Japan*, 56, 61-64, 1978.
- Swinbank, R., and A. O'Neill, A stratosphere-troposphere data assimilation system, *Mon. Wea. Rev.*, 122, 686-702, 1994.
- Taalas, P., and E. Kyrö, 1987-1989 total ozone sounding observations in Northern Scandinavia and Antarctica, and the climatology of the lower stratosphere during 1965-1988 in Northern Finland, *J. Atmos. Terr. Phys.*, 54, 1089-1099, 1992.
- Taalas, P., and E. Kyrö, The stratospheric winter of 1991/2 at Sodankylä in the European Arctic as compared with 1965-92 meteorological and 1988-91 ozone sounding statistics, *Geophys. Res. Lett.*, 21, 1207-1210, 1994.

- Tett, S.F.B., J.F.B. Mitchell, D.E. Parker, and M.R. Allen, Human influence on the atmospheric vertical temperature structure: Detection and observations, *Science*, 274, 1170-1173, 1996.
- Teweles, S., and F.G. Finger, Reduction of diurnal variation in the reported temperatures and heights of stratospheric constant pressure surfaces, *J. Meteorol.*, 17, 177-194, 1960.
- Thompson, D.W.J., and J.M. Wallace, Observed linkages between Eurasian surface air temperature, the North Atlantic Oscillation, Arctic sea-level pressure, and the stratospheric polar vortex, *Geophys. Res. Lett.*, submitted, 1998.
- Tie, X.X., G.P. Brasseur, B. Briegleb, and C. Granier, Two-dimensional simulation of Pinatubo aerosol and its effect on stratospheric ozone, *J. Geophys. Res.*, 99, 20545-20562, 1994.
- Trenberth, K.E., and J.G. Olson, Temperature trends at the South Pole and McMurdo Sound, *J. Clim.*, 2, 1196-1206, 1989.
- van Loon, H., and K. Labitzke, Association between the 11-year solar cycle, the QBO, and the atmosphere: Part IV, The stratosphere, not grouped by the phase of the QBO, *J. Clim.*, 3, 827-837, 1990.
- van Loon, H., and K. Labitzke, The global range of the stratospheric decadal wave: Part I, Its association with the sunspot cycle and its annual mean, and with the troposphere, *J. Clim.*, 11, 1529-1537, 1998.
- Vinnikov, K.Ya., A. Robock, R.J. Stouffer, and S. Manabe, Vertical patterns of free and forced climate variations, *Geophys. Res. Lett.*, 23, 1801-1804, 1996.
- Wang, W.-C., M. P. Dudek, X.-Z. Liang, and J.T. Kiehl, Inadequacy of effective CO₂ as a proxy in simulating the greenhouse effect of other radiatively active gases, *Nature*, 350, 573-577, 1991.
- WMO (World Meteorological Organization), *Atmospheric Ozone: 1985*, Global Ozone Research and Monitoring Project – Report No. 16, Chapter 15, Geneva, 1986.
- WMO (World Meteorological Organization), *Report of the International Ozone Trends Panel: 1988*, Global Ozone Research and Monitoring Project – Report No. 18, Chapter 6, Geneva, 1990a.
- WMO (World Meteorological Organization), *Scientific Assessment of Stratospheric Ozone: 1989*, Global Ozone Research and Monitoring Project – Report No. 20, Chapters 1 and 2, Geneva, 1990b.
- WMO (World Meteorological Organization), *Scientific Assessment of Ozone Depletion: 1991*, Global Ozone Research and Monitoring Project – Report No. 25, Chapters 2 and 7, Geneva, 1992.
- WMO (World Meteorological Organization), *Scientific Assessment of Ozone Depletion: 1994*, Global Ozone Research and Monitoring Project – Report No. 37, Chapter 8, Geneva, 1995.
- WMO (World Meteorological Organization), *SPARC/IOC/GAW Assessment of Trends in the Vertical Distribution of Ozone*, edited by N. Harris, R. Hudson, and C. Phillips, SPARC Report No. 1, World Meteorological Organization Global Ozone Research and Monitoring Project – Report No. 43, Geneva, 1998.
- Zalcik, M.S., Western Canada noctilucent cloud incidence map, *Climatol. Bull.*, 27, 165-169, 1993.
- Zhai, P., and R.E. Eskridge, Analyses of inhomogeneities in radiosonde temperature and humidity time series, *J. Clim.*, 9, 676-705, 1996.